Response to interactive comment of Referee on “Interactive comment on “Characteristics of the Greenhouse Gas Concentration Derived from the Ground-based FTS Spectra at Anmyeondo, Korea” by Young-Suk Oh et al.

T. Blumenstock (Referee)

thomas.blumenstock@kit.edu

Received and published: 24 May 2017

General comments:

The authors present a new TCCON site in Korea. This paper characterizes the instrumentation and gives an example of its application: inter-comparison with OCO-2 satellite data. This site really fills a gap in the existing TCCON network and will be very useful to assessing sink and sources of GHGs. The data and also the comparison with OCO-2 data are of good quality. The subject is appropriate for publication in AMT. The paper is well written and I recommend publication after major revisions, in particular a more comprehensive description.

First of all, we would like to strongly appreciate referee’s very constructive and valuable comments on the manuscript. We have tried to address all the issues (major and minor comments) raised on this paper one by one. The referee makes strong comments to give more details about OASIS and its influence on ILS (Instrumental Line Shape) by including some illustrations so that we added some more brief on it. Our replies and respective changes are described below. Technical comments regarding spellings and grammatical errors are corrected in the final version of the manuscript.

Major comment:

A specific feature of the described instrumentation is the so called OASIS (Operational Automatic System for Intensity of Sunray) system. While analog systems are used in active remote sensing systems, for example laser output control in LIDAR systems, an intensity control of passive systems is typically not used. In the TCCON network the variability of the DC signal is used to quality check and correct the recorded interferograms and resulting spectra. Since you remove this signal you cannot apply this kind of quality check anymore. Do you record and use the actual setting of the aperture to do so?

Response

In addition to OASIS system, we have also simultaneously used the variability of DC signal similar to TCCON network for quality control of the spectra and its retrieval results. Yes, the spectra are recorded with the actual setting of the aperture having a diameter of 0.8 mm throughout the observation period.

If the motivation to introduce such a system is to limit the intensity to avoid non-linear response a smaller constant aperture or smaller preamp gain or a smaller sensitivity of the detector might be more appropriate. Would you please add a statement for the motivation to add this system? Or a comparison of XCO_2 time series recorded with and without OASIS system which might demonstrate the difference, for example in terms of signal to noise ratio.

Response

The OASIS system is developed for improving the quality of the spectra. To ensure the quality of the spectra, this system will be useful for minimizing the noise that induced in the spectra due to rapid intensity fluctuations of the incoming solar radiation that reaches to the instrument. This rapid intensity fluctuations are be occurred in the presence of clouds, aerosol loading etc. along the path of incoming radiation within the instrument field of view. To minimize this intensity fluctuations due to the changing weather conditions, OASIS system regulates in such a way that by varying the aperture size at the source compartment based on the signals from photon sensor which depends on the levels of incoming sunlight intensity. Thereby, it avoids non-linear response of a smaller constant aperture or smaller preamp gain or a smaller sensitivity of the detector. In this study, we are not able to show the whole time series of XCO_2 without OASIS system during the study period since all spectra that are used for analysis of species are obtained after the OASIS system equipped to our FTS spectrometer. However, for a typical example, we illustrated the time series of XCO_2 in both cases.

Based on TCCON community suggestions regarding the OASIS system, it would be recommended to use a consistent g-b FTS measurement set up throughout TCCON network so that we plan to fix a constant aperture size at the source compartment during the FTS operation at Anmyeondo station.

Where is the variable aperture positioned?

Response

A variable aperture is placed inside the OASIS system which is at the source compartment.

Is it in the parallel or focused beam?

Response

It is a focused beam.

Did you check the influence on the ILS (Instrumental Line Shape) due to the variable aperture while scanning?

Response

Yes, we assessed the influence of ILS due to the variable aperture and the result showed that it has no impact on the ILS.

I assume a lamp was used and hence the OASIS system was not active while performing cell measurements. Cell measurements using the sun as source might be an option to check the ILS while the OASIS system is active. Or, if the HCl lines in the atmospheric spectrum are covered by interfering species you might do cell measurements with the lamp using different fixed aperture settings to check the influence of the OASIS system on the ILS. How does your system and its influence on the ILS compares with the results of the recent paper by Sun et al, AMT, 2017 on the 'Sensitivity of instrumental line shape monitoring for the ground-based high-resolution FTIR spectrometer with respect to different optical attenuators'? While most of the site complies with the TCCON standard setup the OASIS system does not. Therefore a more detailed description is needed as well as a discussion on its influence on the ILS.

Response

We have carried out experiments to investigate the influences of ILS due to the presence of OASIS system, and then considered HCl cell measurements using sun as source while OASIS system active and tungsten lamp as a source while OASIS inactive. The result confirmed that the ILS was not affected by the variable aperture during the operation of OASIS system. Sun et al. (2017) reported the detailed characteristics of the ILS with respect to applications of different optical attenuators to FTIR spectrometers within the TCCON and NDACC networks. They used both lamp and sun cell measurements which were conducted after the insertion of five different attenuators in front of and behind the interferometer. In Sun et al. (2017) paper, the ILS result was indicated by considering optical attenuator no .1 which is in good agreement with our findings.

Specific comments:

- In Chapter 3.1 the time series of the O_2 columns is compared with atmospheric pressure. Therefore including surface pressure in Fig. 8 might support your statement.

Response

The time series of surface pressure is included in bottom panel of Fig. 8 and compared with the time series of O_2 column.

- The errors are shown in Fig. 9. How is the error calculated and which sources of errors are included?

Response

The main sources of errors are; laser sampling error, zero level offsets, ILS error, smoothing error, atmospheric apriori temperature, atmospheric apriori pressure, surface

pressure, and random noise. The total error is then computed from the sum of each error components.

- Can you specify 'regular cell measurements'?

Response

Regular cell measurements are conducted one time approximately in every month.

Technical comments:

- p.1 + 12: were generally agreed => generally agreed

….,both instruments generally agreed in capturing seasonal variations of the target species….

- p.2: space born => space borne

…a number of instruments deployed in various platforms (e.g., ground-based, space-borne)…

- p.3: area is; => area is:

…..climatic condition of the area is: the minimum temperature…..

- p.4: with oil-free => with oil-free pump

….FTS is kept at 0.1 to 0.2 hPa with oil-free pump to maintain the stability of the system….

- p.5: beamspliters =< beamsplitters

In Table 1. Beamsplitters

- p. 7: to these derived => to those derived (?)

…mole fractions were used only to those derived (?) below the solar zenith angle…

- p. 9:

- orbit, devoted => orbit. It is devoted

launched on July 2, 2014 into low-Earth orbit. It is devoted to observing

- can available => is available

….instrument is available in different papers……

- p.10: are varied => varied

…column amounts varied ….

- p.11:

- over the land => over land

…the OCO-2 data over land within….

- square => squares

..RMSE - Root Mean Squares Error….

- p.12:

- and this suggesting => suggesting

....OCO-2, suggesting that the variability.....

- new page within Table 4

p.13:

- the source and sink of them. => their sources and sinks.

...for investigating their sources and sinks......

- outcome this => outcome of this

Therefore, the outcome of this study reflects.....

- Is ': : : to be withered that turns out to be weak photosynthesis : : : a grammatically correct sentence?

….. weak photosynthesis phenomenon is occurred because of low plant flourishing and CO_2 reaches the highest values..........

Interactive comment on Atmos. Meas. Tech. Discuss., doi:10.5194/amt-2017-88, 2017.

First referee revision.

Characteristics of the Greenhouse Gas Concentration Derived from the Ground-based FTS Spectra at Anmyeondo, Korea

Young-Suk Oh[1,4*], Samuel Takele Kenea[1], Tae-Young Goo[1], Gawon Kim[1], Kyu-Sun Chung[4], David Griffith[3], Voltaire Velacco[3], Jae-Sang Rhee[1], Me-Lim Oh[2], Haeyoung Lee[2], and Young-Hwa Byun[1]

[1]Climate Research Division, National Institute of Meteorological Sciences, Jeju−do, Korea

[2]Climate Change Monitoring Division, Korea Meteorological Administration, Seoul, Korea

[3]University of Wollongong, Wollongong, Australia

[4]Department of Electrical Eng. & Center for Edge Plasma Science, Hanyang University, Seoul, Korea

Correspondence to: Young-Suk Oh (ysoh306@gmail.com)

Abstract. Since the late 1990s, the meteorological observatory established in Anmyeondo (36.5382˚ N, 126.3311˚ E, and 30 m above mean sea level), has been monitoring several greenhouse gases such as CO_2, CH_4, N_2O, CFCs, and SF_6, as part of the Global Atmosphere Watch (GAW) Program. A high resolution ground-based (g-b) Fourier Transform Spectrometer (FTS, IFS-125HR model) was installed at such observation site in 2013, and has been fully operated within the frame work of the Total Carbon Column Observing Network (TCCON) since August, 2014. The solar spectra recorded by the g-b FTS are covered in the range between 3,800 and 16,000 cm^{-1} at the spectral resolution of 0.02 cm^{-1} during the measurement period between 2013 and 2016. In this work, the GGG2014 version of the TCCON standard retrieval algorithm was used to retrieve XCO_2 concentrations from the FTS spectra. Two spectral bands (at 6220.0 and 6339.5 cm^{-1} center wavenumbers) were used to derive the XCO_2 concentration within the spectral residual of +0.01 %. All sources of errors were thoroughly analyzed. In this paper, we introduced a new home made OASIS (Operational Automatic System for Intensity of Sunray) system to our g-b FTS instrument and that allows reducing the solar intensity variations (SIV) below 2 %. A comparison of the XCO_2 concentration in g-b FTS and OCO-2 (Orbiting Carbon Observatory) satellite observations were presented only for the measurement period between 2014 and 2015. Nine coincident observations were selected on a daily mean basis. It was obtained that OCO-2 exhibited low bias with respect to the g-b FTS, which is about -0.065 ppm with the standard deviation of 1.66 ppm, and revealed a strong correlation (R=0.85). Based on seasonal cycle comparisons, both instruments generally agreed in capturing seasonal variations of the target species with its maximum and minimum levels in spring and late summer respectively.

In the future, it is planned to exert further works in utilizing the FTS measurements for the evaluation of satellite observations such as Greenhouse Gases Observing Satellite (GOSAT) at observation sites. This is the first report of the g-b FTS observations of XCO_2 species over the Anmyeondo station.

Key words: XCO_2, Retrievals, G-b FTS, TCCON, Infrared spectra, OASIS

1 Introduction

Monitoring of greenhouse gases (GHGs) is a crucial issue in the context of the global climate change. Carbon dioxide (CO_2) is one of the key greenhouse gas and its global annual mean concentration has been increased rapidly from 278 to 400 ppm since 1750, pre-industrial year (WMO greenhouse gas bulletin, 2016). Radiative forcing of atmospheric CO_2 accounts for approximately 65 % of the total radiative forcing by long-lived GHGs (Ohyama et al., 2015 and reference therein). Human activities, such as burning of fossil fuels, land use change, etc., are the primary drivers of the continuing increase in atmospheric greenhouse gases and the gases involved in their chemical production (Kiel et al., 2016 and reference therein), In the fact that it is a global concern for demanding accurate and precise long-term measurements of greenhouse gases.

In the field of remote sensing techniques, solar absorption infrared spectroscopy is an essential technique, which has been increasingly used to determine changes in atmospheric constituents. Nowadays, a number of instruments deployed in various platforms (e.g., ground-based, space-borne) have been operated for measuring GHGs such as CO_2. Our g-b FTS at the Anmyeondo station has been measuring several atmospheric GHGs operated within the framework of the Total Carbon Column Observing Network (TCCON). XCO_2 retrievals from the g-b FTS have been reported at different TCCON sites (e.g, Ohyama et al., 2009; Deutscher et al., 2010; Messerschmidt et al., 2010, 2012; Miao et al., 2013; Kivi and Heikkinen, 2016). TCCON achieves the accuracy and precision in measuring the total column of CO_2 as about 0.25 % that is less than 1 ppm (Wunch et al., 2010), which is essential to get information about sinks and sources, as well as validating satellite products (Rayner and O'Brien, 2001; Miller et al., 2007). It is reported that the precision of CO_2 even 0.1 % can be achieved during clear sky conditions (Messerschmidt et al., 2010; Deutscher et al., 2010). The network aims to improve global carbon cycle studies and to supply the primary validation data of different atmospheric trace gases derived from space-based instruments, e.g., the Orbiting Carbon Observatory 2 (OCO-2), the Greenhouse Gases Observing Satellite (GOSAT) (Frankenberg et al., 2015; Morino et al., 2011).

The objective of this study is focused on the characteristics of XCO_2 concentration retrievals from g-b FTS spectra and is to implement a preliminary comparison against OCO-2 over the Anmyeondo station. The FTS spectra have been processed using the TCCON standard GGG2014 (Wunch et al., 2015) retrieval software. One of the interesting issues in this work is that we introduce a new home made OASIS system to our g-b FTS instrument, by which we were able to attain SVI (solar intensity variations) below 2 %.

This paper is organized as follows: Sect. 2 introduces instrumentations and measurement site descriptions. Sect. 3 represents results and discussion. The conclusion is given in Sect. 4.

2 Site and instrumentation

2.1 Site description

The G-b FTS observatory was established in the Anmyeondo (AMY) station, which is located at 36.32˚ N, 126.19˚ E, and 30 m above sea level. This station is situated on the west coast of the Korean Peninsula, which is 180 kilometer away from Seoul, the capital city of Korea. Figure 1 displays the Anmyeondo station. It is also a regional GAW (Global Atmosphere Watch) station that belongs to the Climate Change Monitoring Network of KMA (Korean Meteorological Administration). The AMY station has been monitoring various atmospheric compositions such as greenhouse gases, aerosols, ultraviolet radiation, ozone, and precipitation since 1999. The total area of Anmyeondo is estimated to be ~87.96 km^2 and approximately 1.25 million people reside in this island. Some of the residents over this area are engaged in agricultural activities. The topographic feature of the area consists of low level hills, on average it is about 100 m above sea level. The climatic condition of the area is: the minimum temperature is occurred on winter season with an average of 2.7 ˚C, and the maximum temperature is about 25.6 ˚C during summer season. In addition, the annual precipitation amount is estimated to be 1,155 mm; and the high amount of snows would be observed in winter. Such observation site has been designated as part of TCCON site since August 2014. The AMY site's on TCCON wiki page is kept available and can be found at: https://tccon-wiki.Anmyeondo.edu/Sites/Anmyeondo.

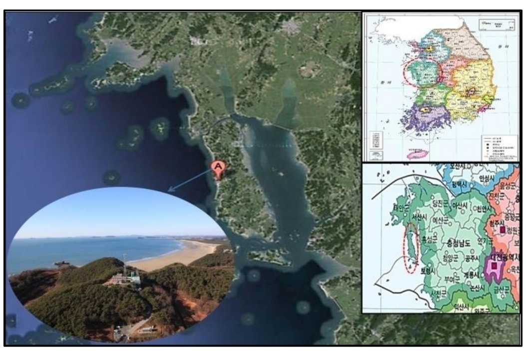

Figure 1: Anmyeondo(AMY) station

2.2 G-b FTS instrument

Solar spectra are acquired by operating a Bruker IFS 125HR spectrometer (Bruker Optics, Germany) under the framework of TCCON. Currently, our g-b FTS instrument operation is semi-automated for taking the routine measurements under clear sky conditions. It is planned to make an FTS operation mode to be fully automated by this year. The solar tracker (Tracker A 547, BrukerOptics, Germany) is mounted inside a dome. The tracking ranges in terms of both azimuthal and elevation angles are about 0˚ to 315˚ and 10˚ to 85˚ degrees, respectively, while the tracking speed is about 2 degrees per second. The tracking accuracy of ±4 minutes of arc can be achieved by the Camtracker mode. Under clear sky conditions, the dome is opened and set to an automatic-turning mode, so that the mirrors are moved automatically to search for the position where the sunspot is seen by the camera. Then, the solar tracker is activated in such a way that the mirrors are finely and continuously controlled to fix the beam into the spectrometer. Figure 2 displays an overview of the general data acquisition system. This ensures that all spectra were recorded under clear weather conditions. The other important feature that has been made on the FTS spectrometer is the implementation of the interferogram sampling method (Brault, 1996), that takes advantage of modern analog-digital converters (ADCs) to improve the signal-to-noise ratio.

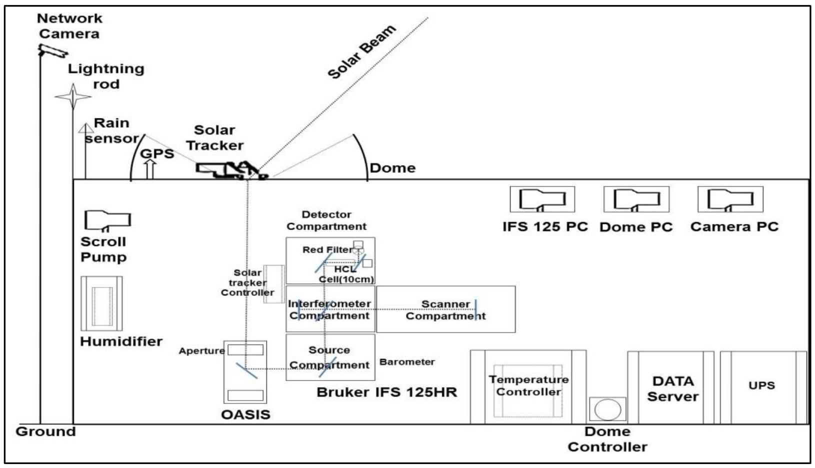

Figure 2: Photographs of the automated FTS laboratory. The Bruker Solar Tracker type A547 is mounted in the custom made dome. A servo controlled solar tracker directs the solar beam through a CaF_2 window to the FTS (125HR) in the laboratory. The server computer uses custom data acquisition software. PC1, PC2 and PC3 are used for controlling the spectrometer, solar tracker, dome, camera, pump, GPS satellite time, and humidity sensor.

The spectrometer has equipped with two room temperature detectors; an Indium-Gallium-Arsenide (InGaAs) detector, which covers the spectral region from 3,800 to 12,800 cm^{-1}, and a Silicon (Si) diode detector (9,000 – 25,000 cm^{-1}) used in a dual-acquisition mode with a dichroic optic (Omega Optical, 10,000 cm^{-1} cut-on). A filter (Oriel Instruments 59523; 15,500 cm^{-1} cut-on) prior to the Si diode detector blocks visible light, which would otherwise be aliased into a near-infrared spectral domain. TCCON measurements are routinely recorded at a maximum optical path difference (OPD_{max}) of 45 cm leading to a spectral resolution of 0.02 cm^{-1}. Two scans, one forward and one backward, are performed and individual interferograms are recorded. A single scan in one measurement takes about 110 s. The pressure inside FTS is kept at 0.1 to 0.2 hPa with oil-free pump to maintain the stability of the system and to ensure clean and dry conditions.

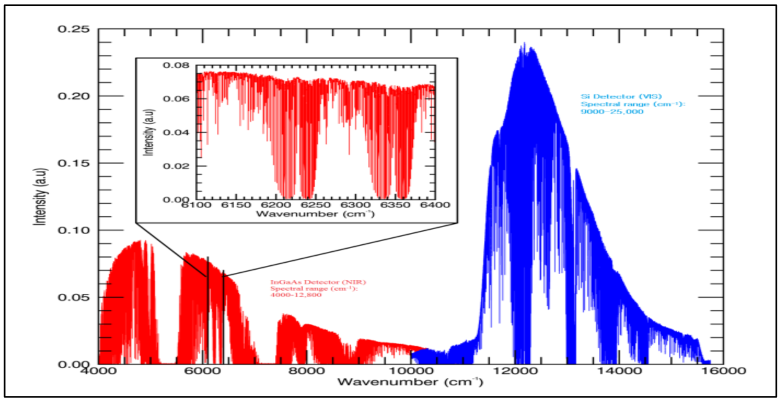

Figure 3: Single spectrum recorded on 4 October 2014 with a resolution of 0.02 cm^{-1}. Signal-to-noise ratio is ~900 for the InGaAs detector (A) and ~500 for the Si diode detector (B). A typical example for the spectrum of XCO_2 is shown in the inset.

Table 1. Measurement setting for the Anmyeondo g-b FTS spectrometer of the Bruker 125HR model

Item	Setting
Aperture	0.8 mm
Detectors	RT-Si Diode DC, RT-InGaAs DC
Beamsplitters	CaF_2
Scanner velocity	10 kHz
Low pass filter	10 kHz
High folding limit	15798.007031
Spectral Resolution	0.02 cm^{-1}
Optical path difference	45 cm
Acquisition mode	Single sided, forward-backward
Sample scan	2
Sample scan time	~110 s

2.3 Operational Automatic System for the Intensity of Sunray (OASIS)

The main function of the OASIS is to control the aperture diameter of inlet through which the incoming radiation goes to the interferometer. This aperture is placed inside the OASIS system, which is different from the actual aperture that is located inside the interferometer compartment. The aperture size varies in the range of 26 to 32 mm with respect to the photon sensor signals at the OASIS system, which is operated at voltage ranges of approximately 0 to 219 mV. Figure 4 depicts the schematic views of the OASIS systems. As can be seen in the figure, the basic components of the OASIS system such as photoelectric sensor, stepping motor, and sunray controller are shown clearly. In fact, the detail characteristic of the operation is beyond the scope of this paper. The fundamental purpose of this system is to optimize the measurement of the solar spectra by reducing the effect of the fluctuations (sudden drops) of the intensity of the incoming light occurred due to changes in thin clouds and aerosols loads or interceptions by any other objects along the line of sight over the measurement site. The maximum threshold value of the solar intensity variation (SIV) is 5 % that is the TCCON standard value (Ohyama et al., 2015). Therefore, we have reduced this value to 2 % in our case by introducing a new home made OASIS system to our g-b FTS since December 2014. This allows us to ensure for having high quality spectra from the instrument. In this work, we have used this quality criterion to screen out the quality of the spectra. Figure 5 illustrates an example, taken on date 4 April 2015, on variations in levels of intensity with and without equipped the OASIS system to the g-b FTS instrument. It is clearly seen that the large amplitude of the solar intensity variation is filtered in the spectra. Note that the solar intensity difference was exhibited as can be seen in the figure, which was due to the measurement time difference.

Table 2. HCL Cell spectrum comparison with OASIS system (tungsten, solar light)

Light Source	Tungsten	Solar(Sun)	Solar(Sun)	Range
S/N (signal to noise ratio)	183.2 : 1	162.7 : 1	167.1 : 1	_
Resolution ($5687.65cm^{-1}$)	0.0137	0.0143	0.0145	0.0135~0.0149
Transmission	-0.0005 to 0.0005	-0.001 to 0.001	-0.001 to 0.001	_
Mod. eff	99.99 %	99.98 %	99.96 %	99.96 ~99.99 %
OASIS run	**OFF**	**OFF**	**ON**	_
Analysis Parameter	(Same Parameter) Resolution: 0.015cm-1, Scans: 50, Beamspliter: CaF2, Aperture: 0.8mm, Detector: RT-InGaAs DC, Scanner velocity: 10kHz, High pass filter: open, Low pass filter: 10kHz (Different Parameter) Source setting: Emission back parallel input/ NIR			

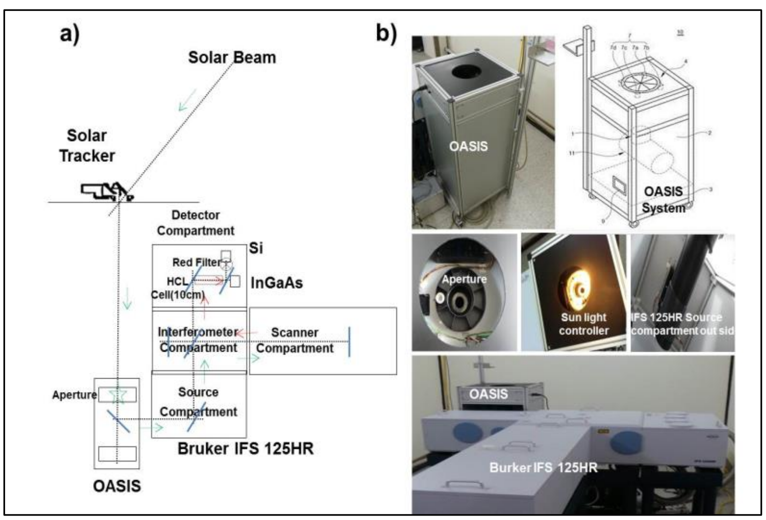

Figure 4: Schematic views of the OASIS system

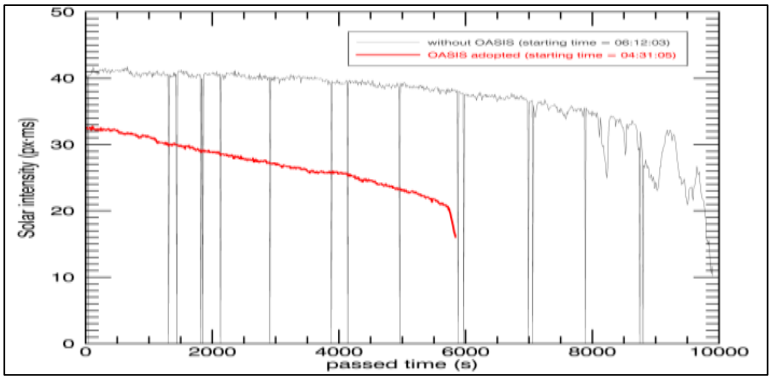

Figure 5: Typical example for solar intensity versus time with and without OASIS is given. (Taken on 04 April, 2015)

2.4 Retrieval methodology

The TCCON standard GGG2014 (version 4.8.6) (Wunch et al., 2015) retrieval software developed by JPL is used to determine the abundances of XCO_2 from the FTS spectra. Within the GGG package, there is a GFIT (version 4.37) section, which is a nonlinear least squares spectral fitting program developed for analyzing FTS spectra (Messerschmidt et al., 2010; Wunch et al., 2011). GFIT is developed in such a way that its "forward model" is independent of and separable from its "inverse method". The forward model is an algorithm that computes the atmospheric spectra compared to the observed spectra, incorporating radiative transfer and molecular physics along with assumed gas distributions (Connor et al., 2016).

Table 3. Spectral windows used for the retrievals of the columns of CO_2 and O_2.

Gas	Center of spectral window (cm^{-1})	Width (cm^{-1})	Interfering gas
O_2	7885.0	240.0	H_2O, HF, CO_2
CO_2	6220.0	80.0	H_2O ,HDO, CH_4
CO_2	6339.5	85.0	H_2O ,HDO

The GFIT forward model calculation uses 70 vertical levels spaced at 1 km intervals to represent the atmosphere. The CO_2 column amount is retrieved from two spectral windows centered at 6220 and 6339.5 cm^{-1} (see Table 2). The calculated and the measured spectra are compared, and the residual is minimized by iteratively scaling the gas VMR profiles (Messerschmidt et al., 2012). A typical example for the measured spectrum of CO_2 in these bands is shown in the inset of Fig. 3. The spectroscopic line parameters for the CO_2 retrieval are taken from the High Resolution Transmission data (HITRAN) 2012 (Rothman et al., 2013). The inverse method retrieves a state vector of parameters, such as volume mixing ratio of the target species, by computing values that provide a best fit to the spectrum by employing other assumptions and constraints (Connor et al., 2016). The apriori profiles generated by the TCCON retrieval algorithm are based on the National Centre for Environment Prediction (NCEP) reanalysis data (http://www.cdc.noaa.gov/data/gridded/data.ncep.reanalysis.html) for temperature, pressure, and humidity. The a priori profile of CO_2 is derived based on a model fitted to the GLOBALVIEW data.

The standard TCCON retrieval uses O_2 retrieved from the same spectra as the target gases in the band at 7885 cm^{-1} to estimate the total dry-air column. The retrieved CO_2 column is then divided by the retrieved O_2 column to compute the column average dry-air mole fraction.

$$XCO_2 = \frac{CO_{2\,column}}{O_{2\,column}} \times 0.2095 \,, \quad (1)$$

Computing the ratio using Eq. (1) minimizes systematic and correlated errors such as errors in solar zenith angle, surface pressure, and instrumental line shape that existed in the retrieved CO_2 and O_2 columns (Messerschmidt et al., 2012, Washenfelder et al., 2006). In addition, the retrieved dry−air mole fractions were used by filtering the data points with high solar zenith angle of (> 80°) (Buschmann et al., 2016).

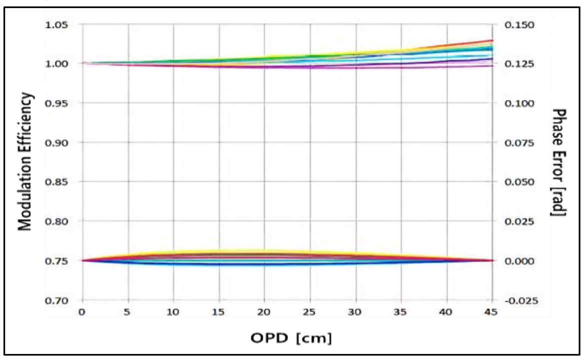

Figure 6: Time series modulation efficiency and phase error (rad) of HCl measurements from the g-b FTS are displayed in the period from October 2013 to September, 2014. Resolution: 0.015 cm^{-1}, Aperture: 0.8 mm, and Detector: RT-InGaAs DC (from 2013.10 (red) to 2016.09 (black)).

2.5 Characterization of FTS-instrumental line shapes

For the accurate retrieval of total column values of the species of interest, a good alignment of the g-b FTS is essential. The instrument line shape (ILS) is retrieved from the regular HCl cell measurement that is an important indicator of the status of the FTS's alignment (Hase et al., 1999). The analyses of the measurements were performed using a linefit spectrum fitting algorithm (LINFIT14 software) (Hase et al., 2013). The time series of the modulation efficiency and phase error (rad) in the HCl measurement obtained from the Anmyeondo g-b FTS in the period from October 2013 to September 2016 are depicted in Fig. 6. Modulation amplitudes for well alignment should be controlled in a limit of 5 % loss at the maximum optical difference (Wunch et al., 2011). In our g-b FTS measurements, it is found that the maximum loss of modulation efficiency at the maximum OPD is about 3 %, which is quite close to the ideal value. The phase errors are less than 0.009. Hase et al. (2013) reported that this level of small disturbances from the ideal value of the modulation efficiency is common to all well-aligned instruments. This result confirmed that the g-b FTS instrument is well aligned and stable during the whole operation period.

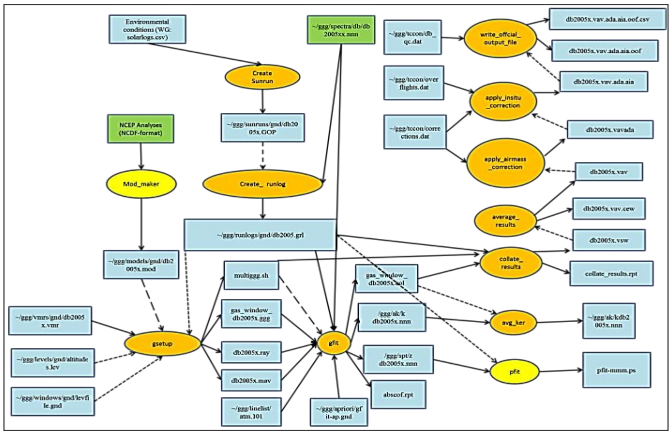

Figure 7: Schematic views of the TCCON GGG2014 standard retrieval software.

2.6 OCO-2

Orbiting Carbon Observatory-2 (OCO-2) is NASA's first Earth-orbiting satellite, which was successfully launched on July 2 2014 into low-Earth orbit. It is devoted to observing atmospheric carbon dioxide (CO_2) to get better insight for the carbon cycle. The primary mission is to measure carbon dioxide with high precision and accuracy in order to characterize its sources and sinks at different spatial and temporal scales (Boland et al., 2009; Crisp, 2008, 2015). The instrument measures the near infrared spectra (NIR) of sunlight reflected off the Earth's surface. Using a retrieval algorithm, it provides results of atmospheric abundances of carbon dioxide and related atmospheric parameters at the nadir, sun glint and targets modes. Detailed information about the instrument is available in different papers (Connor et al., 2008; O'Dell et al., 2012). In this work, we used the OCO-2 version 7Br bias corrected data.

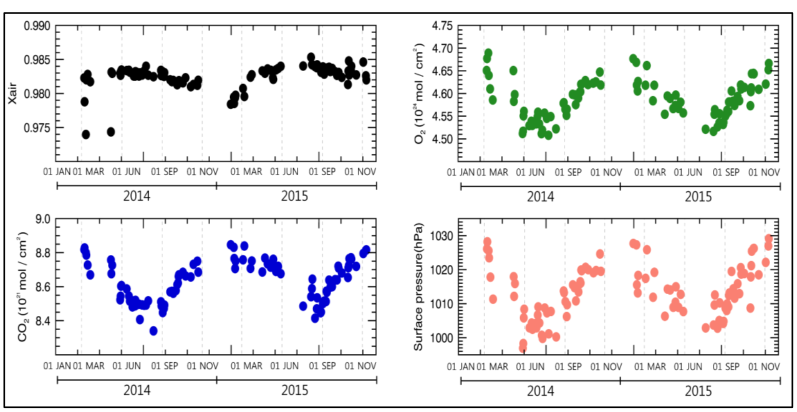

Figure 8: Time series of X_{air}, total column amounts of CO_2, total column amounts of O_2, and surface pressure (pout) from the g-b FTS is depicted during 2014- 2015 from top to bottom, respectively.

3 Result and discussion

3.1 Time series of X_{air} and columns of CO_2 and O_2

The time series of column-averaged abundance of dry air (X_{air}) is given in the top panel of Fig. 8. It shows that the values of X_{air} are fluctuated between 0.974 and 0.985, and the mean value is 0.982 with a standard deviation of 0.0015 in which the scatter for X_{air} is about 0.15 %. The low variability in time series of X_{air} indicates the stability of the measurements.

The temporal distributions of the g-b FTS total column amounts of CO_2 and O_2 on daily mean basis during the period from February 2014 to December 2015 are depicted in Fig. 8. As can be seen in the middle panel of the plot, the CO_2 column amounts varied from 8.40×10^{21} to 8.84×10^{21} molecules cm^{-2} during the whole observation period, while O_2 varied between 4.5×10^{24} and 4.7×10^{24} molecules cm^{-2}, with the corresponding mean of 4.52×10^{24} molecules cm^{-2} and a standard deviation of 2.59×10^{22} molecules cm^{-2}, respectively. The scatter for column O_2 is estimated to be 0.57 %, which is comparable with the variation of atmospheric pressure.

3.2 Comparison of the daily average XCO_2 between the g-b FTS and OCO-2

In this section, we present a comparison of XCO_2 between the g-b FTS and OCO-2 version 7Br data (bias corrected data) over Anmyeondo station during the period between 2014 and 2015. For making a comparison of the g-b FTS measurements, we applied the spatial coincidence criteria for the OCO-2 data over land within 4° latitude/longitude of the FTS station, as well as setting up a time window of 1 day. In addition, a direct comparison was made between the g-b FTS and OCO-2, without considering the effects of different apriori profiles and averaging kernels since we do not have the CO_2 profile that reflects the actual variability over the measurement site. Based on the coincidence criteria, we obtained nine coincident measurements, which were not sufficient to infer a robust conclusion. But it gives a preliminary result for indicating a level of agreement between them. We showed that the comparison of the time series on daily mean basis of XCO_2 concentrations derived from the g-b FTS and OCO-2 along with the time series of its retrieval errors from FTS during the measurement period between 2014 and 2015, as depicted in Fig. 8. As can be seen in the plot, the g-b FTS measurement exhibits some gaps occurred due to bad weather conditions, instrument failures, and absences of an instrument operator. In the present analysis, the XCO_2 concentrations from FTS were considered only when its retrieval error was below 1.5 ppm (see the bottom panel of Figure 8). Recently, Wunch et al. (2016) reported that the comparison of XCO_2 derived from the OCO-2 version 7Br data against a co-located ground-based TCCON data that indicates the median differences between the OCO-2 and TCCON data were less than 0.5 ppm, a corresponding RMS differences less than 1.5 ppm. The overall results of our comparisons are comparable with the report made by Wunch et al. (2016). The OCO-2 product of XCO_2 was biased (satellite minus g-b FTS) with respect to the g-b FTS, which was lowered by 0.065 ppm with a standard deviation of 1.66 ppm. This bias could be attributed to the instrument uncertainty. In addition to that, we also obtained a strong correlation between them, which was quantified as a correlation coefficient of 0.85.

Table 4. Summary of the statistics of the XCO_2 comparisons between OCO-2 and the g-b FTS from 2014 to 2015 are presented. N–coincident number of data, R-correlation coefficient, RMSE - Root Mean Squares Error.

N	Abso. diff. (ppm)	Rel. diff (%)	R	RMSE (ppm)
9	-0.065±1.665	-0.0167±0.418	0.854	1.571

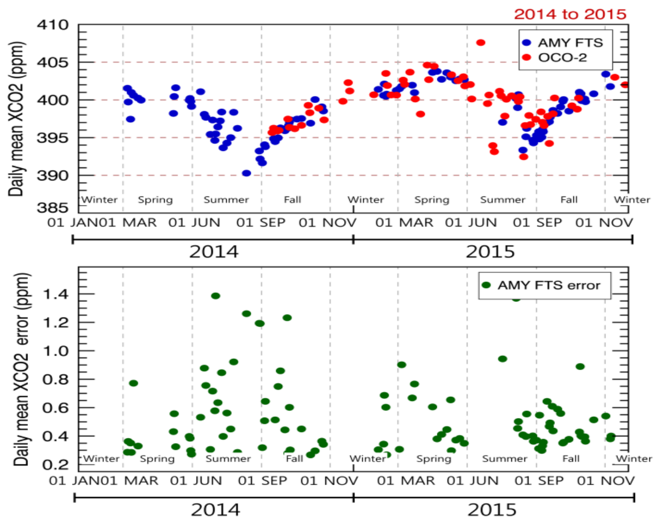

Figure 9: Top Panel: The time series of XCO_2 from the g-b FTS (blue dot) and OCO-2 (red dot) over the Anmyeondo site from 2014 to 2015. Bottom panel: The time series of FTS XCO_2 errors. All results are given on daily mean basis.

3.3 Comparison of seasonal cycle of XCO_2

In this section, the main focus of this issue is to deal with the comparison of the seasonal cycle of XCO_2 between the g-b FTS and OCO-2 over the Anmyeondo station. The top panel of Fig. 9 exhibits the time series of the daily mean XCO_2 from 2014 to 2015. The overall result indicates that both instruments are generally agreed in capturing the seasonal variability of XCO_2 at the measurement site. As it is clearly seen from the temporal distribution of FTS XCO_2, the maximum and minimum values are observed in spring and late summer seasons, respectively. It was found that its mean values in spring and summer were 402.63 and 396.58 ppm, respectively (see Table 4). This is because the seasonal variation of XCO_2 is controlled mainly by the photosynthesis in the terrestrial ecosystem, and this explains the larger XCO_2 values in the northern hemisphere in late April (Schneising et al. 2008, and references therein). The minimum value of XCO_2 occurs in August due to uptake of carbon into the biosphere, which is associated with the period of plant growth. Furthermore, both instruments showed high standard deviations during summer, about 2.56 ppm in FTS and 3.41 ppm in OCO-2, suggesting that the variability reflects strong sources and sink signals.

Table 5. Seasonal mean and standard deviations of XCO_2 from the g-b FTS and OCO-2 in the period between 2014 and 2015 are given below.

Season	g-b FTS XCO_2 mean ±std (ppm)	OCO-2 XCO_2 mean ±std (ppm)
Winter	401.01 ± 0.62	401.57 ± 1.17
Spring	402.63 ± 0.87	402.43 ± 1.81
Summer	396.58 ± 2.56	398.94 ± 3.41
Fall	398.62 ± 2.21	397.49 ± 1.58

4 Conclusions

Monitoring of greenhouse gases is an essential issue in the context of the global climate change. Accurate and precise continuous long-term measurements of the greenhouse gases (GHGs) are substantial for investigating their source and sinks. Nowadays, several remote sensing instruments operated on different platforms are dedicated for measuring GHGs.
XCO_2 measurements have been made using the g-b FTS at the Anmyeondo site since 2013. However, in this work, we focused on the measurements taken during 2014 and 2015. The instrument has been operated in a semi-automated mode since then. The FTS instrument has been stable during the whole measurement period. Regular instrument alignments using the HCl cell measurements are performed. The other important feature is that the home made OASIS system is installed in our FTS instrument, which enables to improve the solar intensity fluctuations. Thus, it guarantees the quality of the spectra. The TCCON standard GGG2014 retrieval software is used to retrieve XCO_2 from the g-b FTS spectra.

In this work, the preliminary comparison results of XCO_2 between FTS and OCO-2 were presented over the Anmyeondo station. The mean absolute difference of XCO_2 between FTS and OCO-2 was calculated on daily mean basis, and it was estimated to be -0.065 ppm, along with a standard deviation of 1.67 with respect to the g-b FTS. This bias could be attributed with instrument uncertainty. Based on the seasonal cycle comparison, both the g-b FTS and OCO-2 illustrated a consistent pattern in capturing the seasonal variability of XCO_2, with maximum in spring and minimum in summer. In summer and fall, plants are flourishing and CO_2 is consumed by photosynthesis. However, in winter and spring, weak photosynthesis phenomenon is occurred because of low plant flourishing and CO_2 reaches the highest values particularly in April. Therefore, the outcome of this study reflects the suitability of the measurements for improving the understanding of the carbon cycle, as well as for evaluating the remote sensing data.

5 Acknowledgements

This research was supported by the Research and Development for KMA Weather, Climate, and Earth system Services (NIMS-2016-3100).

References

Boland, S., Brown L. R., Burrows J. P., Ciais P., Connor B. J., Crisp D., Denning S., Doney S. C., Engelen R., Fung I. Y., Griffith P., Jacob D. J., Johnson B., Martin-Torres J., Michalak A. M., Miller C. E., Polonsky I., Potter C., Randerson J. T., Rayner P. J., Salawitch R. J., Santee M., Tans P. P., Wennberg P. O., Wunch D., Wofsy S. C., and Yung Y. L.: The Need for Atmospheric Carbon Dioxide Measurements from Space: Contributions from a Rapid Reflight of the Orbiting Carbon Observatory, 2009, http://www.nasa.gov/pdf/363474main_OCO_Reflight.pdf.

Buschmann M., Nicholas M., Deutscher M., Sherlock V., Palm M., Warneke T., and Notholt J.: Retrieval of XCO2 from ground-based mid-infrared (NDACC) solar absorption spectra and comparison to TCCON, Atmos. Meas. Tech., 9, 577–585, 2016.

Brault, J. W.: New approach to high-precision Fourier transform spectrometer design. Appl. Opt. 35, 2891–2896, 1996.

Connor B. J., Bösch H., Toon G., Sen B., Miller C. E., and Crisp D.: Orbiting carbon observatory: Inverse method and prospective error analysis, J. Geophys. Res., 113 doi: 10.1029/2006JD008336, 2008.

Connor B. J., Sherlock V., Toon G., Wunch D., and Wennberg P. O.: GFIT2: an experimental algorithm for vertical profile retrieval from near-IR spectra, Atmos. Meas. Tech., 9(8), 3513–3525, doi:10.5194/amt-9-3513-2016, 2016.

Crisp D., Miller C. E., DeCola P. L.: NASA Orbiting Carbon Observatory: measuring the column averaged carbon dioxide mole fraction from space. J. Appl. Remote Sens., 2, 023508, doi:10.1117/1.2898457, 2008.

Crisp D. for the OCO-2 Team: Measuring Atmospheric Carbon Dioxide from Space with the Orbiting Carbon Observatory-2 (OCO-2), Proc. SPIE 9607, Earth Observing Systems XX, 960702, doi: 10.1117/12.2187291, 2015.

Deutscher, N. M., Griffith, D. W. T., Bryant, G. W., Wennberg, P. O., Toon, G. C., Washenfelder, R. A., Keppel-Aleks, G., Wunch, D., Yavin, Y., Allen N. T., Blavier, J.-F., Jiménez R., Daube, B. C., Bright, A. V., Matross, D. M., Wofsy, S. C., and Park, S.: Total column CO2 measurements at Darwin, Australia-site description and calibration against in situ aircraft profiles, Atmos. Meas. Tech., 3, 947-958, doi:10.5194/amt-3-947-2010, 2010.

Frankenberg, C., Pollock, R., Lee, R. A. M., Rosenberg, R., Blavier, J.-F., Crisp, D., O'Dell C. W., Osterman, G. B., Roehl, C., Wennberg, P. O., and Wunch, D.: The Orbiting Carbon Observatory (OCO-2): spectrometer performance evaluation using pre-launch direct sun measurements. Atmospheric Measurement Techniques, 8(1), 301–313. doi:10.5194/amt-8-301-2015, 2015.

Geibel, M. C., Gerbig, C., and Feist, D. G.: A new fully automated FTIR system for total column measurements of greenhouse gases, Atmospheric Measurement Techniques, 3(5), 1363-1375, doi:10.5194/amt-3-1363-2010, 2010.

Hase, F., Blumenstock, T., and Paton-Walsh, C.: Analysis of the instrumental line shape of high resolution Fourier transform IR spectrometers with gas cell measurements and new retrieval software, Appl. Optics, 38, 3417–3422, doi:10.1364/AO.38.003417,1999.

Hase, F., Drouin, B. J., Roehl C. M., Toon, G. C., Wennberg, P. O., Wunch, D., Blumenstock, T., Desmet F., Feist, D. G., Heikkinen, P., De Mazière, M., Rettinger, M., Robinson, J., Schneider, M., Sherlock, V., Sussmann, R., Té Y., Warneke, T., and Weinzierl, C.: Calibration of sealed HCl cells used for TCCON instrumental line shape monitoring, Atmospheric Measurement Techniques, 6(12), 3527–3537, doi:10.5194/amt-6-3527-2013, 2013.

Kiel, M., Wunch, D., Wennberg, P. O., Toon, G. C., Hase, F., and Blumenstock, T.: Improved retrieval of gas abundances from near-infrared solar FTIR spectra measured at the Karlsruhe TCCON station, Atmos. Meas. Tech., 9(2), 669–682, doi:10.5194/amt-9-669-2016, 2016.

Kivi, R. and Heikkinen, P.: Fourier transform spectrometer measurements of column CO2 at Sodankylä, Finland, Geosci. Instrum. Method. Data Syst., 5, 271–279, 2016.

Messerschmidt, J., Macatangay, R., Notholt, J., Petri C., Warneke, T., and Weinzierl, C.: Side by side measurements of CO2 by ground-based Fourier transform spectrometry (FTS), Tellus B, 62(5), 749-758, doi:10.1111/j.1600-0889.2010.00491.x., 2010.

Messerschmidt, J., H. Chen, N. M. Deutscher, C. Gerbig, P. Grupe, K. Katrynski, F.-T. Koch, J. V. Lavrič, J. Notholt, C. Rödenbeck, W. Ruhe, T. Warneke, and Weinzierl, C.: Automated ground-based remote sensing measurements of greenhouse gases at the Białystok site in comparison with collocated in situ measurements and model data, Atmospheric Chemistry and Physics, 12(15), 6741–6755, doi:10.5194/acp-12-6741-2012, 2012.

Miao, R., Lu N., Yao L., Zhu, Y., Wang, J., and Sun, J.: Multi-Year Comparison of Carbon Dioxide from Satellite Data with Ground-Based FTS Measurements (2003–2011), Remote Sensing, 5(7), 3431–3456, doi:10.3390/rs5073431, 2013.

Miller, C. E., Crisp, D. DeCola, P. L., Olsen, S. C., Randerson, J. T., Michalak, A. M., Alkhaled, A., Rayner, P., Jacob, D. J., Suntharalingam, P., Jones, D. B. A., Denning, A. S., Nicholls, M. E., Doney, S. C., Pawson, S., Boesch, H., Connor B. J., Fung I. Y., O'Brien, D., Salawitch, R. J., Sander, S. P., Sen, B., Tans, P., Toon, G. C., Wennberg, P. O., Wofsy, S. C., Yung, Y. L., and Law, R. M.: Precision requirements for space-based XCO2 data, J. Geophys. Res-Atmos., 109, D02301, doi: 10.1029/2006JD007659, 2007.

Morino, I., Uchino, O., Inoue, M., Yoshida, Y., Yokota T., Wennberg, P. O., Toon, G. C., Wunch, D., Roehl, C. M., Notholt, J., Warneke, T., Messerschmidt, J., Griffith, D. W. T., Deutscher, N. M., Sherlock, V., Connor, B. J., Robinson, J., Sussmann, R., and Rettinger, M.: Preliminary validation of column-averaged volume mixing ratios of carbon dioxide and methane retrieved from GOSAT short-wavelength infrared spectra, Atmospheric Measurement Techniques, 4(6), 1061-1076, doi:10.5194/amt-4-1061-2011, 2011.

O'Dell, C. W., Connor, B., Bösch, H., O'Brien, D., Frankenberg C., Castano, R., Christi, M., Eldering, D., Fisher, B., Gunson, M., McDuffie, J., Miller, C. E., Natraj, V., Oyafuso, F., Polonsky, I., Smyth, M., Taylor, T., Toon, G. C., Wennberg, P. O., and Wunch, D.: The ACOS CO2 retrieval algorithm – Part 1: Description and validation against synthetic observations, Atmospheric Measurement Techniques, 5, 99–121, doi: 10.5194/amt-5-99-2012, http://www.atmos-meas-tech.net/5/99/2012/, 2012.

Ohyama, H., Morino, I., Nagahama, T., Machida, T., Suto H., Oguma, H., Sawa, Y., Matsueda, H., Sugimoto, N., Nakane, H., and Nakagawa, K.: Column-averaged volume mixing ratio of CO2 measured with ground-based Fourier transform spectrometer at Tsukuba, J. Geophys. Res., 114, D18303 doi:10.1029/2008JD011465, 2009.

Ohyama, H., Kawakami, S., Tanaka, T., Morino, Uchino, I., O., Inoue, M., Sakai, T., Nagai, T., Yamazaki, A., Uchiyama, A., Fukamachi, T., Sakashita, M., Kawasaki, T., Akaho, T., Arai, K., and Okumura, H.: Observations of XCO2 and XCH4 with ground-based high-resolution FTS at Saga, Japan, and comparisons with GOSAT products, Atmos. Meas. Tech., 8(12), 5263–5276, doi:10.5194/amt-8-5263-2015.

Schneising O., Buchwitz M., Burrows J. P., Bovensmann H., Reuter M., Notholt J., Macatangay R., and Warneke T.: Three years of greenhouse gas column-averaged dry air mole fractions retrieved from satellite-Part 1: Carbon dioxide, Atmos. Chem. Phys., 8, 3827-3853, 2008.

Rayner P. J., and O'Brien D. M.: The utility of remotely sensed CO2 concentration data in surface source inversions, Geophys. Res. Lett., 28, 175–178, doi: 10.1029/2000GL011912, 2001.

Rothman et al. (2013). The HITRAN 2012 Molecular Spectroscopic Database, J. Quant. Spectrosc. Ra., Elsevier, ISSN 0022-4073.

Washenfelder R. A., Toon G. C., Blavier J-F., Yang Z., Allen N. T., Wennberg P. O., Vay S. A., Matross D. M., and Daube B. C.: Carbon dioxide column abundances at the Wisconsin Tall Tower site, Journal of Geophysical Research, 2006, 111, doi:10.1029/2006JD00715, 2000.
Warneke, T., Yang, Z., Olsen, S., Korner, S., Notholt J., Toon, G. C., Velazco, V., Schultz, A., and Schrems, O.: Seasonal and latitudinal variations of column averaged volume-mixing ratios of atmospheric CO2, Geophysical Research Letters, 32(3), 2-5, doi:10.1029/2004GL021597, 2005.

Wunch, D., Toon G. C., Wennberg, P. O., Wofsy, S. C., Stephens, B., Fisher, M. L., Uchino O., Abshire, J. B., Bernath, P. F., Biraud, S. C., Blavier J.-F. L., Boone, C. D., Bowman, K. P., Browell, E. V., Campos, T., Connor, B. J., Daube, B. C., Deutscher, N. M., Diao M., Elkins J. W., Gerbig C., Gottlieb E., Griffith, D. W. T., Hurst, D. F., Jiménez, R., Keppel-Aleks G., Kort E. A., Macatangay R., Machida T., Matsueda, H., Moore F. L., Morino I., Park S., Robinson J., Roehl C. M., Sawa Y., Sherlock V., Sweeney C., Tanaka T., and Zondlo M. A.: Calibration of the Total Carbon Column Observing Network using aircraft profile data, Atmospheric Measurement Techniques, 3(5), 1351-1362, doi:10.5194/amt-3-1351-2010.

Wunch, D., Toon, G. C., Blavier, J.-F. L., Washenfelder, R. A., Notholt, J., Connor, B. J., Griffith, D. W. T., Sherlock V., and Wennberg P. O.: The Total Carbon Column Observing Network, Philos. T. R. Soc. A, 369, 2087–2112, doi:10.1098/rsta.2010.0240, 2011.

Wunch, D., Toon G. C., Sherlock V., Deutscher N. M., Liu X., Feist D. G., and Wennberg P. O.: The Total Carbon Column Observing Network's GGG2014 Data Version. doi:10.14291/tccon.ggg2014.documentation.R0/1221662, 2015.

Wunch, D., Wennberg, P.O.,, Osterman, G., Fisher, B.,Naylor, B.,, Roehl, C. M., O'Dell, C., Mandrake, L.,Viatte, C., Griffith, D. W. T., Deutscher, N. M., Velazco, V. A., Notholt, J.,Warneke, T.,Petri, C., Maziere, M. De, Sha, M. K., Sussmann,R., Rettinger, M., Pollard, D., Robinson, J.,Morino, I., Uchino O.,Hase, F., Blumenstock, T., Kiel, M., Feist, D. G., Arnold S.G., Strong, K., Mendonca, J., Kivi, R.,Heikkinen, P., Iraci, L., Podolske, J., Hillyard, P. W., Kawakami, S., Dubey, M. K., Parker, H. A., Sepulveda, E., Rodriguez, O. E. G., Te, Y., Jeseck, P., Gunson, M. R., Crisp, D., and Eldering A., Comparisons of the Orbiting Carbon Observatory-2 (OCO-2) XCO2 measurements with TCCON, Atmos. Meas. Tech. Discuss., doi:10.5194/amt-2016-227, 2016.

Youwen, S., Mathias, P., Christine, W., Christof, P., Justus, N., Yuting, W., and Cheng, L., Technical note: Sensitivity of instrumental line shape monitoring for the ground-based high-resolution FTIR spectrometer with respect to different optical attenuators, Atmos. Meas. Tech. Discuss., doi:10.5194/amt-10-989- 2017.

Response to interactive comment of Referee on "Interactive comment on "Characteristics of the Greenhouse Gas Concentration Derived from the Ground-based FTS Spectra at Anmyeondo, Korea" by Young-Suk Oh et al.

Anonymous (Referee 2)

Received and published: 14 August 2017

"Interactive comment on "Characteristics of the Greenhouse Gas Concentration Derived from the Ground-based FTS Spectra at Anmyeondo, Korea" by Young-Suk Oh et al.

General comments:

First of all, we would like to strongly appreciate referee's very constructive and valuable comments, suggestions, and feedbacks on the manuscript. On the basis of this, we have tried to address all the issues raised on this manuscript. We have discussed the feature of OASIS system and its performance in a detail manner in the revised manuscript. We have included other TCCON site data for comparison purpose, and also added some species such as CO, and CH_4 derived from Anmyeondo FTS instrument.

Comments:

Section 2.2: What exactly does "operation is semi-automated" mean and how does it affect e.g. the number of measurements as opposed to fully automated like many other TCCON instruments?

Response: The FTS instrument is operated in semi-automated, which mean that some systems are operated by manual (someone should be there for controlling certain systems). However, this mode of operation does not affect the measurements.

Section 2.3: OASIS

I think this is the most interesting technical part of this TCCON site but the description and analysis is not thorough enough. Especially, I miss a detailed discussion of the pros and cons of a system like OASIS. For example: what is the dynamic range of OASIS?

Response: We tried to elaborate regarding Operational Automatic System for the Intensity of Sunray (OASIS) system to some extent in section 2.3, which may not be sufficient to get in-depth information about it. We planned to address all issues like the pros and cons of this system on the measurements, as well as other technical details based on sufficient experiments on a special issue.
(*The OASIS part was decided to write a separate paper on TCCON.)

How large is the quality difference of clear-sky spectra with OASIS compared to without? - In the example in Fig. 5, why is the signal with OASIS lower than without?

Response: In this particular example, the spectra were taken with and without OASIS April 04, 2015 (starting time in the case of without OASIS was 06:12:03 and ending time 08:46:40 while the starting time in the case of OASIS was 04:31:00 and approximately ending time 05:40:00). The solar intensity differences are occurred due to measurement time differences. Unfortunately, we did not conduct experiment in assessment of the quality of spectra measured with and without OASIS during clear sky condition. In next work, this will be examined. (*The OASIS part was decided to write a separate paper on TCCON.)

Does the better stability with OASIS compensate the loss in intensity and hence in signal-to noise?

Response: Yes, it would improve well the stability and signal-to-noise ratio of the spectra. (*The OASIS part was decided to write a separate paper on TCCON.)

do you log what OASIS is doing? Can you still distinguish between observations with truly clear sky and such with thin clouds or other intensity fluctuations? May be some would better be dropped rather than compensated. Is a system like OASIS worth the effort? How many more spectra do you get compared to the TCCON approach of dropping ones with SIV>5%?

Response: Yes, this OASIS system controls the aperture size based on the external sun light intensity. In the meantime, we do not have clear idea to distinguish observations with truly clear sky and such with thin clouds since we did not perform experiments. We obtained around 1230 number of spectra more as compared to TCCON approach of dropping ones with SIV > 5%. It is required further effort to briefly explain the impact of the OASIS system on the measurements. (*The OASIS part was decided to write a separate paper on TCCON.)

In Fig. 5, it looks like there were only a few events with strong drops in intensity. And I wonder if they could actually be corrected by OASIS. Certainly, a thick cloud moving in from of the sun cannot be compensated. How does OASIS affect the pointing accuracy of your solar tracker?

Response: Yes surely, a thick cloud moving in from of the sun cannot be compensated. (*The OASIS part was decided to write a separate paper on TCCON.)

Section 2.4:
This whole subsection only describes standard TCCON retrieval procedure without any obvious site-specific adaptions. I think the whole subsection can be left out and be replaced by a single sentence and a reference to Wunch et al. 2015.

Response: We have removed the unnecessary part of Section 2.4 retrieval methodology, and modified this section; please see section 2.5 Data processing in revised manuscript.

Section 3.1:
- you should explain a little better what X_{air} is and how it can be used as an indicator of stability. what are the plots in Fig. 8 showing? Obviously not single retrievals! Are these daily means or medians or something else?

Response: The X_{air} would be unity for an ideal retrieval, however, due to spectroscopic limitations there is a TCCON wide bias and solar zenith angle (SZA) dependence. The X_{air} is a useful indicator of the quality of measurements, with retrievals deviating more than 1% from the nominal value of 0.98 demonstrating systematic error. Initially, Fig. 8 showed the time series of X_{air}, surface pressure, and column amounts of O_2 and CO_2 in daily means in the period between February 2014 and December 2015, but we have re-plotted this figure again, where we considered only X_{air} and others are excluded.

- Plotting and discussing CO_2 and O_2 separately here is a poor choice. The whole idea behind TCCON is to remove airmass-related effects to produce high-precision observations. What we see here is simply the change in airmass probably due to the seasonal change of the sun's position in the sky (and a small part from ground pressure changes). All carbon-cycle related effects are completely hidden by this effect.

Response: We appreciate this very nice comment. We understood that discussing CO_2 and O_2 separately is not relevant so that we removed this discussion part.

Section 3.2:
- I don't understand the argument about the comparison between g-b FTS and OCO-2. A priori profiles and averaging kernels are available for both observations. What CO_2 profile do you mean with "... since we do not have the CO_2 profile that reflects the actual variability over the measurement site."?

Response: We have improved the arguments about the comparison between g-b FTS and OCO-2. Please see the discussion in section 3.4 in revised manuscript.

Section 3.3:
- Is this really all you can see: XCO_2 variability because of photosynthesis? Are there no in-situ observations nearby so one could separate CO_2 in the Planetary Boundary Layer (PBL) from CO_2 in the free troposphere or at least look for differences in PBL and total column?

Response: We strongly appreciate the comment. We included the in-situ tower observation data and compared the seasonal cycle of CO_2 with g-b FTS XCO_2. The seasonal cycle of FTS XCO_2 followed nearly same pattern as that of in-situ observations, this would suggest that seasonal cycle of CO_2 is most likely controlled by the imbalance of terrestrial ecosystem exchange, even though it is required further work to examine other effect like the role of transport. Please see section 3.1 in revised manuscript.

- Especially in this section, the other observed species like CH_4, CO, and N_2O might have been really useful. I doubt that all you can see at your site are local effects and maybe some seasonal background variation. There must be transport from other regions which would probably show up in CH_4 or CO.

Response: In addition of XCO_2, we have also considered other species such as XCO and XCH_4. The XCO_2 along with the retrievals of XCO and XCH_4 obtained from g-b FTS spectra are presented in Figure 8 (panel a-c), in the time period of February 2014–December 2016. (Please see section 3.1). Furthermore, we have discussed the relation between XCO and XCO_2 at our site, which is presented in section 3.2 in revised manuscript.

Minor corrections:

- please make sure that all acronyms and abbreviations (liek "g-b") are defined in the main text, even if they have been defined in the abstract already.

Response: We corrected and checked all acronyms and abbreviations throughout the text in the manuscript.

- p. 1, l. 31: "G-b FTS" is not a very good choice for a keyword. Neither is "OASIS" as it is not a unique term and also not a well-established acronym (yet).

Response: We have removed "G-b FTS" and "OASIS" as key words.
(*The OASIS part was decided to write a separate paper on TCCON.)

- p. 2, l. 15: "TCCON achieves the accuracy and precision in measuring the total column of CO2 ..." -> TCON achieves this precision and accuracy for the column averaged dry air mole fraction of CO2 (XCO_2), not for the total column!

Response: We have corrected as "TCCON achieves the accuracy and precision in measuring the column averaged dry air mole fraction of CO_2 about 0.25 %..........."

- p. 2, l. 12: you mention "several atmospheric GHGs" but you neither say which nor discuss them in any way in this manuscript. Why?

Response: It is very nice comment. We described the GHGs that have been measured with our instruments at Anmyeondo site. Those prominent GHGs are CO_2, CH_4, CO, N_2O, and H_2O. We included CH_4 and CO results obtained from g-b FTS and discussed.

- p. 2, l. 25: "a new home made OASIS system" sounds as if "OASIS" was an established acronym. It is not, it is just your internal name for your device. It might also be better to define the acronym OASIS in the main text rather than in the abstract. My suggestion for the sentence would be "One of the interesting issues in this work is a new home made addition to our g-b FTS instrument (see Sect. 2.3) that reduces the solar intensity variations from the 5% maximum allowed in TCCON to less than 2%."

Response: Thanks to the comment. We have defined the acronym OASIS in the main text as well. We have replaced the previous sentence written in Sect. 2.3 by "One of the interesting issues in

this work is a new home made addition to our g-b FTS instrument (see Sect. 2.3) that reduces the solar intensity variations from the 5% maximum allowed in TCCON to less than 2%."
(*The OASIS part was decided to write a separate paper on TCCON.)

- p. 2, l. 25: "SIV" instead of "SVI"! In fact, you don’t need this acronym at all. It is TCCON jargon and only used three times in the whole manuscript (and you spelled it out each time!).

Response: We made correction “SVI” by “SIV”.

- p. 2, l. 27-28: there is no need to provide an outline of the sections and numbers. Scientific papers typically don’t have a table of contents. Just drop these two lines.

Response: We improved it. Please see the last paragraph of the introduction section in revised manuscript.

- p. 3, l- 3: Please replace "G-b" with "g-b" throughout the text unless it starts a sentence.

Response: We corrected it.

- p. 3, l. 5: "... Seoul, the capital city of Korea." -> I don’t want get into politics here but isn’t the country officially named "Republic of Korea"? "South Korea" would probably also be clear, maybe even clearer to the general reader.

Response: Thanks for the comment. The country official name is "Republic of Korea". We corrected the sentence “… Seoul, the capital city of Republic of Korea.”

- p. 3, l. 22-23: avoid the line break for "A 547". In fact, I believe the tracker model number is "A547" (w/o space).

Response: Replaced "A 547" by "A547".

- p. 3, l. 23: "... are about 0_ to 315_ and 10_ to 85_ degrees ..." -> (1) "_" and "degrees" are redundant, (2) is the elevation range really only 10 to 85 degrees? Does that mean the tracker cannot point to the horizon or zenith at all?

Response: We removed the redundant of "_" and "degrees" from the text. The tracker can point to the horizon and zenith as well.

- p. 4, l. 3: "oil-free" -> "vacuum pump" is missing. Is the pump running continuously?

Response: The vacuum pump is running continuously.

- p. 5, l. 9: "... voltage ranges of approximately 0 to 219 mV." This information is hardly useful for anyone outside your department. Especially since you claim that "... the detail characteristic of the operation is beyond the scope of this paper."

Response: We omitted "…voltage ranges of approximately 0 to 219 mV…." from the text, since the detail characteristic of the operation is beyond the scope of this paper.

- p. 5, l. 13-14: "the intensity of the incoming light occurred due to changes in thin clouds and aerosols loads or interceptions by any other objects along the line of sight over the measurement site." -> thin clouds is clear but aerosol load should not really change during a 2-minute measurement. And what objects could be passing the line of sight often enough to justify such a system?

Response: We understood that this sentence "…interceptions by any other objects along the line of…." is irrelevant so that we omitted the sentence "…interceptions by any other objects …." in the text.

- p. 6, l. 13: GGG is not developed "by JPL" even though the main developer works there. But there are also other main developers who work at different institutions even outside Caltec/JPL. It would be correct to say that GGG is developed by the TCCON community.

Response: We thank the referee's comments. We corrected it accordingly.

- p. 8, l. 9: "LINFIT" -> "LINEFIT"!
Response: Corrected "LINFIT" by "LINEFIT"

Figures
Response: All figures have been replaced. Data analysis period and quality improved.

- Fig. 1: (1) picture quality is not very good, (2) country borders and maybe the location of Seoul would be helpful, (3) For the insets: the upper one is clear but what is the lower one? The labels are Korean only.

- Fig. 2: (1) "server" instead of "sever", (2) you used "solar tracker" throughout the text, so you should not use "sun tracker" in the figure, (3) "Photographs of the automated FTS laboratory."

- Fig. 3: how is signal-to-noise defined here?

- Fig. 4: low quality/resolution

- Fig. 5: (1) low quality/resolution, (2) is this the same day for both plots? (3) why does signal drop off to the right with OASIS even though start time is earlier? (3) better plot this over solar zenith angle than over time!

- Fig. 6: very low quality with obvious JPEG compression artifacts. This should be redone in a lossless compression format like PNG or a vector format like PDF!

- Fig. 7: (1) not referenced in the text at all! (2) Should probably belong to Sec. 2.4 which means it should appear before (!) Fig. 6. (3) I don't know why this Figure is even part of the manuscript.

Is this an original figure created by the authors or taken from somewhere else? (4) similar quality problem as with the other figures. The box labels are basically unreadable.

- Fig. 8: (1) low quality/resolution (2) why not just plot XCO2? The variations in column are mostly due to seasonal airmass variation (as can be seen in O2 column). XCO2 would tell you something about carbon-cycle related effects at your site!

- Fig. 9: unlike the other figures, this one has acceptable quality. I would still suggest to plot daily medians instead of means.

Second referee revision

Characteristics of the Greenhouse Gas Concentration Derived from the Ground-based FTS Spectra at Anmyeondo, Korea

Young-Suk Oh[1,2*], Samuel Takele Kenea[1], Tae-Young Goo[1], Gawon Kim[1], Kyu-Sun Chung[2], David W. T. Griffith[3], Voltaire A. Velazco[3], Jae-Sang Rhee[1], Me-Lim Oh[4], Haeyoung Lee[4], and Young-Hwa Byun[1]

1. Climate Research Division, National Institute of Meteorological Sciences (NIMS), Jeju-do, Korea
2. Department of Electrical Eng. & Centre for Edge Plasma Science, Hanyang University, Seoul, Korea
3. School of Chemistry, University of Wollongong, Wollongong, Australia
4. Climate Change Monitoring Division, Korea Meteorological Administration, Seoul, Korea

*Correspondence to: Young-Suk Oh (ysoh306@korea.com)

Abstract. Since the late 1990s, the meteorological observatory established in Anmyeondo (36.5382˚ N, 126.3311˚ E, and 30 m above mean sea level), has been monitoring several greenhouse gases such as CO_2, CH_4, N_2O, CFCs, and SF_6, as part of the Global Atmosphere Watch (GAW) Program. A high resolution ground-based (g-b) Fourier Transform Spectrometer (FTS, IFS-125HR model) was installed at such observation site in 2013, and has been fully operated within the frame work of the Total Carbon Column Observing Network (TCCON) since August, 2014. The solar spectra recorded by the g-b FTS are covered in the range between 3,800 and 16,000 cm^{-1} at the spectral resolution of 0.02 cm^{-1} during the measurement period between 2013 and 2016. In this work, the GGG2014 version of the TCCON standard retrieval algorithm was used to retrieve XCO_2 concentrations from the FTS spectra. Two spectral bands (at 6220.0 and 6339.5 cm^{-1} centre wavenumbers) were used to derive the XCO_2 concentration within the spectral residual of +0.01 %. All sources of errors were thoroughly analyzed. In this paper, we introduced a new home made OASIS (Operational Automatic System for Intensity of Sunray) system to our g-b FTS instrument and that allows reducing the solar intensity variations (SIV) below 2 %. A comparison of the XCO_2 concentration in g-b FTS and OCO-2 (Orbiting Carbon Observatory) satellite observations were presented only for the measurement period between 2014 and 2015. Nine coincident observations were selected on a daily mean basis. It was obtained that OCO-2 exhibited low bias with respect to the g-b FTS, which is about -0.065 ppm with the standard deviation of 1.66 ppm, and revealed a strong correlation (R=0.85). Based on seasonal cycle comparisons, both instruments generally agreed in capturing seasonal variations of the target species with its maximum and minimum values in spring and late summer, respectively.

In the future, it is planned to exert further works in utilizing the FTS measurements for the evaluation of satellite observations such as Greenhouse Gases Observing Satellite (GOSAT) at observation sites. This is the first report of the g-b FTS observations of XCO_2 species over the Anmyeondo station.

Key words: XCO_2, GOSAT, TCCON, Infrared spectra

1 Introduction

Monitoring of greenhouse gases (GHGs) is a crucial issue in the context of the global climate change. Carbon dioxide (CO_2) is one of the key greenhouse gas and its global annual mean concentration has been increased rapidly from 278 to 400 ppm since 1750, pre-industrial year (WMO greenhouse gas bulletin, 2016). Radiative forcing of atmospheric CO_2 accounts for approximately 65 % of the total radiative forcing by long-lived GHGs (Ohyama et al., 2015 and reference therein). Human activities, such as burning of fossil fuels, land use change, etc., are the primary drivers of the continuing increase in atmospheric greenhouse gases and the gases involved in their chemical production (Kiel et al., 2016 and reference therein), In the fact that it is a global concern for demanding accurate and precise long-term measurements of greenhouse gases.

In the field of remote sensing techniques, solar absorption infrared spectroscopy is an essential technique, which has been increasingly used to determine changes in atmospheric constituents. Nowadays, a number of instruments deployed in various platforms (e.g., ground-based, space-borne) have been operated for measuring GHGs such as CO_2. Our g-b FTS at the Anmyeondo station has been measuring several atmospheric GHGs such as CO_2, CH_4, CO, N_2O, and H_2O operated within the framework of the Total Carbon Column Observing Network (TCCON). XCO_2

retrievals from the g-b FTS have been reported at different TCCON sites (e.g, Ohyama et al., 2009; Deutscher et al., 2010; Messerschmidt et al., 2010, 2012; Miao et al., 2013; Kivi and Heikkinen, 2016). TCCON achieves the accuracy and precision in measuring the column averaged dry air mole fraction of CO_2 (XCO_2), as about 0.25 % that is less than 1 ppm (Wunch et al., 2010), which is essential to get information about sinks and sources, as well as validating satellite products (Rayner and O'Brien, 2001; Miller et al., 2007). It is reported that the precision of CO_2 even 0.1 % can be achieved during clear sky conditions (Messerschmidt et al., 2010; Deutscher et al., 2010). The network aims to improve global carbon cycle studies and to supply the primary validation data of different atmospheric trace gases derived from space-based instruments, e.g., the Orbiting Carbon Observatory 2 (OCO-2), the Greenhouse Gases Observing Satellite (GOSAT) (Frankenberg et al., 2015; Morino et al., 2011).

The objective of this study is focused on the characteristics of XCO_2 concentration retrievals from g-b FTS spectra and is to implement a preliminary comparison against OCO-2 over the Anmyeondo station. The FTS spectra have been processed using the TCCON standard GGG2014 (Wunch et al., 2015) retrieval software. One of the interesting issues in this work is a new home made addition to our g-b FTS instrument that reduces the solar intensity variations from the 5% maximum allowed in TCCON to less than 2%. This paper is organized as follows: Sect. 2 introduces instrumentations and measurement site descriptions. Sect. 3 represents results and discussion. The conclusion is given in Sect. 4.

2 Site and instrumentation

2.1 Site description

The G-b FTS observatory was established in the Anmyeondo (AMY) station, which is located at 36.32˚ N, 126.19˚ E, and 30 m above sea level. This station is situated on the west coast of the Korean Peninsula, which is 180 kilometre away from Seoul, the capital city of Republic of Korea. Figure 1 displays the Anmyeondo station. It is also a regional GAW (Global Atmosphere Watch) station that belongs to the Climate Change Monitoring Network of KMA (Korean Meteorological Administration). The AMY station has been monitoring various atmospheric compositions such as greenhouse gases, aerosols, ultraviolet radiation, ozone, and precipitation since 1999. The total area of Anmyeondo is estimated to be ~87.96 km^2 and approximately 1.25 million people reside in this island. Some of the residents over this area are engaged in agricultural activities. The topographic feature of the area consists of low level hills, on average it is about 100 m above sea level. The climatic condition of the area is: the minimum temperature is occurred on winter season with an average of 2.7 ˚C, and the maximum temperature is about 25.6 ˚C during summer season. In addition, the annual precipitation amount is estimated to be 1,155 mm; and the high amount of snows would be observed in winter. Such observation site has been designated as part of TCCON site since August 2014. The AMY site's on TCCON wiki page is kept available and can be found at: https://tccon-wiki.Anmyeondo.edu/Sites/Anmyeondo.

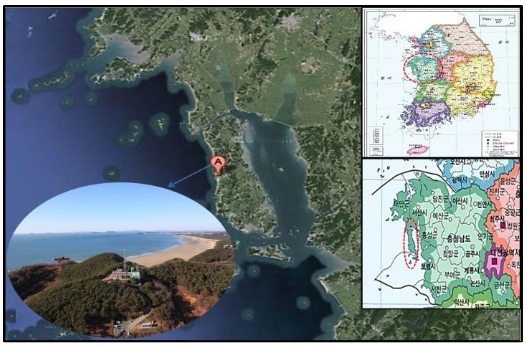

Figure 10: Anmyeondo (AMY) station

- Fig. 1: (1) picture quality is not very good, (2) country borders and maybe the location of Seoul would be helpful, (3) For the insets: the upper one is clear but what is the lower one? The labels are Korean only.

2.2 G-b FTS instrument

Solar spectra are acquired by operating a Bruker IFS 125HR spectrometer (Bruker Optics, Germany) under the framework of TCCON. Currently, our g-b FTS instrument operation is semi-automated for taking the routine measurements under clear sky conditions. It is planned to make an FTS operation mode to be fully automated by this year. The solar tracker (Tracker A547, BrukerOptics, Germany) is mounted inside a dome. The tracking ranges in terms of both azimuthal and elevation angles are about 0 to 315 and 10 to 85 degrees, respectively, while the tracking speed is about 2 degrees per second. The tracking accuracy of ±4 minutes of arc can be achieved by the Camtracker mode. Under clear sky conditions, the dome is opened and set to an automatic-turning mode, so that the mirrors are moved automatically to search for the position where the sunspot is seen by the camera. Then, the solar tracker is activated in such a way that the mirrors are finely and continuously controlled to fix the beam into the spectrometer. Figure 2 displays an overview of the general data acquisition system. This ensures that all spectra were recorded under clear weather conditions. The other important feature that has been made on the FTS spectrometer is the implementation of the interferogram sampling method (Brault, 1996), that takes advantage of modern analog-digital converters (ADCs) to improve the signal-to-noise ratio.

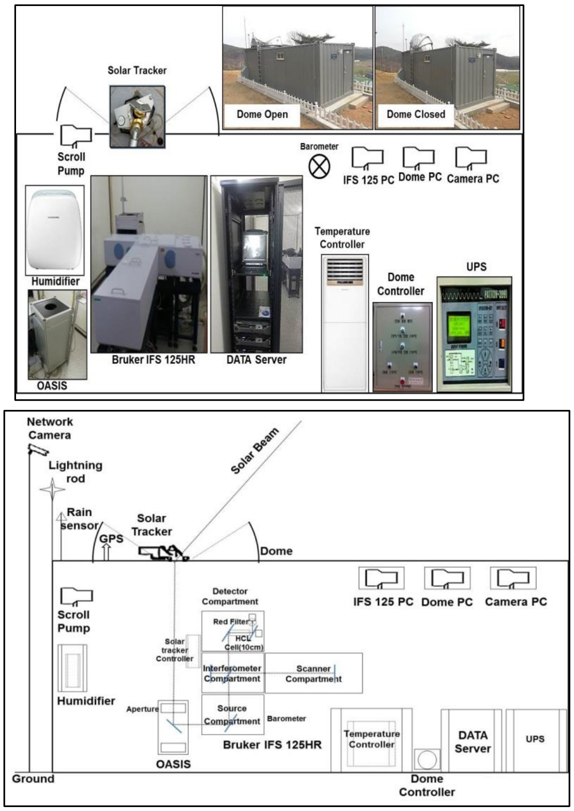

Figure 11: Photographs of the automated FTS laboratory. The Bruker Solar Tracker type A547 is mounted in the custom made dome. A servo controlled solar tracker directs the solar beam through a CaF_2 window to the FTS (125HR) in the laboratory. The server computer is used for data acquisition. PC1, PC2 and PC3 are used for controlling the spectrometer, solar tracker, dome, camera, pump, GPS satellite time, and humidity sensor.

- Fig. 2: (1) "server" instead of "sever", (2) you used "solar tracker" throughout the text, so you should not use "sun tracker" in the figure, (3) "Photographs of the automated FTS laboratory."

The spectrometer has equipped with two room temperature detectors; an Indium-Gallium-Arsenide (InGaAs) detector, which covers the spectral region from 3,800 to 12,800 cm^{-1}, and a Silicon (Si) diode detector (9,000 – 25,000 cm^{-1}) used in a dual-acquisition mode with a dichroic optic (Omega Optical, 10,000 cm^{-1} cut-on). A filter (Oriel Instruments 59523; 15,500 cm^{-1} cut-on) prior to the Si diode detector blocks visible light, which would otherwise be aliased into a near-infrared spectral domain. TCCON measurements are routinely recorded at a maximum optical path difference (OPD_{max}) of 45 cm leading to a spectral resolution of 0.02 cm^{-1}. Two scans, one forward and one backward, are performed and individual interferograms are recorded. A single scan in one measurement takes about 110 s. The pressure inside FTS is kept at 0.1 to 0.2 hPa with vacuum pump to maintain the stability of the system and to ensure clean and dry conditions.

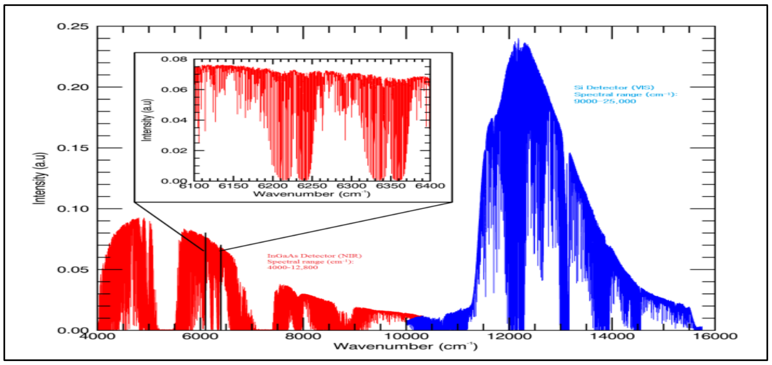

Figure 12: Single spectrum recorded on 4 October 2014 with a resolution of 0.02 cm^{-1}. A typical example for the spectrum of XCO_2 is shown in the inset.

Table 6. Measurement setting for the Anmyeondo g-b FTS spectrometer of the Bruker 125HR model

Item	Setting
Aperture	0.8 mm
Detectors	RT-Si Diode DC, RT-InGaAs DC
Beamsplitters	CaF_2
Scanner velocity	10 kHz
Low pass filter	10 kHz
High folding limit	15798.007031
Spectral Resolution	0.02 cm^{-1}
Optical path difference	45 cm
Acquisition mode	Single sided, forward-backward
Sample scan	2 scans
Sample scan time	~110 s

2.3 Operational Automatic System for the Intensity of Sunray (OASIS)

The OASIS system is developed for improving the quality of the spectra recorded by the spectrometer. To ensure the quality of the spectra, this system is beneficial for minimizing the noise that induced in the spectra due to rapid intensity fluctuations of the incoming solar radiation that reaches to the instrument. The main function of the OASIS is to control the aperture diameter of inlet through which the incoming radiation goes to the interferometer. This aperture is placed inside the OASIS system, which is different from the actual aperture that is located inside the interferometer compartment. The aperture size varies in the range of 26 to

32 mm with respect to the photon sensor signals at the OASIS system. Figure 4 depicts the schematic views of the OASIS systems. As can be seen in the figure, the basic components of the OASIS system such as photoelectric sensor, stepping motor, and sunray controller are shown clearly. In fact, the detail characteristic of the operation is beyond the scope of this paper. The fundamental purpose of this system is to optimize the measurement of solar spectra by reducing the effect of the fluctuations (sudden drops) of the intensity of the incoming light occurred due to changes in thin clouds along the line of sight over the measurement site. The maximum threshold value of the solar intensity variation (SIV) is 5 % that is the TCCON standard value (Ohyama et al., 2015). Therefore, we have reduced this value to 2 % in our case by introducing a new home made OASIS system to our g-b FTS since December 2014. This allows us to ensure for having high quality spectra from the instrument. In this work, we have used this quality criterion to screen out the quality of the spectra. Figure 5 illustrates an example, taken on date 4 April 2015, on variations in levels of intensity with and without equipped the OASIS system to the g-b FTS instrument. It is clearly seen that the large amplitude of the solar intensity variation is filtered in the spectra. Note that the solar intensity difference was exhibited as can be seen in the figure, which was due to the measurement time difference.

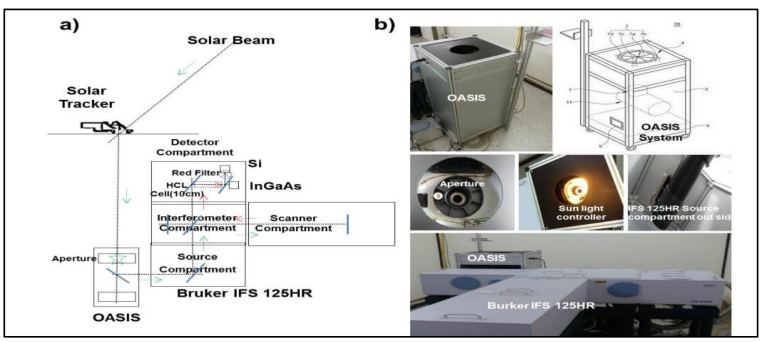

Figure 13: a) Shows the configuration of installed equipment and the path of solar beam and (b) Schematic views of the OASIS system.

- Fig. 4: low quality/resolution

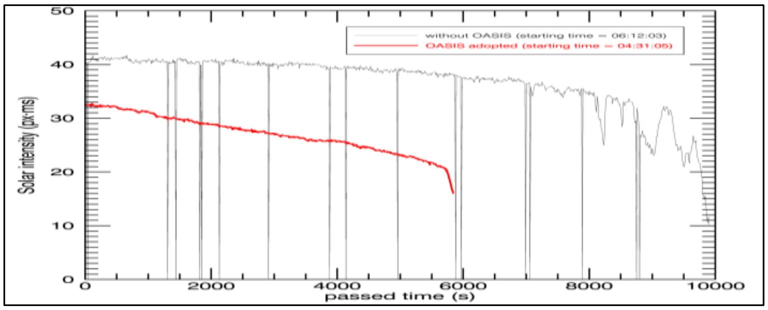

Figure 14: Typical example for solar intensity versus time with and without OASIS is given. (Taken on 04 April, 2015)

- Fig. 5: (1) low quality/resolution, (2) is this the same day for both plots? (3) why does signal drop off to the right with OASIS even though start time is earlier? (3) better plot this over solar zenith angle than over time!

Table 2. Spectral windows used for the retrievals of the columns of CO_2 and O_2.

Gas	Center of spectral window (cm^{-1})	Width (cm^{-1})	Interfering gas
O_2	7885.0	240.0	H_2O, HF, CO_2
CO_2	6220.0	80.0	H_2O ,HDO, CH_4
CO_2	6339.5	85.0	H_2O ,HDO

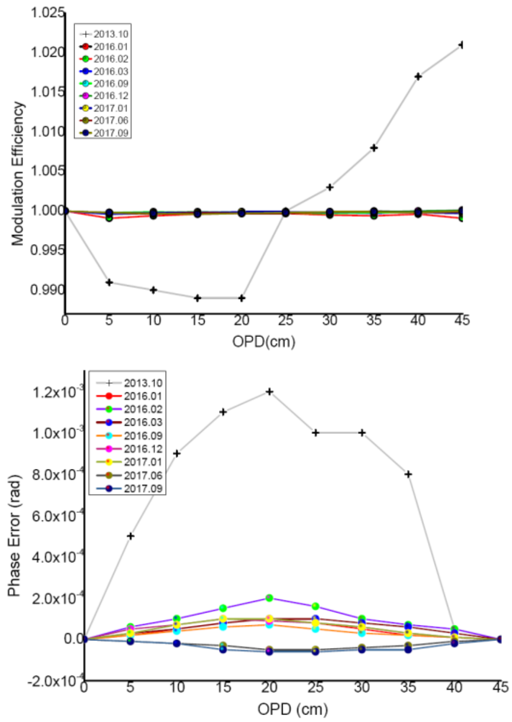

Figure 15: Modulation efficiency and phase error (rad) of HCl measurements from the g-b FTS are displayed in the period from October 2013 to September, 2014. Resolution: 0.015 cm^{-1}, Aperture: 0.8 mm, and Detector: RT-InGaAs DC (from 2013.10 (red) to 2016.09 (black)).

- Fig. 6: very low quality with obvious JPEG compression artifacts. This should be redone in a lossless compression format like PNG or a vector format like PDF!

2.5 Characterization of FTS-instrumental line shapes

For the accurate retrieval of total column values of the species of interest, a good alignment of the g-b FTS is essential. The instrument line shape (ILS) is retrieved from the regular HCl cell measurement that is an important indicator of the status of the FTS's alignment (Hase et al., 1999). The analyses of the measurements were performed using a linefit spectrum fitting algorithm (LINEFIT14 software) (Hase et al., 2013). Here, we have carried out experiments to investigate the influences of ILS with and without to the presence of OASIS system, and then we considered HCl cell measurements using sun as source while OASIS system active and tungsten lamp as a source while OASIS inactive. Without OASIS system, we showed the time series of the modulation efficiency and phase error (rad) in the HCl measurement using the source of light from tungsten lamp in the period of October 2013 to September 2016, which is depicted in Fig.

6. Modulation amplitudes for well alignment should be controlled in a limit of 5 % loss at the maximum optical difference (Wunch et al., 2011). In our g-b FTS measurements, it is found that the maximum loss of modulation efficiency at the maximum OPD is about 3 %, which is quite close to the ideal value. The phase errors are less than 0.009. Hase et al. (2013) reported that this level of small disturbances from the ideal value of the modulation efficiency is common to all well-aligned instruments. This result confirmed that the g-b FTS instrument is well aligned and stable during the whole operation period.

In the case OASIS system in active mode, we also confirmed that the ILS was not affected by the variable aperture during the operation of this system. The modulation efficiency and phase error were estimated to be 99.96 % and 0.009 rad, respectively (see Table 3). Sun et al. (2017) reported the detailed characteristics of the ILS with respect to applications of different optical attenuators to FTIR spectrometers within the TCCON and NDACC networks. They used both lamp and sun cell measurements which were conducted after the insertion of five different attenuators in front of and behind the interferometer. In Sun et al. (2017) paper, the ILS result was indicated by considering optical attenuator no .1 which is in good agreement with our findings.

Table 3. ILS measurements with and without OASIS system (sources of light are tungsten lamp and solar light).

Light Source	Tungsten	Solar(Sun)	Solar(Sun)	Range
S/N (signal to noise ratio)	183.2 : 1	162.7 : 1	167.1 : 1	_
Center wavenumber	5687.65 cm^{-1}	5687.65 cm^{-1}	5687.65 cm^{-1}	
~~Residual (measured minus simulated spectra)~~	~~-0.0005 to 0.0005~~	~~-0.001 to 0.001~~	~~-0.001 to 0.001~~	_
Mod. eff	99.99 %	99.98 %	99.96 %	99.96 ~99.99 %
Phase error (rad)	0.007	0.009	0.009	0.007 – 0.009
OASIS run	**OFF**	**OFF**	**ON**	_
Parameter	Spectral Resolution: 0.015cm^{-1}, Scans: 50, Beamsplitter: CaF_2, Aperture: 0.8 mm, Detector: RT-InGaAs DC, Scanner velocity: 10 kHz, High pass filter: open, Low pass filter: 10 kHz, Optical Path Difference (OPD) = 45 cm Source setting: Emission back parallel input/ NIR			

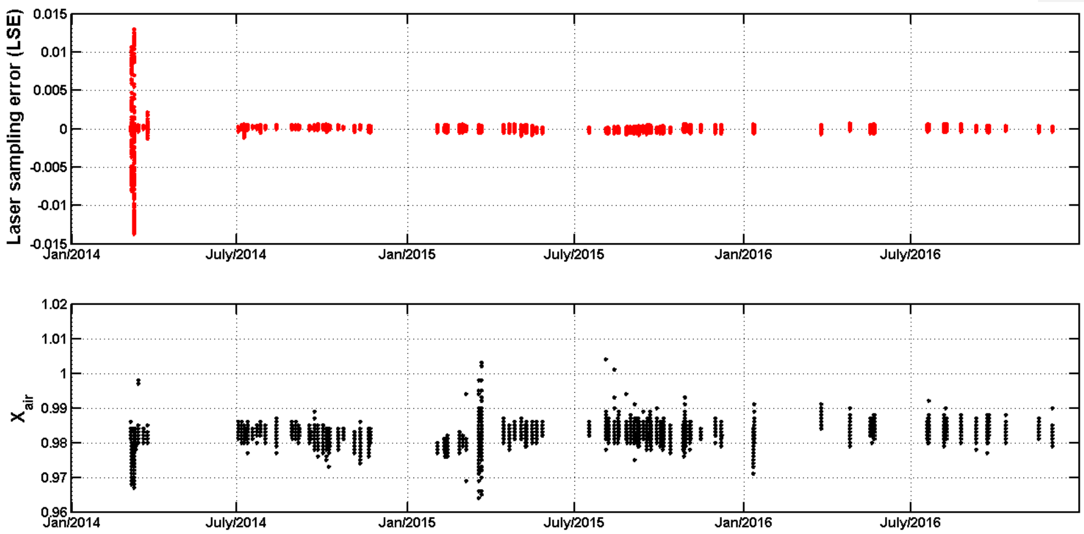

Figure 16: Time series of LSE (top panel) and X_{air} (bottom panel) from the g-b FTS during 2014-2016. Each marker represents a single measurement.

2.6 Data processing

Within the TCCON standard retrieval strategy, we have derived the column-averaged dry-air mole fraction CO_2 (XCO_2) and other atmospheric gases using GFIT algorithm. In this work, the TCCON standard GGG2014 (version 4.8.6) retrieval software was used to obtained abundance of the species from FTS spectra (Wunch et al., 2015). However, there is a slightly different setup of instrumentation in Anmyondo FTS site where all spectra are recorded after the OASIS system equipped, which is described a little bit in section...The XCO_2 is the ratio of retrieved CO_2 column to retrieved O_2 column ,

$$XCO_2 = \frac{CO_{2\,\mathrm{column}}}{O_{2\,\mathrm{column}}} \times 0.2095 , \quad (1)$$

Computing the ratio using Eq. (1) minimizes systematic and correlated errors such as errors in solar zenith angle, surface pressure, and instrumental line shape that existed in the retrieved CO_2 and O_2 columns (Messerschmidt et al., 2012, Washenfelder et al., 2006). Top panel of Fig.7 depicts the time series of LSE obtained from InGaAs spectra at Anmyondo FTS station in the measurement period of 2014 to 2016. We conducted the laser adjustment or laser replacement on 10 March, 2014, at which large LSE values were shown (see top panel of Fig. 7).

The X_{air} is a useful indicator of the quality of measurements and the instrument performance. The X_{air} would be unity for an ideal retrieval, however, due to spectroscopic limitations there is a TCCON wide bias and solar zenith angle (SZA) dependence. The retrieval of X_{air} deviating more than 1% from the nominal value of 0.98 would suggest a systematic error. The time series of X_{air} are shown in the bottom panel of Fig. 7. The X_{air} record reveals that the instrument has been stable during the measurement period. It shows that the values of X_{air} are fluctuated between 0.974 and 0.985, and the mean value is 0.982 with a standard deviation of 0.0015 in which the scatter for X_{air} is about 0.15 %. The low variability in time series of X_{air} indicates the stability of the measurements.

2.6 OCO-2

Orbiting Carbon Observatory-2 (OCO-2) is NASA's first Earth-orbiting satellite, which was successfully launched on July 2, 2014 into low-Earth orbit. It is devoted to observing atmospheric carbon dioxide (CO_2) to get better insight for the carbon cycle. The primary mission is to measure carbon dioxide with high precision and accuracy in order to characterize its sources and sinks at different spatial and temporal scales (Boland et al., 2009; Crisp, 2008, 2015). The instrument measures the near infrared spectra (NIR) of sunlight reflected off the Earth's surface. Using a retrieval algorithm, it provides results of atmospheric abundances of carbon dioxide and related atmospheric parameters at the nadir, sun glint and targets modes. Detailed information about the instrument is available in different papers (Connor et al., 2008; O'Dell et al., 2012). In this work, we used the OCO-2 version 7Br bias corrected data.

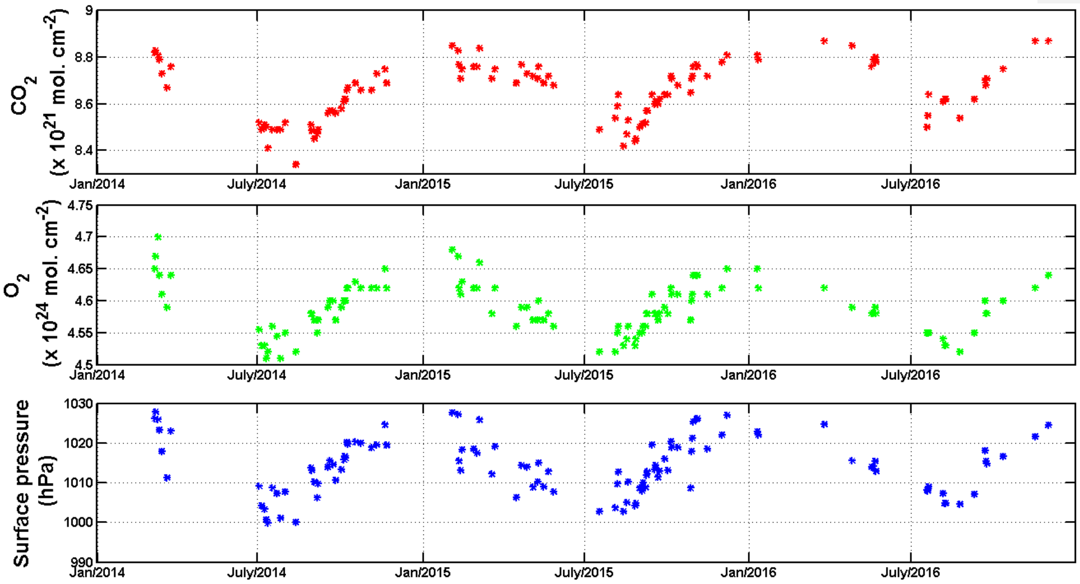

Figure 8: Time series of CO_2 (top panel) and O_2 (middle panel) column amounts and surface pressure (bottom right panel) from the g-b FTS are depicted during 2014- 2016. All results are on basis of daily median basis.

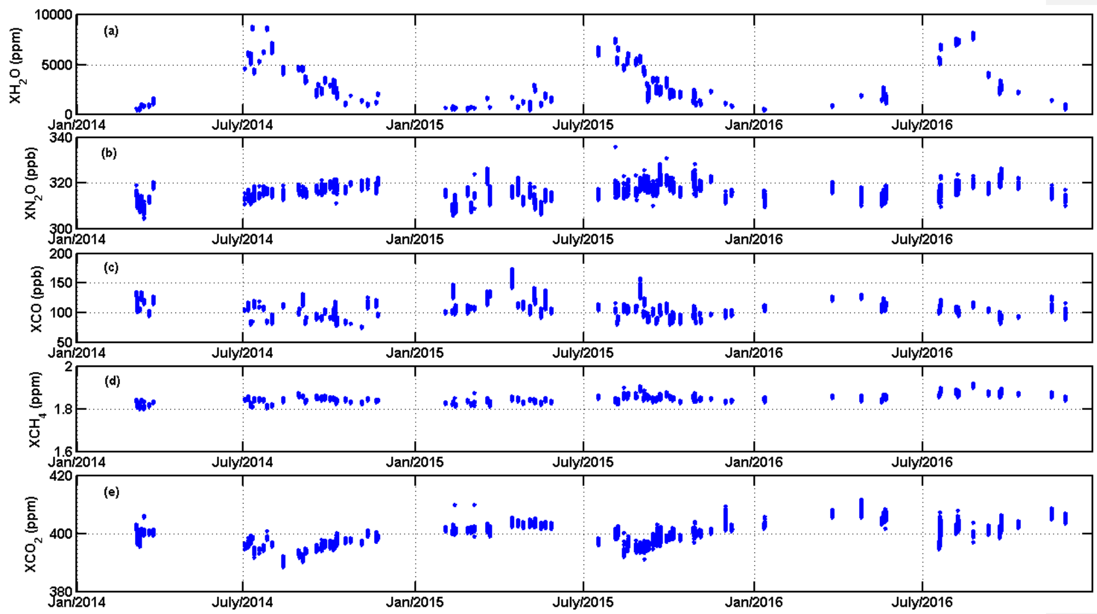

Figure 9. Time series of XH_2O, XN_2O, XCO, XCH_4, and XCO_2 from top to bottom panels (a-e), respectively in the period between 2014 - 2016. Each marker indicates a single retrieval.

3 Results and discussion

3.1 Time series of g-b FTS columns of CO_2 and O_2

The XCO_2 along with other retrievals g-b FTS are presented in Fig. 8 (panel e), in the time period of 2014 – 2016. We also incorporated time series of other greenhouse gases (such as XH_2O, XN_2O, XCO, and XCH_4) that are retrieved together with the XCO_2, which are depicted in Fig 9.(panel a-d). The temporal distributions of the g-b FTS total column amounts of CO_2 and O_2 on daily median basis during the period from February 2014 to December 2016 are depicted in the left bottom and right top panels of Fig. 8, respectively. It was shown that the CO_2 column amounts varied within 8.40×10^{21} to 8.84×10^{21} molecules cm^{-2} during the whole observation period, while O_2 varied between 4.5×10^{24} and 4.7×10^{24} molecules cm^{-2}, with the corresponding mean of 4.52×10^{24} molecules cm^{-2} and a standard deviation of 2.59×10^{22} molecules cm^{-2}, respectively. The scatter for column O_2 is estimated to be 0.57 %, which is comparable with the variation of atmospheric pressure (see Fig. 8 right top and bottom panels).

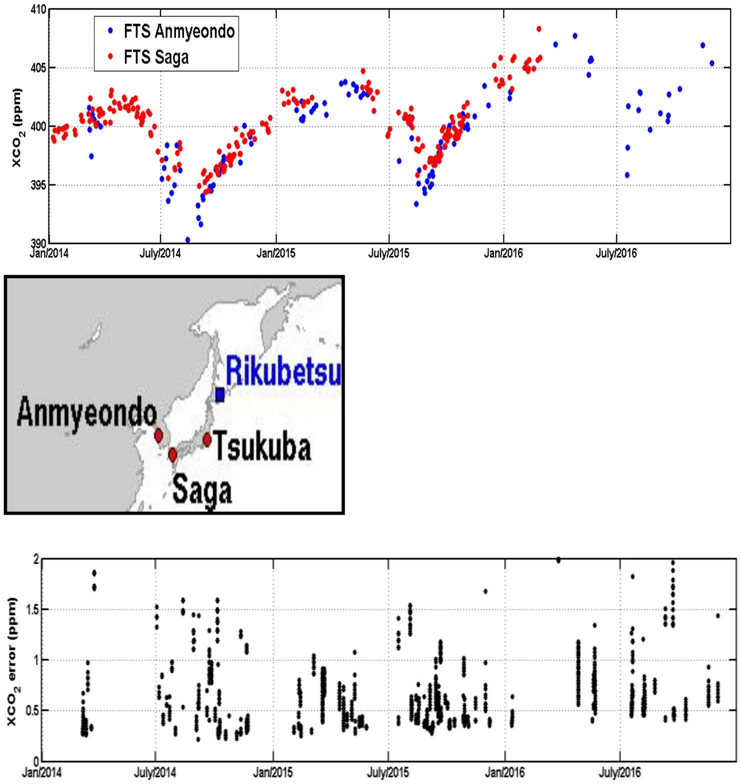

Figure 10. Time series of XCO_2 retrieval (top left panel) and its retrieval error (bottom left panel) from Anmyeondo FTS and Saga FTS in the period of 2014 – 2016. Top right panel depicts map of TCCON sites which are close to our site.

3.2 Comparison of Anmyeondo XCO_2 with nearby TCCON site

We compared our FTS XCO_2 data with similar ground-based high resolution FTS observations at Saga TCCON station (33.26 N, 130.29 E) in Japan, which is the closest TCCON station to our site (see right panel of Fig 10). Among those TCCON sites, Rikubetsu, Tsukuba, and Saga are located in Japan and Hefei is located in China (Wang et al., 2017). To demonstrate the comparison between them, we have shown the daily averaged XCO_2 of two sites during the period of 2014 to 2016 in Fig. 10 left panel. As can be seen, variations of XCO_2 at the Saga site agreed well with Anmyeondo site. The daily averaged XCO_2 revealed the same seasonal cycle as that of our site. The lowest XCO_2 appeared in late summer (August and September), and the highest value was in spring (April).

3.3 Comparison of XCO_2 between the g-b FTS and OCO-2

In this section, we present a comparison of XCO_2 between the g-b FTS and OCO-2 version 7Br data (bias corrected data) over Anmyeondo station during the period between 2014 and 2016. For making a direct comparison of the g-b FTS measurements against OCO-2, we applied the spatial coincidence criteria for the OCO-2 data within 3° latitude/longitude of the FTS station, as well as setting up a time window of 3 hours. Based on the coincidence criteria, we obtained thirteen (13) coincident measurements, which were not sufficient to infer a robust conclusion. But it gives a preliminary result for indicating a level of agreement between them. We showed that the comparison of the time series XCO_2 concentrations derived from the g-b FTS and OCO-2 on daily medians basis along with the time series of its retrieval errors from FTS during the measurement period between 2014 and 2016, as depicted in Fig. 10. As can be seen in the plot, the g-b FTS measurement exhibits some gaps occurred due to bad weather conditions, instrument failures, and absences of an instrument operator. In the present analysis, the XCO_2 concentrations from FTS were considered only when its retrieval error was below 1.5 ppm (see the bottom panel of Figure 8), which is the sum of all error components such as laser sampling error, zero level offsets, ILS error, smoothing error, atmospheric apriori temperature, atmospheric apriori pressure, surface pressure, and random noise. Recently, Wunch et al. (2016) reported that the comparison of XCO_2 derived from the OCO-2 version 7Br data against a co-located ground-based TCCON data that indicates the median differences between the OCO-2 and TCCON data were less than 0.5 ppm, a corresponding RMS differences less than 1.5 ppm. The overall results of our comparisons are comparable with the report made by Wunch et al. (2016). The OCO-2 product of XCO_2 was biased (satellite minus g-b FTS) with respect to the g-b FTS, which was slightly higher by 0.179 ppm with a standard deviation of 1.194 ppm. This bias could be attributed to the instrument uncertainty. In addition to that, we also obtained a strong correlation between them, which was quantified as a correlation coefficient of 0.936 (see Table 2).

Table 4. Summary of the statistics of XCO_2 comparisons between OCO-2 and the g-b FTS from 2014 to 2016 are presented. N –coincident number of data, R - Pearson correlation coefficient, RMSE - Root Mean Squares Error.

N	Mean Absolute. diff. (ppm)	Mean Relative diff (%)	R	RMSE (ppm)
13	0.179±1.194	0.0443±0.298	0.936	1.161

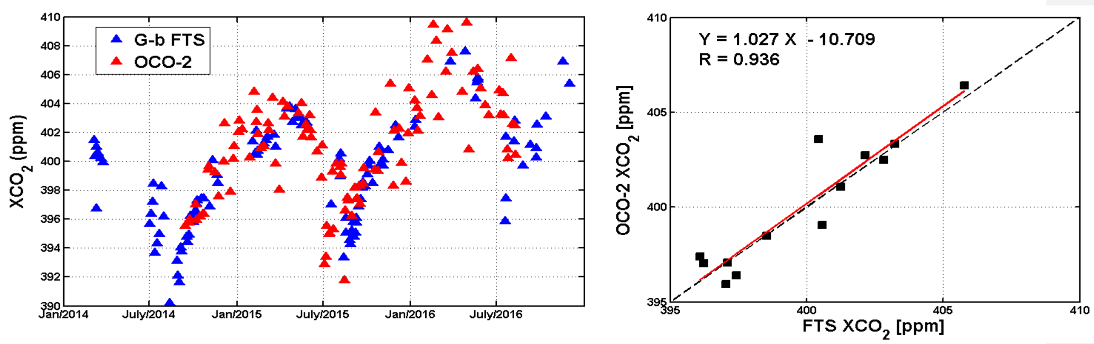

Figure 11: Left panel: The time series of XCO_2 from the g-b FTS (blue triangle) and OCO-2 (red triangle) over the Anmyeondo site from 2014 to 2016. Right panel: The linear regression curve between FTS and OCO-2. All results are given on daily medians basis.

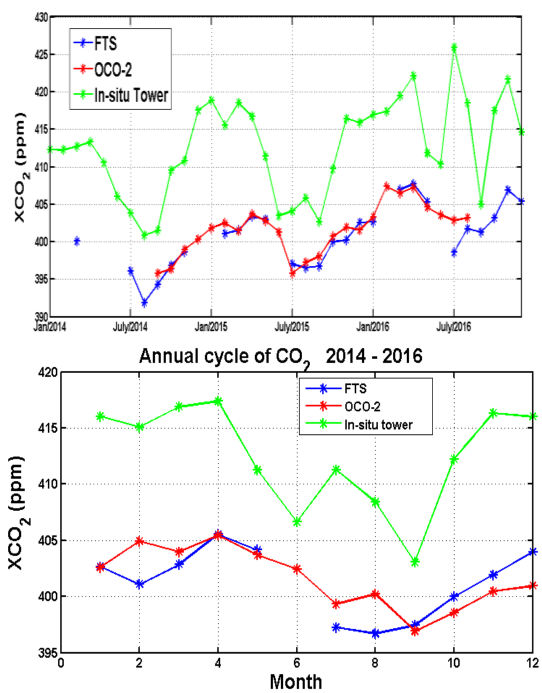

Figure 12: Left panel: The time series of XCO_2 on monthly mean basis, whereas left panel depicted annual cycle of XCO_2.

3.4 Seasonal cycle of XCO_2

In this section, the main focus of this issue is to deal with the comparison of the seasonal cycle of XCO_2 between the g-b FTS and OCO-2 over the Anmyeondo station. In order to understand the role of local influence, we have tried to show the seasonal and annual cycle of CO_2 derived from in-situ tower observation. Fig. 12 exhibits the time series of the monthly mean XCO_2 and annual cycle for the measurement period of 2014 to 2016 from FTS (blue), OCO-2 (red) and in-situ tower (green solid lines with dot marker). The overall result indicates that both instruments are generally agreed in capturing the seasonal variability of XCO_2 at the measurement site. As it is clearly seen from the temporal distribution of FTS XCO_2, the maximum and minimum values are observed in spring and late summer seasons, respectively. It was found that its mean values in spring and summer were 402.72 and 396.92 ppm, respectively (see Table 5). This is because the seasonal variation of XCO_2 is controlled mainly by the photosynthesis in the terrestrial ecosystem, and this explains the larger XCO_2 values in the northern hemisphere in late April (Schneising et al. 2008, and references therein). The minimum value of XCO_2 occurs in August, which is most likely due to uptake of carbon into the biosphere in associated with the period of plant growth. Furthermore, both instruments showed high standard deviations during summer, about 3.28 ppm in FTS and 3.77 ppm in OCO-2, suggesting that the variability reflects strong sources and sink signals. However, photosynthesis is not the only driver of the seasonal cycle during the local growing season. The site is also influenced by regional anthropogenic emissions under the prevailing winds.

Table 5. Seasonal mean and standard deviations of XCO_2 from the g-b FTS and OCO-2 in the period between 2014 and 2016 are given below.

Season	g-b FTS XCO_2 mean ± std (ppm)	OCO-2 XCO_2 mean ± std (ppm)
Winter	401.52 ± 0.85	402.67 ± 2.67
Spring	402.72 ± 2.79	403.96 ± 2.77
Summer	396.92 ± 3.28	399.68 ± 3.77
Autumn	398.01 ± 2.83	398.48 ± 2.41

4 Conclusions

Monitoring of greenhouse gases is an essential issue in the context of the global climate change. Accurate and precise continuous long-term measurements of the greenhouse gases (GHGs) are substantial for investigating their source and sinks. Nowadays, several remote sensing instruments operated on different platforms are dedicated for measuring GHGs.

XCO_2 measurements have been made using the g-b FTS at the Anmyeondo site since 2013. However, in this work, we focused on the measurements taken during 2014 and 2016. The instrument has been operated in a semi-automated mode since then. The FTS instrument has been stable during the whole measurement period. Regular instrument alignments using the HCl cell measurements are performed. The other important feature is that the home made OASIS system is installed in our FTS instrument, which enables to improve the solar intensity fluctuations. Thus, it guarantees the quality of the spectra. The TCCON standard GGG2014 retrieval software is used to retrieve XCO_2 from the g-b FTS spectra.

In this work, the preliminary comparison results of XCO_2 between FTS and OCO-2 were presented over the Anmyeondo station. The mean absolute difference of XCO_2 between FTS and OCO-2 was calculated on daily mean basis, and it was estimated to be -0.065 ppm, along with a standard deviation of 1.67 with respect to the g-b FTS. This bias could be attributed with instrument uncertainty. Based on the seasonal cycle comparison, both the g-b FTS and OCO-2 illustrated a consistent pattern in capturing the seasonal variability of XCO_2, with maximum in spring and minimum in summer. In summer and fall, plants are flourishing and CO_2 is consumed by photosynthesis. However, in winter and spring, weak photosynthesis phenomenon is occurred because of low plant flourishing and CO_2 reaches the highest values particularly in April. Therefore, the outcome of this study reflects the suitability of the measurements for improving the understanding of the carbon cycle, as well as for evaluating the remote sensing data.

5 Acknowledgements

This research was supported by the Research and Development for KMA Weather, Climate, and Earth system Services (NIMS-2016-3100). We would greatly acknowledge the two anonymous reviewers who helped to improve this manuscript well.

References

Boland, S., Brown L. R., Burrows J. P., Ciais P., Connor B. J., Crisp D., Denning S., Doney S. C., Engelen R., Fung I. Y., Griffith P., Jacob D. J., Johnson B., Martin-Torres J., Michalak A. M., Miller C. E., Polonsky I., Potter C., Randerson J. T., Rayner P. J., Salawitch R. J., Santee M., Tans P. P., Wennberg P. O., Wunch D., Wofsy S. C., and Yung Y. L.: The Need for Atmospheric Carbon Dioxide Measurements from Space: Contributions from a Rapid Reflight of the Orbiting Carbon Observatory, 2009, http://www.nasa.gov/pdf/363474main_OCO_Reflight.pdf.

Buschmann M., Nicholas M., Deutscher M., Sherlock V., Palm M., Warneke T., and Notholt J.: Retrieval of XCO_2 from ground-based mid-infrared (NDACC) solar absorption spectra and comparison to TCCON, Atmos. Meas. Tech., 9, 577–585, 2016.

Brault, J. W.: New approach to high-precision Fourier transform spectrometer design. Appl. Opt. 35, 2891–2896, 1996.

Connor B. J., Bösch H., Toon G., Sen B., Miller C. E., and Crisp D.: Orbiting carbon observatory: Inverse method and prospective error analysis, J. Geophys. Res., 113 doi: 10.1029/2006JD008336, 2008.

Connor B. J., Sherlock V., Toon G., Wunch D., and Wennberg P. O.: GFIT2: an experimental algorithm for vertical profile retrieval from near-IR spectra, Atmos. Meas. Tech., 9(8), 3513–3525, doi:10.5194/amt-9-3513-2016, 2016.

Crisp D., Miller C. E., DeCola P. L.: NASA Orbiting Carbon Observatory: measuring the column averaged carbon dioxide mole fraction from space. J. Appl. Remote Sens., 2, 023508, doi:10.1117/1.2898457, 2008.

Crisp D. for the OCO-2 Team: Measuring Atmospheric Carbon Dioxide from Space with the Orbiting Carbon Observatory-2 (OCO-2), Proc. SPIE 9607, Earth Observing Systems XX, 960702, doi: 10.1117/12.2187291, 2015.

Deutscher, N. M., Griffith, D. W. T., Bryant, G. W., Wennberg, P. O., Toon, G. C., Washenfelder, R. A., Keppel-Aleks, G., Wunch, D., Yavin, Y., Allen N. T., Blavier, J.-F., Jiménez R., Daube, B. C., Bright, A. V., Matross, D. M., Wofsy, S. C., and Park, S.: Total column CO_2 measurements at Darwin, Australia-site description and calibration against in situ aircraft profiles, Atmos. Meas. Tech., 3, 947-958, doi:10.5194/amt-3-947-2010, 2010.

Frankenberg, C., Pollock, R., Lee, R. A. M., Rosenberg, R., Blavier, J.-F., Crisp, D., O'Dell C. W., Osterman, G. B., Roehl, C., Wennberg, P. O., and Wunch, D.: The Orbiting Carbon Observatory (OCO-2): spectrometer performance evaluation using pre-launch direct sun measurements. Atmospheric Measurement Techniques, 8(1), 301–313. doi:10.5194/amt-8-301-2015, 2015.

Geibel, M. C., Gerbig, C., and Feist, D. G.: A new fully automated FTIR system for total column measurements of greenhouse gases, Atmospheric Measurement Techniques, 3(5), 1363-1375, doi:10.5194/amt-3-1363-2010, 2010.

Hase, F., Blumenstock, T., and Paton-Walsh, C.: Analysis of the instrumental line shape of high resolution Fourier transform IR spectrometers with gas cell measurements and new retrieval software, Appl. Optics, 38, 3417–3422, doi:10.1364/AO.38.003417,1999.

Hase, F., Drouin, B. J., Roehl, C. M., Toon, G. C., Wennberg, P. O., Wunch, D., Blumenstock, T., Desmet F., Feist, D. G., Heikkinen, P., De Mazière, M., Rettinger, M., Robinson, J., Schneider, M., Sherlock, V., Sussmann, R., Té Y., Warneke, T., and Weinzierl, C.: Calibration of sealed HCl cells used for TCCON instrumental line shape monitoring, Atmospheric Measurement Techniques, 6(12), 3527–3537, doi:10.5194/amt-6-3527-2013, 2013.

Kiel, M., Wunch, D., Wennberg, P. O., Toon, G. C., Hase, F., and Blumenstock, T.: Improved retrieval of gas abundances from near-infrared solar FTIR spectra measured at the Karlsruhe TCCON station, Atmos. Meas. Tech., 9(2), 669–682, doi:10.5194/amt-9-669-2016, 2016.

Kivi, R. and Heikkinen, P.: Fourier transform spectrometer measurements of column CO_2 at Sodankylä, Finland, Geosci. Instrum. Method. Data Syst., 5, 271–279, 2016.

Messerschmidt, J., Macatangay, R., Notholt, J., Petri C., Warneke, T., and Weinzierl, C.: Side by side measurements of CO_2 by ground-based Fourier transform spectrometry (FTS), Tellus B, 62(5), 749-758, doi:10.1111/j.1600-0889.2010.00491.x., 2010.

Messerschmidt, J., H. Chen, N. M. Deutscher, C. Gerbig, P. Grupe, K. Katrynski, F.-T. Koch, J. V. Lavrič, J. Notholt, C. Rödenbeck, W. Ruhe, T. Warneke, and Weinzierl, C.: Automated ground-based remote sensing measurements of greenhouse gases at the Białystok site in comparison with collocated in situ measurements and model data, Atmospheric Chemistry and Physics, 12(15), 6741–6755, doi:10.5194/acp-12-6741-2012, 2012.

Miao, R., Lu N., Yao L., Zhu, Y., Wang, J., and Sun, J.: Multi-Year Comparison of Carbon Dioxide from Satellite Data with Ground-Based FTS Measurements (2003–2011), Remote Sensing, 5(7), 3431–3456, doi:10.3390/rs5073431, 2013.

Miller, C. E., Crisp, D. DeCola, P. L., Olsen, S. C., Randerson, J. T., Michalak, A. M., Alkhaled, A., Rayner, P., Jacob, D. J., Suntharalingam, P., Jones, D. B. A., Denning, A. S., Nicholls, M. E., Doney, S. C., Pawson, S., Boesch, H., Connor B. J., Fung I. Y., O'Brien, D., Salawitch, R. J., Sander, S. P., Sen, B., Tans, P., Toon, G. C., Wennberg, P. O., Wofsy, S. C., Yung, Y. L., and Law, R. M.: Precision requirements for space-based XCO2 data, J. Geophys. Res-Atmos., 109, D02301, doi: 10.1029/2006JD007659, 2007.

Morino, I., Uchino, O., Inoue, M., Yoshida, Y., Yokota T., Wennberg, P. O., Toon, G. C., Wunch, D., Roehl, C. M., Notholt, J., Warneke, T., Messerschmidt, J., Griffith, D. W. T., Deutscher, N. M., Sherlock, V., Connor, B. J., Robinson, J., Sussmann, R., and Rettinger, M.: Preliminary validation of column-averaged volume mixing ratios of carbon dioxide and methane retrieved from GOSAT short-wavelength infrared spectra, Atmospheric Measurement Techniques, 4(6), 1061-1076, doi:10.5194/amt-4-1061-2011, 2011.

O'Dell, C. W., Connor, B., Bösch, H., O'Brien, D., Frankenberg C., Castano, R., Christi, M., Eldering, D., Fisher, B., Gunson, M., McDuffie, J., Miller, C. E., Natraj, V., Oyafuso, F., Polonsky, I., Smyth, M., Taylor, T., Toon, G. C., Wennberg, P. O., and Wunch, D.: The ACOS CO2 retrieval algorithm – Part 1: Description and validation against synthetic observations, Atmospheric Measurement Techniques, 5, 99–121, doi: 10.5194/amt-5-99-2012, http://www.atmos-meas-tech.net/5/99/2012/, 2012.

Ohyama, H., Morino, I., Nagahama, T., Machida, T., Suto H., Oguma, H., Sawa, Y., Matsueda, H., Sugimoto, N., Nakane, H., and Nakagawa, K.: Column-averaged volume mixing ratio of CO_2 measured with ground-based Fourier transform spectrometer at Tsukuba, J. Geophys. Res., 114, D18303 doi:10.1029/2008JD011465, 2009.

Ohyama, H., Kawakami, S., Tanaka, T., Morino, Uchino, I., O., Inoue, M., Sakai, T., Nagai, T., Yamazaki, A., Uchiyama, A., Fukamachi, T., Sakashita, M., Kawasaki, T., Akaho, T., Arai, K., and Okumura, H.: Observations of XCO_2 and XCH_4 with ground-based high-resolution FTS at Saga, Japan, and comparisons with GOSAT products, Atmos. Meas. Tech., 8(12), 5263–5276, doi:10.5194/amt-8-5263-2015.

Rayner P. J., and O'Brien D. M.: The utility of remotely sensed CO_2 concentration data in surface source inversions, Geophys. Res. Lett., 28, 175–178, doi: 10.1029/2000GL011912, 2001.

Rothman, L., Gordon, I., Babikov, Y., Barbe, A., Benner, D. C., Bernath, P., Birk, M., Bizzocchi, L., Boudon, V., Brown, L., Campargue, A., Chance, K., Cohen, E., Coudert, L., Devi, V., Drouin, B., Fayt, A., Flaud, J.-M., Gamache, R., Harrison, J., Hartmann, J.-M., Hill, C., Hodges, J., Jacquemart, D., Jolly, A., Lamouroux, J., Roy, R. L., Li, G., Long, D., Lyulin, O., Mackie, C., Massie, S., Mikhailenko, S., Müller, H., Naumenko, O., Nikitin, A., Orphal, J., Perevalov, V., Perrin, A., Polovtseva, E., Richard, C., Smith, M., Starikova, E., Sung, K., Tashkun, S., Tennyson, J., Toon, G., Tyuterev, V., and Wagner, G.: The HITRAN2012 molecular spectroscopic database, J. Quant. Spectrosc. Ra., 130, 4–50, doi:10.1016/j.jqsrt.2013.07.002, 2013.

Schneising O., Buchwitz M., Burrows J. P., Bovensmann, H., Reuter, M., Notholt, J., Macatangay, R., and Warneke, T.: Three years of greenhouse gas column-averaged dry air mole fractions retrieved from satellite-Part 1: Carbon dioxide, Atmos. Chem. Phys., 8, 3827-3853, 2008.

Sun, Y., Palm, M., Weinzierl, C., Peteri, C., Notholt, J., Wang, Y., and Liu, C.: Technical note: Sensitivity of instrumental line shape monitoring for the ground-based high-resolution FTIR spectrometer with respect to different optical attenuators, Atmos. Meas. Tech. Discuss., doi:10.5194/amt-10-989- 2017.

Wang, W., Tian, Y., Liu, C., Sun, Y., Liu, W., Xie, P., Liu, J., Xu, J., Morino, I., Velazco, V., Griffith, D., Notholt, J., and Warneke, T.: Investigating the performance of a greenhouse gas observatory in Hefei, China, Atmos. Meas. Tech., 10, 2627–2643, 2017.

Washenfelder R. A., Toon G. C., Blavier J-F., Yang Z., Allen N. T., Wennberg P. O., Vay S. A., Matross, D. M., and Daube B. C.: Carbon dioxide column abundances at the Wisconsin Tall Tower site, Journal of Geophysical Research, 2006, 111, doi:10.1029/2006JD00715, 2000.
Warneke, T., Yang, Z., Olsen, S., Korner, S., Notholt J., Toon, G. C., Velazco, V., Schultz, A., and Schrems, O.: Seasonal and latitudinal variations of column averaged volume-mixing ratios of atmospheric CO_2, Geophysical Research Letters, 32(3), 2-5, doi:10.1029/2004GL021597, 2005.

Wunch, D., Toon G. C., Wennberg, P. O., Wofsy, S. C., Stephens, B., Fisher, M. L., Uchino O., Abshire, J. B., Bernath, P. F., Biraud, S. C., Blavier, J.-F. L., Boone, C. D., Bowman, K. P., Browell, E. V., Campos, T., Connor, B. J., Daube, B. C., Deutscher, N. M., Diao M., Elkins, J. W., Gerbig, C., Gottlieb, E., Griffith, D. W. T., Hurst, D. F., Jiménez, R., Keppel-Aleks, G., Kort, E. A., Macatangay, R., Machida, T., Matsueda, H., Moore, F. L., Morino, I., Park, S., Robinson, J., Roehl, C. M., Sawa, Y., Sherlock, V., Sweeney, C., Tanaka, T., and Zondlo, M. A.: Calibration of the Total Carbon Column Observing Network using aircraft profile data, Atmospheric Measurement Techniques, 3(5), 1351-1362, doi:10.5194/amt-3-1351-2010.

Wunch, D., Toon, G. C., Blavier, J.-F. L., Washenfelder, R. A., Notholt, J., Connor, B. J., Griffith, D. W. T., Sherlock, V., and Wennberg, P. O.: The Total Carbon Column Observing Network, Philos. T. R. Soc. A, 369, 2087–2112, doi:10.1098/rsta.2010.0240, 2011.

Wunch, D., Toon, G. C., Sherlock, V., Deutscher, N. M., Liu X., Feist, D. G., and Wennberg, P. O.: The Total Carbon Column Observing Network's GGG2014 Data Version. doi:10.14291/tccon.ggg2014.documentation.R0/1221662, 2015.

Wunch, D., Wennberg, P.O.,, Osterman, G., Fisher, B., Naylor, B., Roehl, C. M., O'Dell, C., Mandrake, L.,Viatte, C., Griffith, D. W. T., Deutscher, N. M., Velazco, V. A., Notholt, J.,Warneke, T.,Petri, C., Maziere, M. De, Sha, M. K., Sussmann,R., Rettinger, M., Pollard, D., Robinson, J.,Morino, I., Uchino O., Hase, F., Blumenstock, T., Kiel, M., Feist, D. G., Arnold S.G., Strong, K., Mendonca, J., Kivi, R.,Heikkinen, P., Iraci, L., Podolske, J., Hillyard, P. W., Kawakami, S., Dubey, M. K., Parker, H. A., Sepulveda, E., Rodriguez, O. E. G., Te, Y., Jeseck, P., Gunson, M. R., Crisp, D., and Eldering A., Comparisons of the Orbiting Carbon Observatory-2 (OCO-2) XCO_2 measurements with TCCON, Atmos. Meas. Tech. Discuss., doi:10.5194/amt-2016-227, 2016

Co-authors and TCCON comments.

- You can also add the comparison with the KORUS-AQ in situ profile to strengthen the paper.

- Then write a separate paper focussed on OASIS, using these measurements with and without OASIS.

Response: I will follow the TCCON measurement guidelines. I will re-work my existing paper without OASIS content.(I will follow your suggestion). , I will write a separate paper for the OASIS section through further study. The KORUS-AQ in situ profile add in the paper.

Co-authors and TCCON member first comment revision.

Characteristics of the Greenhouse Gas Concentration Derived from the Ground-based FTS Spectra at Anmyeondo, Korea

Young-Suk Oh[1,2*], Samuel Takele Kenea[1], Tae-Young Goo[1], Kyu-Sun Chung[2], David W. T. Griffith[3], Paul. Wennberg[4], Voltaire A. Velazco[3], Jae-Sang Rhee[1], Mi-Lim Ou[5], and Young-Hwa Byun[1]

1. Climate Research Division, National Institute of Meteorological Sciences (NIMS), Jeju-do, Republic of Korea
2. Department of Electrical Eng. & Centre for Edge Plasma Science, Hanyang University, Seoul, Republic of Korea
3. School of Chemistry, University of Wollongong, Wollongong, Australia
4. California Institute of Technology, California, USA
5. Climate Change Monitoring Division, Korea Meteorological Administration, Seoul, Republic of Korea

*Correspondence to: Young-Suk Oh (ysoh306@gmail.com)

Abstract.

Since the late 1990s, the meteorological observatory established in Anmyeondo (36.5382˚ N, 126.3311˚ E, and 30 m above mean sea level), has been monitoring several greenhouse gases such as CO_2, CH_4, N_2O, CFCs, and SF_6, as part of the Global Atmosphere Watch (GAW) Program. A high resolution ground-based (g-b) Fourier Transform Spectrometer (FTS, IFS-125HR model) was installed at such observation site in 2013, and has been fully operated within the frame work of the Total Carbon Column Observing Network (TCCON) since August, 2014. The solar spectra recorded by the g-b FTS are covered in the range between 3,800 and 16,000 cm^{-1} at the spectral resolution of 0.02 cm^{-1} during the measurement period between 2014 and 2016. In this work, the GGG2014 version of the TCCON standard retrieval algorithm was used to retrieve

XCO_2 concentrations from the FTS spectra. Two spectral bands (at 6220.0 and 6339.5 cm^{-1} centre wavenumbers) were used to derive the XCO_2 concentration within the spectral residual of +0.01 %. All sources of errors were thoroughly analyzed. In this paper, we introduced aircraft observation campaigns over Anmyeondo station were carried out during the period between 2012 and 2016. A comparison of the XCO_2 concentration in g-b FTS and OCO-2 (Orbiting Carbon Observatory) satellite observations was presented only for the measurement period between February 2014 and December 2016. The 13 coincident observations were selected on a daily median basis. It was obtained that OCO-2 exhibited slightly higher bias with respect to the g-b FTS, which is about 0.189 ppm with the standard deviation of 1.19 ppm, and revealed a strong correlation (R=0.94). Based on seasonal cycle comparisons, both instruments generally agreed in capturing seasonal variations of the target species with its maximum and minimum values in spring and late summer, respectively. In the future, it is planned to exert further works in utilizing the FTS measurements for the evaluation of satellite observations such as Greenhouse Gases Observing Satellite (GOSAT) at observation sites. This is the first report of the g-b FTS observations of XCO_2 species over the Anmyeondo station.

Key words: Aircraft**,** XCO_2, OCO-2, TCCON, Infrared spectra

1. Introduction

Monitoring of greenhouse gases (GHGs) is a crucial issue in the context of the global climate change. Carbon dioxide (CO_2) is one of the key greenhouse gas and its global annual mean concentration has been increased rapidly from 278 to 400 ppm since 1750, pre-industrial year (WMO greenhouse gas bulletin, 2016). Radiative forcing of atmospheric CO_2 accounts for approximately 65 % of the total radiative forcing by long-lived GHGs (Ohyama et al., 2015 and reference therein). Human activities, such as burning of fossil fuels, land use change, etc., are the primary drivers of the continuing increase in atmospheric greenhouse gases and the gases involved in their chemical production (Kiel et al., 2016 and reference therein). In the fact that it is a global concern for demanding accurate and precise long-term measurements of greenhouse gases.

In the field of remote sensing techniques, solar absorption infrared spectroscopy is an essential technique, which has been increasingly used to determine changes in atmospheric constituents. Nowadays, a number of instruments deployed in various platforms (e.g., ground-based, space-borne) have been operated for measuring GHGs such as CO_2. Our g-b FTS at the Anmyeondo station has been measuring several atmospheric GHGs such as CO_2, CH_4, CO, N_2O, and H_2O operated within the framework of the Total Carbon Column Observing Network (TCCON). XCO_2

retrievals from the g-b FTS have been reported at different TCCON sites (e.g, Ohyama et al., 2009; Deutscher et al., 2010; Messerschmidt et al., 2010, 2012; Miao et al., 2013; Kivi and Heikkinen, 2016). TCCON achieves the accuracy and precision in measuring the column averaged dry air mole fraction of CO_2 (XCO_2), as about 0.25 % that is less than 1 ppm (Wunch et al., 2010), which is essential to get information about sinks and sources, as well as validating satellite products (Rayner and O'Brien, 2001; Miller et al., 2007). It is reported that the precision of CO_2 even 0.1 % can be achieved during clear sky conditions (Messerschmidt et al., 2010; Deutscher et al., 2010). The network aims to improve global carbon cycle studies and supply the primary validation data of different atmospheric trace gases derived from space-based instruments, e.g., the Orbiting Carbon Observatory 2 (OCO-2), the Greenhouse Gases Observing Satellite (GOSAT) (Morino et al., 2011; Frankenberg et al., 2015).

The objective of this study is focused on the characteristics of XCO_2 concentration retrievals from g-b FTS spectra and is implement a preliminary comparison against OCO-2 over the Anmyeondo station. The FTS spectra have been processed using the TCCON standard GGG2014 (Wunch et al., 2015) retrieval software. One of the interesting issues in this work is a new home made addition to our g-b FTS instrument that reduces the solar intensity variations from the 5% maximum allowed in TCCON to less than 2%. This paper presents introduction to instrumentation and measurement site, and next to that, provides results and discussion followed by conclusions.

2 Station and instrumentation

2.1 Station description

The G-b FTS observatory was established in the Anmyeondo (AMY) station, which is located at 36.32˚ N, 126.19˚ E, and 30 m above sea level. This station is situated on the west coast of the Korean Peninsula, which is 180 kilometres away from Seoul, the capital city of Republic of Korea. Figure 1 displays the Anmyeondo station. It is also a regional GAW (Global Atmosphere Watch) station that belongs to the Climate Change Monitoring Network of KMA (Korean Meteorological Administration). The AMY station has been monitoring various atmospheric compositions such as greenhouse gases, aerosols, ultraviolet radiation, ozone, and precipitation since 1999. The total area of Anmyeondo is estimated to be ~87.96 km^2 and approximately 1.25 million people reside in this island. Some of the residents over this area are engaged in agricultural activities. Vegetated areas consisting of mainly pine trees are located in and around the FTS observatory. The topographic feature of the area consists of low level hills, on average it is about 100 m above sea level. The climatic condition of the area is: the minimum temperature occurred on winter season with an average of 2.7 ˚C, and the maximum temperature is about 25.6 ˚C during summer season. In addition, the annual precipitation amount is estimated to be 1,155 mm; and the high amount of snows would be observed in winter. Such a observation site has been designated as part of TCCON site since August 2014. The AMY Station's on TCCON wiki page is kept available and can be found at: [https://tccon-wiki.Anmyeondo.edu]

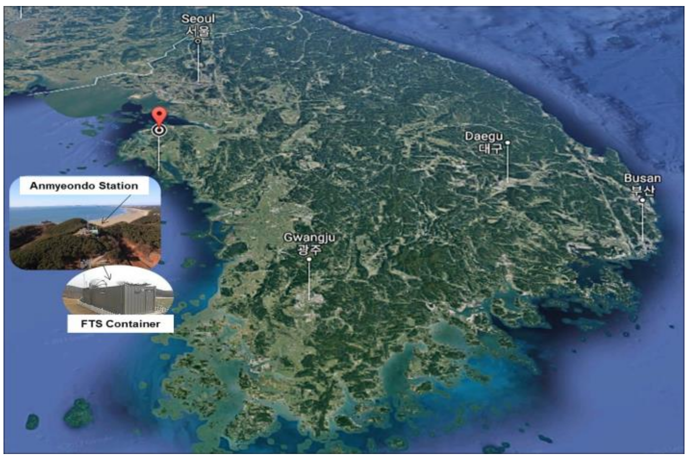

Figure 17. Anmyeodo (AMY) g-b FTS station

2.2 G-b FTS instrument

Solar spectra are acquired by operating a Bruker IFS 125HR spectrometer (Bruker Optics, Germany) under the framework of TCCON. Currently, our g-b FTS instrument operation is semi-automated for taking the routine measurements under clear sky conditions. It is planned to make an FTS operation mode to be fully automated by this year. The solar tracker (Tracker A547, Bruker Optics, Germany) is mounted inside a dome. The tracking ranges in terms of both azimuthal and elevation angles are about 0 to 315 and -10 to 85 degrees, respectively, while the tracking speed is about 2 degrees per second. The tracking accuracy of ±4 minutes of arc can be achieved by the Camtracker mode. Under clear sky conditions, the dome is opened and set to an automatic-turning mode, in order that the mirrors are moved automatically to search for the position where the sunspot is seen by the camera. Then, the solar tracker is activated in such a way that the mirrors are finely and continuously controlled to fix the beam into the spectrometer. Figure 2 displays an overview of the general data acquisition system. This ensures that all spectra were recorded under clear weather conditions. The other important feature that has been made on the FTS spectrometer is the implementation of the interferogram sampling method (Brault, 1996), that takes advantage of modern analogue-digital converters (ADCs) to improve the signal-to-noise ratio.

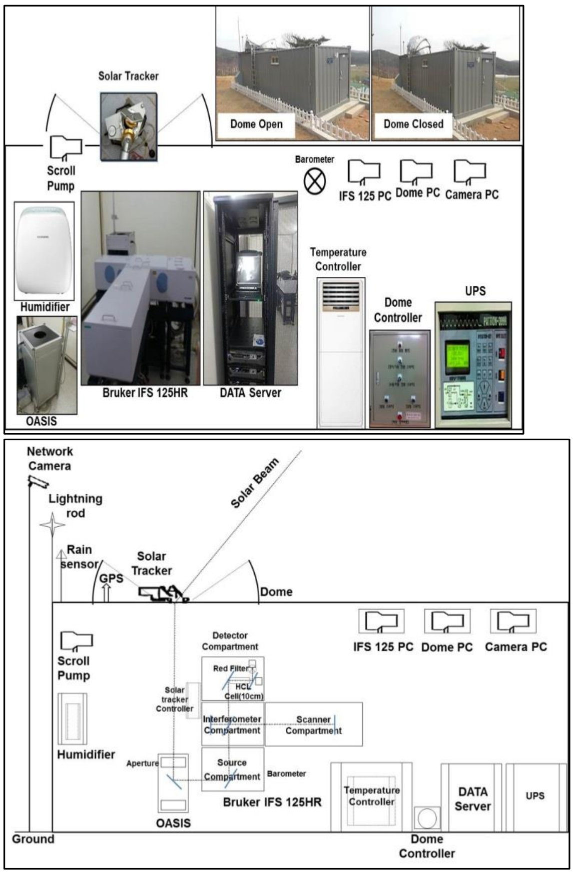

Figure 2. Photographs of the automated FTS laboratory. The Bruker Solar Tracker type A547 is mounted in the custom made dome. A servo controlled solar tracker directs the solar beam through a CaF_2 window to the FTS (125HR) in the laboratory. The server computer is used for data acquisition. PC1 and PC2 are used for controlling the spectrometer, solar tracker, dome, camera, pump, GPS satellite time, and humidity sensor.

The spectrometer is equipped with two room temperature detectors; an Indium-Gallium-Arsenide (InGaAs) detector, which covers the spectral region from 3,800 to 12,800 cm^{-1}, and Silicon (Si) diode detector (9,000 – 25,000 cm^{-1}) used in a dual-acquisition mode with a dichroic optic (Omega Optical, 10,000 cm^{-1} cut-on). A filter (Oriel Instruments 59523; 15,500 cm^{-1} cut-on) prior to the Si diode detector blocks visible light, which would otherwise be aliased into a near-infrared spectral domain. TCCON measurements are routinely recorded at a maximum optical path difference (OPD_{max}) of 45 cm leading to a spectral resolution of 0.02 cm^{-1}. Two scans, one forward and one backward, are performed and individual interferograms are recorded. As an example, Figure 3 shows a single spectrum recorded on 4 October 2014 with a resolution of

0.02 cm^{-1}. A single scan in one measurement takes about 110 s. Measurement setting for the Anmyeondo g-b FTS spectrometer of the Bruker 125HR model is summarized in Table 1. The pressure inside FTS is kept at 0.1 to 0.2 hPa with vacuum pump to maintain the stability of the system and to ensure clean and dry conditions.

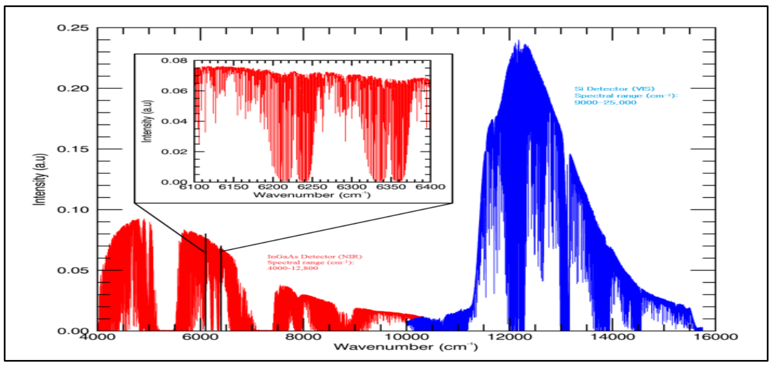

Figure 3. Single spectrum recorded on 4 October 2014 with a resolution of 0.02 cm^{-1}. A typical example for the spectrum of XCO_2 is shown in the inset.

Table 7. Measurement setting for the Anmyeondo g-b FTS spectrometer of the Bruker 125HR model.

Item	Setting
Aperture	0.8 mm
Detectors	RT-Si Diode DC, RT-InGaAs DC
Beamsplitters	CaF_2
Scanner velocity	10 kHz
Low pass filter	10 kHz
High folding limit	15798.007031
Spectral Resolution	0.02 cm^{-1}
Optical path difference	45 cm
Acquisition mode	Single sided, forward backward
Sample scan	2 scans
Sample scan time	~110 s

2.3 Characterization of FTS-instrumental line shapes

For the accurate retrieval of total column values of the species of interest, a good alignment of the g-b FTS is essential. The instrument line shape (ILS) is retrieved from the regular HCl cell measurement that is an important indicator of the status of the FTS's alignment (Hase et al., 1999). The analyses of the measurements were performed using a linefit spectrum fitting algorithm (LINEFIT14 software) (Hase et al., 2013). Here, we have carried out experiments to investigate the influences of ILS. We showed the time series of the phase error (rad) (left panel) and modulation efficiency (right panel) in the HCl measurement using the source of light from tungsten lamp in the period of October 2013 to September 2017, which is depicted in Figure 4. Modulation amplitudes for well alignment should be controlled in a limit of 5 % loss at the maximum optical difference (Wunch et al., 2011). In our g-b FTS measurements, it is found that the maximum loss of modulation efficiency is less than 1 %, which is quite close to the ideal value. The phase errors are less than 0.0001. Hase et al. (2013) reported that this level of small disturbances from the ideal value of the modulation efficiency is common to all well-aligned instruments. This result confirmed that the g-b FTS instrument is well aligned and stable during the whole operation period.

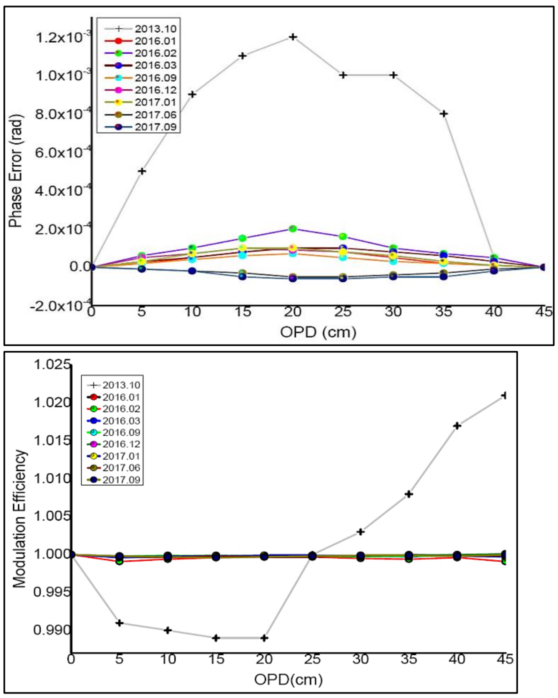

Figure 4. Phase error (rad) (left panel) and Modulation efficiency (right panel) of HCl measurements from the g-b FTS are displayed in the period from October 2013 to September 2017. Resolution = 0.015 cm^{-1}, Aperture = 0.8 mm.

We also confirmed that the ILS was not affected by the variable aperture during the operation of this system. The modulation efficiency and phase error were estimated to be 99.98 % and 0.0001 rad. Sun et al. (2017) reported the detailed characteristics of the ILS with respect to applications of different optical attenuators to FTIR spectrometers within the TCCON and NDACC networks. They used both lamp and sun cell measurements which were conducted after the insertion of five different attenuators in front of and behind the interferometer. In Sun et al.

(2017), the ILS result was indicated by considering optical attenuator number 1 which is in good agreement with our findings.

Table 2. Spectral windows used for the retrievals of the columns of CO_2 and O_2.

Gas	Center of spectral window (cm^{-1})	Width (cm^{-1})	Interfering gas
O_2	**7885.0**	**240.0**	**H_2O, HF, CO_2**
CO_2	**6220.0**	**80.0**	**H_2O ,HDO, CH_4**
CO_2	**6339.5**	**85.0**	**H_2O ,HDO**

2.4 Data processing

Within the TCCON standard retrieval strategy, we have derived the column-averaged dry-air mole fraction CO_2 (XCO_2) and other atmospheric gases (O_2, CO, CH_4, N_2O, and H_2O) using GFIT algorithm. The spectral windows used for the retrieval of CO_2 and O_2 are given in Table 2. The TCCON standard GGG2014 (version 4.8.6) retrieval software was used to obtain the abundance of the species from FTS spectra (Wunch et al., 2015). The XCO_2 is the ratio of retrieved CO_2 column to retrieved O_2 column,

$$XCO_2 = \frac{CO_{2\,\mathrm{column}}}{O_{2\,\mathrm{column}}} \times 0.2095\,, \qquad (1)$$

Computing the ratio using Eq. (1) minimizes systematic and correlated errors such as errors in solar zenith angle, surface pressure, and instrumental line shape that existed in the retrieved CO_2 and O_2 columns (Washenfelder et al., 2006, Messerschmidt et al., 2012). Top panel of Fig.6 depicts the time series of laser sampling error (LSE) obtained from InGaAs spectra at the Anmyeondo FTS station in the measurement period of February 2014 to December 2016. LSE is small and centered around zero in an ideal case. Slightly large LSE values were shown on 10 March, 2014 (see top panel of Fig. 7). On this date, we conducted the laser adjustment in FTS.

The X_{air} is a useful indicator of the quality of measurements and the instrument performance. The X_{air} would be unity for an ideal retrieval, however, due to spectroscopic limitations there is a TCCON wide bias and solar zenith angle (SZA) dependence. The retrieval of X_{air} deviating more than 1% from the nominal value of 0.98 would suggest a systematic error. The time series of X_{air} is shown in the bottom panel of Figure 5. The X_{air} record reveals that the instrument has been stable during the measurement period. It shows that the values of X_{air} are fluctuated between 0.974 and 0.985, and the mean value is 0.982 with a standard deviation of 0.0015 in which the scatter for X_{air} is about 0.15 %. The low variability in time series of X_{air} indicates the stability of the measurements.

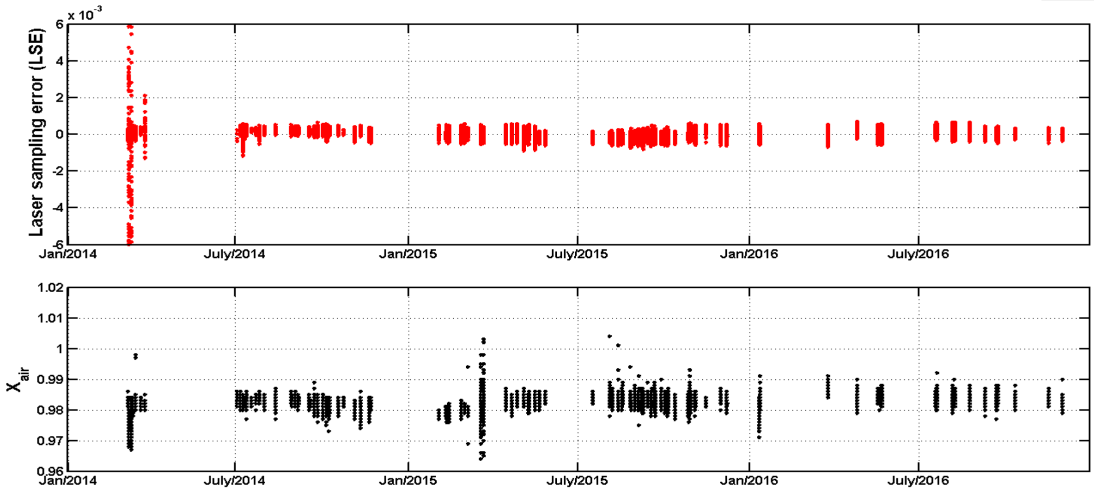

Figure 5. Time series of LSE (top panel) and X_{air} (bottom panel) from the g-b FTS during 2014- 2016 is shown. Each marker represents a single measurement.

2.5 Aircraft observation campaigns over Anmyeondo station

In this section, we have discussed a preliminary comparison results made between aircraft observations and g-b FTS over the Anmyeondo station. The aircraft campaign conducted over Anmyeondo station was monitored by National Institute of Meteorological Sciences (NIMS). The aircraft was equipped with a Wavelength Scanned Cavity Ring Down Spectrometer (CRDS; Picarro, G2401-mc) providing mixing ratio data recorded at 0.3 Hz intervals. The position of the aircraft was monitored by GPS, and information on the outside temperature, static pressure, and ground speed was provided by the aircraft's instruments. Data observed during ascent and descent of the aircraft are considered as vertical profiles of CO_2 and CH_4 over the measurement station. The temperature and pressure of the gas sample have to be tightly controlled at 45 ℃ and 140 Torr in the CRDS, which leads to highly stable spectroscopic features (Chen et al., 2010). Any deviations from these values cause a reduction of the instrument's precision. Data recorded beyond these range of variations in cavity pressure and temperature were discarded in this analysis. Variance of the cavity pressure and temperature in flight result in variance in the CO_2 and CH_4 mixing ratios. The Picarro CRDS instrument has been regularly calibrated with respect to the standard gases within the error range recommend by World Meteorological Organization (CO_2 is 380.23 ± 0.1 ppm, CH_4 is 1.825 ± 0.001 ppm)

Several aircraft observation campaigns over Anmyeondo station were carried out during the period between 2012 and 2016. However, a few numbers of aircraft data matched with the remote sensing instruments were available during this observation period. The total number of the aircraft measurements that matched with g-b FTS was only three and all those coincident observations were laid within a period of 2015. The g-b FTS retrieval of XCO_2 and XCH_4 were compared with aircraft measurements. Here, FTS data were averaged over a time window of ± 30 minutes with respect to the aircraft measurement time. In addition, the averaging kernel of the FTS was applied into the aircraft data. The g-b FTS data were corrected for an airmass-dependent artefact for XCO_2 and XCH_4, as well as calibrated with respect to TCCON common scaling factors. This scale factor was derived empirically using aircraft profiles over many TCCON sites in order to place the TCCON data on the WMO standard reference scales (Wunch et al. 2010) for both XCO_2 and XCH_4. This comparison study will be useful for ensuring that the TCCON common scale factors can be applied to our g-b FTS data. The statistical results for XCO_2 and XCH_4 comparisons between aircraft and g-b FTS are summarized in Table 3. The mean absolute difference between FTS and aircraft were found to be -0.798 ± 1.734 ppm, the corresponding mean relative differences of -0.196 ± 0.427 % for XCO_2, while the mean absolute difference of XCH_4 is -0.0079 ± 0.012 ppm, with a corresponding mean relative difference of -0.426 ± 0.632 %. These differences appeared on both species were consistent with the combined total errors of instruments. Wunch et al. (2010) reported that the uncertainties (2σ) of the TCCON common scale are approximately 0.2 % for XCO_2 and 0.4 % for XCH_4. It is determined that our g-b FTS uncertainty was found to be within this range of uncertainties and can be calibrated against WMO standard scale. Here, we also include some results from the aircraft campaign conducted in 2016, which was operated by KORUS-AQ (Korea-U.S.-Air Quality) joint program aiming at advancing the ability to monitor air pollution from space. Figure 6 illustrates the results of XCO_2 and XCH_4 comparisons between the aircraft observation and TCCON sites data. Light blue diamond marks show for Anmyeondo station. Our results laid within the indicated linear regression curves as with other TCCON sites.

Table 3. The statistical results for XCO_2 and XCH_4 comparisons between aircraft and g-b FTS are summarized

Instruments (Aircraft vs. g-b FTS)	No. of coincident measurement	Absolute difference (ppm)	Relative diff. (%)

XCO_2	3	-0.798 ± 1.734	-0.196 ± 0.427
XCH_4	3	-0.0079 ± 0.012	-0.426 ± 0.632

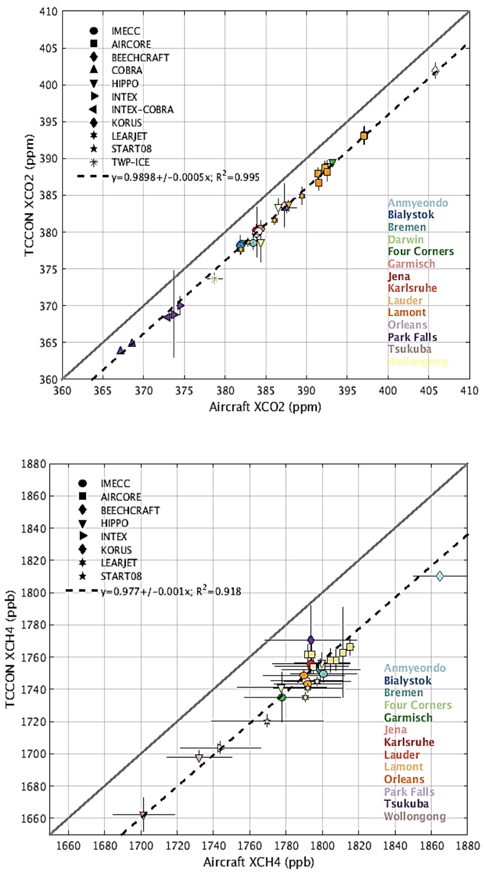

Figure 6. The comparisons of XCO_2 and XCH_4 between the aircraft observation and TCCON sites data are shown. The left side is XCO_2 and the right side is XCH_4 (light blue depicts for Anmyeondo station) .

2.6 OCO-2

Orbiting Carbon Observatory-2 (OCO-2) is NASA's first Earth-orbiting satellite, which was successfully launched on July 2, 2014 into low-Earth orbit. It is devoted to observing atmospheric carbon dioxide (CO_2) to get better insight for the carbon cycle. The primary mission is to measure carbon dioxide with high precision and accuracy in order to characterize its sources and sinks at different spatial and temporal scales (Boland et al., 2009; Crisp, 2008, 2015). The instrument measures the near infrared spectra (NIR) of sunlight reflected off the

Earth's surface. Using a retrieval algorithm, it provides results of atmospheric abundances of carbon dioxide and related atmospheric parameters at the nadir, sun glint and targets modes. Detailed information about the instrument is available in different papers (Connor et al., 2008; O'Dell et al., 2012). In this work, we used the OCO-2 version 7Br bias corrected data.

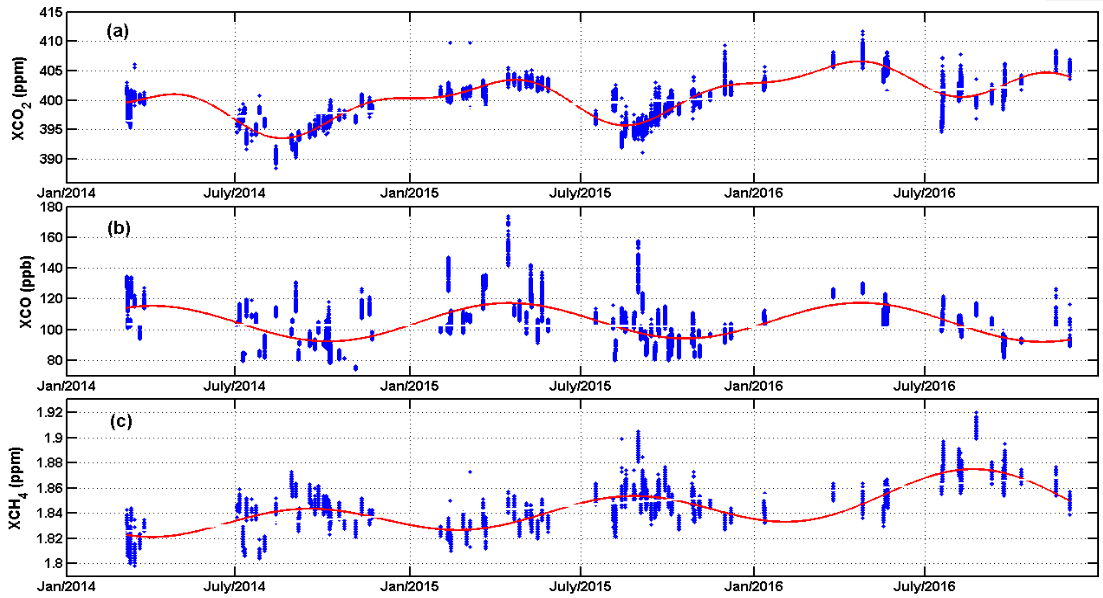

Figure 7. Time series of XCO_2, XCO, and XCH_4 from top to bottom panels (a-c), respectively in the period between February 2014 and December 2016 is given. Each marker indicates a single retrieval. Fitting curves (red solid lines) are also displayed.

Table 4. Annual mean of XCO_2, XCO, and XCH_4 from Anmyeondo g-b FTS from 2014 to 2016 is given.

	Annual mean ± standard deviation		
Gases	**2014**	**2015**	**2016**
XCO_2 (ppm)	**396.91 ± 2.55**	**399.32 ± 2.96**	**402.97 ± 2.74**
XCO (ppb)	**99.42 ± 14.71**	**102.73 ± 14.91**	**105.39 ± 10.68**
XCH_4 (ppm)	**1.837 ± 0.014**	**1.844 ± 0.015**	**1.864 ± 0.015**

3 Results and discussion

3.1 Time series of g-b FTS XCO_2, seasonal and annual cycle

The time series of XCO_2 along with retrievals of other trace gases such as XCO and XCH_4 from g-b FTS is presented in Figure 7 (panel a-c) during the period from February 2014 to December 2016. In such time series plots, each marker represents single retrievals, and the fitting curves of the retrieved values are also depicted (red solid line). We showed the seasonal cycle of XCO_2, XCO, and XCH_4 in the time series using a fitting procedure described by Thoning et al. (1989). Standard deviations of the differences between the retrieved values and the fitting curves are 1.42 ppm, 11.0 ppb, and 10.3 ppb for XCO_2, XCO, and XCH_4, respectively. It is evident that all species have a feature of seasonal cycle. Year to year variability of XCO_2 is highest in spring and lowest during the growing season in June to September. Moreover, the behavior of seasonal cycle of XCO_2 at our site was compared with that of XCO_2 at Saga, Japan, which is discussed in later section. The atmospheric increase of XCO_2 from 2015 to 2016 was 3.65 ppm which is larger than the increase from 2014 to 2015. For the case of XCH_4, its increase from 2015 to 2016 was 0.02 ppm which is higher than the increase from 2014 to 2015, whereas in XCO the rate of increment from year to year was found to be slightly decreased (see Table 4).

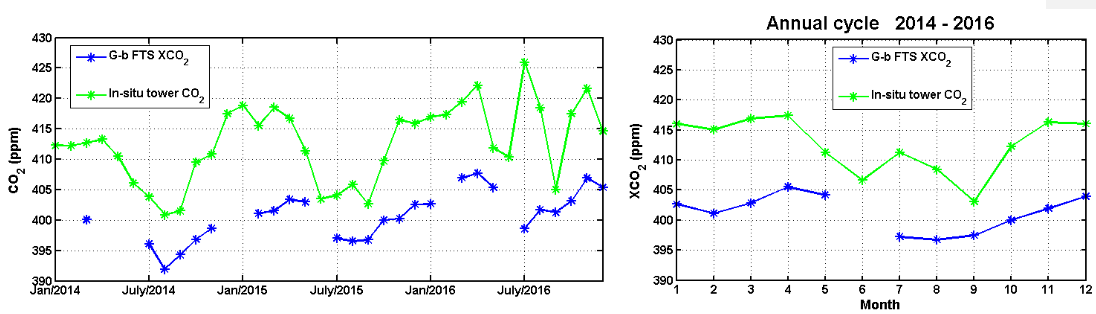

Figure 8. Left panel shows the time series of FTS XCO_2 and in-situ tower CO_2 on monthly mean basis, whereas right panel depicts annual cycle.

Moreover, the seasonal and annual cycles of XCO_2 derived from the g-b FTS were compared with in-situ tower observations of CO_2 over the Anmyeondo station, which are presented in Figure 8. Regarding in-situ data, samples were collected using flask using non-dispersive infrared (NDIR) method at the altitude of 77 meters above sea level at Anmyeondo station (36.53 N, 126.32 E) (details about data are available at http://ds.data.jma.go.jp/jmd/wdcgg/). Nearly 97 % of in-situ data were taken during day time between 04:00 – 08:40 UTC (13:00 – 17:40 Korea Standard Time (KST)) so that the early morning and night time observations of CO_2 were almost neglected. In-situ CO_2 monthly means are generated by first averaging all valid event measurements with a unique sample date and time. The values are then extracted at weekly intervals from a smooth curve (Thoning et al., 1989) fitted to the averaged data and then these weekly values are averaged for each month. As can be seen in Figure 8, the overall patterns of seasonal and annual cycle of FTS XCO_2 tend to be similar with that of in-situ tower CO_2 over there. This could suggest that the amplitude of seasonal cycle was likely to be driven by the imbalance of ecosystem exchange.

3.2 Correlations between XCO_2 and XCO

CO is co-emitted with CO_2 from combustion sources, leading to a significant positive correlation between them when combustion is a significant source of observed CO_2. The midday peaks for each gas reflect the influence of anthropogenic emissions. To examine this effect, we have determined the correlations between ΔXCO and ΔXCO_2 at our site. In order to compute the correlations, first we have selected hourly averaged data for both XCO and XCO_2 that were recorded between 06:00 and 07:00 UTC (i.e 15:00 and 16:00 LST, local standard time), excluding summer data, and then calculated the anomalies by subtracting the hourly averaged data from the mean of the selected data during the measurement period of February 2014 to December 2016. Figure 9 depicts the relationship between hourly CO_2 and CO means of anomalies at Anmyeondo during the whole measurement period, excluding summer data. CO_2 and CO had a correlation of 0.50, and this suggests that there is an influence of combustion emissions on CO_2. However, in a summer season, a negative relationship between them was identified at this site, with the small magnitude of correlation -0.22, and a correlation slope of -0.84. In Ohyama et al., (2015) paper, they derived the correlation coefficients and slopes of $\Delta XCO/\Delta XCO_2$ and $\Delta XCH_4/\Delta XCO$ in order to understand the short term variations of XCO_2, XCO, and XCH_4 in summer seasons during July 2011 and December 2014 at Saga, Japan. The trajectories for the summer season were classified into three types, depending on the origin of the air masses. The trajectories for types I, II, and III relate to transport of air masses from the Asian continent (China), Southeast Asia, and the Pacific Ocean, respectively. The negative slope of the $\Delta XCO/\Delta XCO_2$ ratio for the type I (slope was -3.15 ppb ppm^{-1}) gentler than for the type II (slope was -14.3 ppb ppm^{-1}), which was due to the transport of the air masses that experience the strong biospheric uptake of CO_2 over the Asia. This argument could support for our analysis at Anmyeondo station. The slope that we obtained in our station is close to the slope reported in type III case in Ohyama et al., (2015) paper.

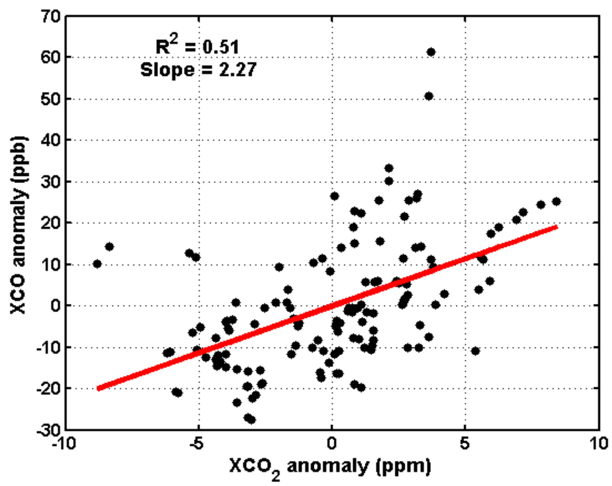

Figure 9. Correlation between XCO_2 versus XCO anomalies at Anmyeondo FTS station between February 2014 and December 2016, excluding summer data, is depicted.

In Wang et al (2010), the diurnal cycles of CO_2 signal was dominated by the biospheric activity from May to September, with a maximum drawdown of 39 ppmv in daily CO_2 in the summer at rural station near Beijing. Biospheric activity, however, has little impact on CO except for the CO source from in situ oxidation of biogenic hydrocarbons. They obtained that the correlation between CO_2 and CO in summer was insignificant. The correlation slope gives the emission ratio of CO to CO_2, which fluctuates with the sources of CO_2, depending on different combustion types and biospheric activity. In our case, the correlation slope of CO to CO_2 was found to be 2.27 ppb ppm^{-1} during the whole measurement period excluding summer, which is smaller than the correlation slope reported in Hefei FTS station where it was estimated to be 5.66 ppb ppm^{-1} (Wang et al., 2017 and references therein), which are primarily attributed to the smaller emission in CO.

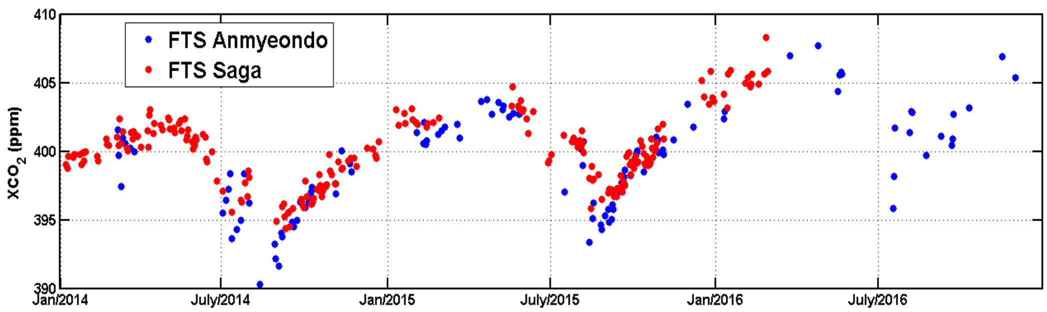

Figure 10. Time series of XCO_2 retrieval from Anmyeondo FTS and Saga FTS in the period of February 2014 to December 2016 is depicted.

3.3 Comparison of Anmyeondo XCO_2 with nearby TCCON station

We presented the comparison of our FTS XCO_2 data with a similar ground-based high resolution FTS observation at Saga TCCON station (33.26 N, 130.29 E) in Japan, which is the closest TCCON station to our site. Among those TCCON station, Rikubetsu, Tsukuba, and Saga are located in Japan (Morino et al., 2011, Ohyama et al., 2009, 2015) and Hefei is located in China (Wang et al., 2017). To demonstrate the comparison between them, we have shown the daily averaged XCO_2 of two stations during the period of 2014 to 2016 in Figure 10. As can be seen, variations of XCO_2 at the Saga station agreed well with Anmyeondo station. The daily averaged XCO_2 revealed the same seasonal cycle as that of our station. The lowest XCO_2 appeared in late summer (August and September), and the highest value was in spring (April).

Ohyama et al., (2015) studied the time series of XCO_2 at Saga, Japan during the period from July 2011 to December 2014. They showed seasonal and interannual variations over there. The peak-to-peak seasonal amplitude of XCO_2 was 6.9 ppm over Saga during July 2011 and December 2014, with a seasonal maximum and minimum in the average seasonal cycle during May and September, respectively. In recent finding of Wang et al. (2017), the g-b FTS temporal distributions of XCO_2 at Hefei, China were reported. The FTS observations in 2014 to 2016 had a clear seasonal cycle XCO_2 reaches a minimum in late summer, and then slowly increases to the highest value in spring. The daily average of XCO_2 ranges from 392.33 ± 0.86 to 411.62 ± 0.90 ppm, and the monthly average value shows a seasonal amplitude of 8.31 and 13.56 ppm from 2014 to 2015 and from 2015 to 2016, respectively. The seasonal cycle was mainly driven by biosphere–atmosphere exchange. Butz et al., (2011) reported that the observations from GOSAT and the co-located ground-based measurements agreed well in capturing the seasonal cycle of XCO_2 with the late summer minimum and the spring maximum for four TCCON stations

(Bialystok, Orleans, Park Falls, and Lamont) in the Northern Hemisphere. We inferred that the variation of XCO_2 over Anmyeondo station is in harmony with the variation pattern in elsewhere in mid-latitude Northern Hemisphere.

3.4 Comparison of XCO_2 between the g-b FTS and OCO-2

In this section, we present a comparison of XCO_2 between the g-b FTS and OCO-2 version 7Br data (bias corrected data) over Anmyeondo station during the period between 2014 and 2016. For making a direct comparison of the g-b FTS measurements against OCO-2, we applied the spatial coincidence criteria for the OCO-2 data within 3° latitude/longitude of the FTS station, as well as setting up a time window of 3 hours (maximum 3 h mismatch between satellite and g-b FTS observations). Based on the coincidence criteria, we obtained 13 coincident measurements, which were not sufficient to infer a robust conclusion. But it gives a preliminary result for indicating a level of agreement between them. The comparison of the time series of XCO_2 concentrations derived from the g-b FTS and OCO-2 on daily medians basis are demonstrated during the measurement period between 2014 and 2016, as depicted in Figure 11. As can be seen in the plot, the g-b FTS measurement exhibits some gaps occurred due to bad weather conditions, instrument failures, and absences of an instrument operator. In the present analysis, the XCO_2 concentrations from FTS were considered only when its retrieval error was below 1.50 ppm (it is not shown here), which is the sum of all error components such as laser sampling error, zero level offsets, ILS error, smoothing error, atmospheric apriori temperature, atmospheric apriori pressure, surface pressure, and random noise. Wunch et al. (2016) reported that the comparison of XCO_2 derived from the OCO-2 version 7Br data against a co-located ground-based TCCON data that indicates the median differences between the OCO-2 and TCCON data were less than 0.50 ppm, a corresponding RMS differences less than 1.50 ppm. The overall results of our comparisons were comparable with the report Wunch et al. (2016). The OCO-2 product of XCO_2 was biased (satellite minus g-b FTS) with respect to the g-b FTS, which was slightly higher by 0.18 ppm with a standard deviation of 1.19 ppm, a corresponding RMS difference of 1.16 ppm. This bias could be attributed to the instrument uncertainty. In addition to that, we also obtained a strong correlation between them, which was quantified as a correlation coefficient of 0.94 (see Table 5).

Table 5. Summary of the statistics of XCO_2 comparisons between OCO-2 and the g-b FTS from 2014 to 2016 are presented. N - coincident number of data, R - Pearson correlation coefficient, RMS - Root Mean Squares differences.

N	Mean Absolute. diff. (ppm)	Mean Relative diff (%)	R	RMS (ppm)
13	0.18±1.19	0.04±0.29	0.94	1.16

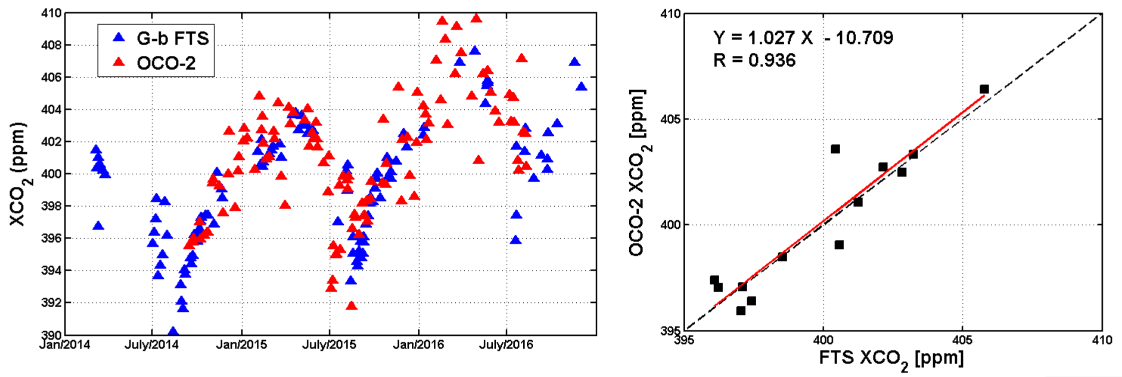

Figure 11. Left panel: The time series of XCO_2 from the g-b FTS (blue triangle) and OCO-2 (red triangle) over the Anmyeondo station from February 2014 to December 2016 are shown. Right panel: The linear regression curve between FTS and OCO-2 is shown. All results are given on daily medians basis.

Table 6. Seasonal mean and standard deviations of XCO_2 from the g-b FTS and OCO-2 in the period between 2014 and 2016 are given below.

Season	g-b FTS XCO_2 mean ± std (ppm)	OCO-2 XCO_2 mean ± std (ppm)
Winter	401.52 ± 0.85	402.67 ± 2.67
Spring	402.72 ± 2.79	403.96 ± 2.77
Summer	396.92 ± 3.28	399.68 ± 3.77
Autumn	398.01 ± 2.83	398.48 ± 2.41

Moreover, both instruments are generally agreed in capturing the seasonal variability of XCO_2 at the measurement station. As can be seen clearly from the temporal distribution of FTS XCO_2, the maximum and minimum values are discernible in spring and late summer seasons, respectively. It was found that its mean values in spring and summer were 402.72 and 396.92 ppm, respectively (see Table 6). This is because the seasonal variation of XCO_2 is most likely to be controlled by the imbalance of the terrestrial ecosystem exchange, and this could explain the larger XCO_2 values in the northern hemisphere in late April (Schneising et al. 2008, and references therein). The minimum value of XCO_2 occurs in August, which is most likely due to uptake of carbon into the biosphere in associated with the period of plant growth. Furthermore, both instruments showed high standard deviations during summer, which are about 3.28 ppm in FTS and 3.77 ppm in OCO-2, and this suggests that the variability reflects strong sources and sink signals.

4 Conclusions

Monitoring of greenhouse gases is an essential issue in the context of the global climate change. Accurate and precise continuous long-term measurements of the greenhouse gases (GHGs) are substantial for investigating their source and sinks. Nowadays, several remote sensing instruments operated on different platforms are dedicated for measuring GHGs. Greenhouse gases such as XCO_2, XCH_4, XH_2O, XN_2O measurements have been made using the g-b FTS at the Anmyeondo station since 2013. However, in this work, we focused on the measurements taken during the period of February 2014 to December 2016. The instrument has been operated in a semi-automated mode since then. The FTS instrument has been stable during the whole measurement period. Regular instrument alignments using the HCl cell measurements are performed. Thus, it guarantees the quality of the spectra. The TCCON standard GGG2014 retrieval software was used to retrieve XCO_2, XCO, and others GHG gases from the g-b FTS spectra.

In this work, the g-b FTS retrieval of XCO_2 and XCH_4 were compared with aircraft measurements that were conducted over Anmyeondo station. We obtained the mean absolute difference between FTS and aircraft were found to be -0.798 ± 1.734 ppm, the corresponding mean relative differences of -0.196 ± 0.427 % for XCO_2, while the mean absolute difference of XCH_4 is -0.0079 ± 0.012 ppm, with a corresponding mean relative difference of -0.426 ± 0.632 %. These differences appeared on both species were consistent with the combined total errors of instruments. The preliminary comparison results of XCO_2 between FTS and OCO-2 were also presented over the Anmyeondo station. The mean absolute difference of XCO_2 between FTS and OCO-2 was calculated on daily median basis, and it was estimated to be 0.18 ppm with a standard deviation of 0.19 with respect to the g-b FTS. This bias could be attributed with instrument uncertainty. Based on the seasonal cycle comparison, both the g-b FTS and OCO-2 illustrated a consistent pattern in capturing the seasonal variability of XCO_2, with maximum in spring and minimum in summer. In summer and fall, plants flourish and CO_2 is most likely to be consumed by photosynthesis. However, in winter and spring, weak photosynthesis phenomenon would be expected to occur because of low plant flourishing and CO_2 reaches the highest values particularly in April. Therefore, the outcome of this study reflects the suitability of the measurements for improving the understanding of the carbon cycle, as well as evaluating the remote sensing data.

5 Acknowledgements

This research was supported by the Research and Development for KMA Weather, Climate, and Earth system Services (NIMS-2016-3100). We would greatly acknowledge the two anonymous reviewers who helped us to improve this manuscript well.

References

Boland, S., Brown L. R., Burrows J. P., Ciais P., Connor B. J., Crisp D., Denning S., Doney S. C., Engelen R., Fung I. Y., Griffith P., Jacob D. J., Johnson B., Martin-Torres J., Michalak A. M., Miller C. E., Polonsky I., Potter C., Randerson J. T., Rayner P. J., Salawitch R. J., Santee M., Tans P. P., Wennberg P. O., Wunch D., Wofsy S. C., and Yung Y. L.: The Need for Atmospheric Carbon Dioxide Measurements from Space: Contributions from a Rapid Reflight of the Orbiting Carbon Observatory, 2009, http://www.nasa.gov/pdf/363474main_OCO_Reflight.pdf.

Brault, J. W.: New approach to high-precision Fourier transform spectrometer design. Appl. Opt. 35, 2891–2896, 1996.

Butz, A., Guerlet, S., Hasekamp, O., Schepers, D., Galli, A., Aben, I., Frankenberg, C., Hartmann, J.-M., Tran, H., Kuze, A., Keppel-Aleks, G., Toon, G., Wunch, D., Wennberg, P., Deutscher, N., Griffith, D., Macatangay, R., Messerschmidt, J., Notholt, J., and Warneke, T.: Toward accurate CO_2 and CH_4 observations from GOSAT, Geophys. Res. Lett., 38, L14812, https://doi.org/10.1029/2011GL047888, 2011.

Chen, H., Winderlich, J., Gerbig, C., Hoefer, A., Rella, C. W., Crosson, E. R., Van Pelt, A. D., Steinbach, J., Kolle, O., Beck, V., Daube, B. C., Gottlieb, E. W., Chow, V. Y., Santoni, G. W., and Wofsy, S. C: High-accuracy continuous airborne measurement of greenhouse gases (CO_2 and CH_4) using the cavity ring-down spectroscopy (CRDS) technique Atmos. Meas. Tech., 3, 375-386, 2010.

Connor B. J., Bösch H., Toon G., Sen B., Miller C. E., and Crisp D.: Orbiting carbon observatory: Inverse method and prospective error analysis, J. Geophys. Res., 113 doi: 10.1029/2006JD008336, 2008.

Crisp D., Miller C. E., DeCola P. L.: NASA Orbiting Carbon Observatory: measuring the column averaged carbon dioxide mole fraction from space. J. Appl. Remote Sens., 2, 023508, doi:10.1117/1.2898457, 2008.

Crisp D. for the OCO-2 Team: Measuring Atmospheric Carbon Dioxide from Space with the Orbiting Carbon Observatory-2 (OCO-2), Proc. SPIE 9607, Earth Observing Systems XX, 960702, doi: 10.1117/12.2187291, 2015.

Deutscher, N. M., Griffith, D. W. T., Bryant, G. W., Wennberg, P. O., Toon, G. C., Washenfelder, R. A., Keppel-Aleks, G., Wunch, D., Yavin, Y., Allen N. T., Blavier, J.-F., Jiménez R., Daube, B. C., Bright, A. V., Matross, D. M., Wofsy, S. C., and Park, S.: Total column CO_2 measurements at Darwin, Australia-site description and calibration against in situ aircraft profiles, Atmos. Meas. Tech., 3, 947-958, doi:10.5194/amt-3-947-2010, 2010.

Frankenberg, C., Pollock, R., Lee, R. A. M., Rosenberg, R., Blavier, J.-F., Crisp, D., O'Dell C. W., Osterman, G. B., Roehl, C., Wennberg, P. O., and Wunch, D.: The Orbiting Carbon Observatory (OCO-2): spectrometer performance evaluation using pre-launch direct sun measurements. Atmospheric Measurement Techniques, 8(1), 301–313. doi:10.5194/amt-8-301-2015, 2015.

Hase, F., Blumenstock, T., and Paton-Walsh, C.: Analysis of the instrumental line shape of high resolution Fourier transform IR spectrometers with gas cell measurements and new retrieval software, Appl. Optics, 38, 3417–3422, doi:10.1364/AO.38.003417,1999.

Hase, F., Drouin, B. J., Roehl, C. M., Toon, G. C., Wennberg, P. O., Wunch, D., Blumenstock, T., Desmet F., Feist, D. G., Heikkinen, P., De Mazière, M., Rettinger, M., Robinson, J., Schneider, M., Sherlock, V., Sussmann, R., Té Y., Warneke, T., and Weinzierl, C.: Calibration of sealed HCl cells used for TCCON instrumental line shape monitoring, Atmospheric Measurement Techniques, 6(12), 3527–3537, doi:10.5194/amt-6-3527-2013, 2013.

Kiel, M., Wunch, D., Wennberg, P. O., Toon, G. C., Hase, F., and Blumenstock, T.: Improved retrieval of gas abundances from near-infrared solar FTIR spectra measured at the Karlsruhe TCCON station, Atmos. Meas. Tech., 9(2), 669–682, doi:10.5194/amt-9-669-2016, 2016.

Kivi, R. and Heikkinen, P.: Fourier transform spectrometer measurements of column CO_2 at Sodankylä, Finland, Geosci. Instrum. Method. Data Syst., 5, 271–279, 2016.

Messerschmidt, J., Macatangay, R., Notholt, J., Petri C., Warneke, T., and Weinzierl, C.: Side by side measurements of CO_2 by ground-based Fourier transform spectrometry (FTS), Tellus B, 62(5), 749-758, doi:10.1111/j.1600-0889.2010.00491.x., 2010.

Messerschmidt, J., H. Chen, N. M. Deutscher, C. Gerbig, P. Grupe, K. Katrynski, F.-T. Koch, J. V. Lavrič, J. Notholt, C. Rödenbeck, W. Ruhe, T. Warneke, and Weinzierl, C.: Automated ground-based remote sensing measurements of greenhouse gases at the Białystok site in comparison with collocated in situ measurements and model data, Atmospheric Chemistry and Physics, 12(15), 6741–6755, doi:10.5194/acp-12-6741-2012, 2012.

Miao, R., Lu N., Yao L., Zhu, Y., Wang, J., and Sun, J.: Multi-Year Comparison of Carbon Dioxide from Satellite Data with Ground-Based FTS Measurements (2003–2011), Remote Sensing, 5(7), 3431–3456, doi:10.3390/rs5073431, 2013.

Miller, C. E., Crisp, D. DeCola, P. L., Olsen, S. C., Randerson, J. T., Michalak, A. M., Alkhaled, A., Rayner, P., Jacob, D. J., Suntharalingam, P., Jones, D. B. A., Denning, A. S., Nicholls, M. E., Doney, S. C., Pawson, S., Boesch, H., Connor B. J., Fung I. Y., O'Brien, D., Salawitch, R. J., Sander, S. P., Sen, B., Tans, P., Toon, G. C., Wennberg, P. O., Wofsy, S. C., Yung, Y. L., and Law, R. M.: Precision requirements for space-based XCO_2 data, J. Geophys. Res-Atmos., 109, D02301, doi: 10.1029/2006JD007659, 2007.

Morino, I., Uchino, O., Inoue, M., Yoshida, Y., Yokota T., Wennberg, P. O., Toon, G. C., Wunch, D., Roehl, C. M., Notholt, J., Warneke, T., Messerschmidt, J., Griffith, D. W. T., Deutscher, N. M., Sherlock, V., Connor, B. J., Robinson, J., Sussmann, R., and Rettinger, M.: Preliminary validation of column-averaged volume mixing ratios of carbon dioxide and methane retrieved from GOSAT short-wavelength infrared spectra, Atmospheric Measurement Techniques, 4(6), 1061-1076, doi:10.5194/amt-4-1061-2011, 2011.

O'Dell, C. W., Connor, B., Bösch, H., O'Brien, D., Frankenberg C., Castano, R., Christi, M., Eldering, D., Fisher, B., Gunson, M., McDuffie, J., Miller, C. E., Natraj, V., Oyafuso, F., Polonsky, I., Smyth, M., Taylor, T., Toon, G. C., Wennberg, P. O., and Wunch, D.: The ACOS CO2 retrieval algorithm – Part 1: Description and validation against synthetic observations, Atmospheric Measurement Techniques, 5, 99–121, doi: 10.5194/amt-5-99-2012, http://www.atmos-meas-tech.net/5/99/2012/, 2012.

Ohyama, H., Morino, I., Nagahama, T., Machida, T., Suto H., Oguma, H., Sawa, Y., Matsueda, H., Sugimoto, N., Nakane, H., and Nakagawa, K.: Column-averaged volume mixing ratio of CO_2 measured with ground-based Fourier transform spectrometer at Tsukuba, J. Geophys. Res., 114, D18303 doi:10.1029/2008JD011465, 2009.

Ohyama, H., Kawakami, S., Tanaka, T., Morino, Uchino, I., O., Inoue, M., Sakai, T., Nagai, T., Yamazaki, A., Uchiyama, A., Fukamachi, T., Sakashita, M., Kawasaki, T., Akaho, T., Arai, K., and Okumura, H.: Observations of XCO_2 and XCH_4 with ground-based high-resolution FTS at Saga, Japan, and comparisons with GOSAT products, Atmos. Meas. Tech., 8(12), 5263–5276, doi:10.5194/amt-8-5263-2015.

Rayner P. J., and O'Brien D. M.: The utility of remotely sensed CO_2 concentration data in surface source inversions, Geophys. Res. Lett., 28, 175–178, doi: 10.1029/2000GL011912, 2001.

Schneising O., Buchwitz M., Burrows J. P., Bovensmann, H., Reuter, M., Notholt, J., Macatangay, R., and Warneke, T.: Three years of greenhouse gas column-averaged dry air mole fractions retrieved from satellite-Part 1: Carbon dioxide, Atmos. Chem. Phys., 8, 3827-3853, 2008.

Sun, Y., Palm, M., Weinzierl, C., Peteri, C., Notholt, J., Wang, Y., and Liu, C.: Technical note: Sensitivity of instrumental line shape monitoring for the ground-based high-resolution FTIR spectrometer with respect to different optical attenuators, Atmos. Meas. Tech. Discuss., doi:10.5194/amt-10-989- 2017.

Thoning, K. W., Tans, P. P. and Komhyr, W. D.: Atmospheric carbon dioxide at Mauna Loa Observatory. Analysis of the NOAA GMCC Data, 1974-1985, J. Geophys. Res., 94, 8549-8565, 1989.

WMO (2016). The state of greenhouse gases in the atmosphere based on global observations through 2015, greenhouse gas. Greenhouse Gas Bulletin 2016. https://library.wmo.int/opac/doc_num.php.

Wang, W., Tian, Y., Liu, C., Sun, Y., Liu, W., Xie, P., Liu, J., Xu, J., Morino, I., Velazco, V., Griffith, D., Notholt, J., and Warneke, T.: Investigating the performance of a greenhouse gas observatory in Hefei, China, Atmos. Meas. Tech., 10, 2627–2643, 2017.

Wang, Y., Munger, J. W., Xu, S., McElroy, M. B., Hao, J., Nielsen, C. P., and Ma, H.: CO2 and its correlation with CO at a rural site near Beijing: implications for combustion efficiency in China, Atmos. Chem. Phys., 10, 8881–8897, https://doi.org/10.5194/acp-10-8881-2010, 2010.

Washenfelder R. A., Toon G. C., Blavier J-F., Yang Z., Allen N. T., Wennberg P. O., Vay S. A., Matross, D. M., and Daube B. C.: Carbon dioxide column abundances at the Wisconsin Tall Tower site, Journal of Geophysical Research, 2006, 111, doi:10.1029/2006JD00715, 2006.
Warneke, T., Yang, Z., Olsen, S., Korner, S., Notholt J., Toon, G. C., Velazco, V., Schultz, A., and Schrems, O.: Seasonal and latitudinal variations of column averaged volume-mixing ratios of atmospheric CO_2, Geophysical Research Letters, 32(3), 2-5, doi:10.1029/2004GL021597, 2005.

Wunch, D., Toon G. C., Wennberg, P. O., Wofsy, S. C., Stephens, B., Fisher, M. L., Uchino O., Abshire, J. B., Bernath, P. F., Biraud, S. C., Blavier, J.-F. L., Boone, C. D., Bowman, K. P., Browell, E. V., Campos, T., Connor, B. J., Daube, B. C., Deutscher, N. M., Diao M., Elkins, J. W., Gerbig, C., Gottlieb, E., Griffith, D. W. T., Hurst, D. F., Jiménez, R., Keppel-Aleks, G., Kort, E. A., Macatangay, R., Machida, T., Matsueda, H., Moore, F. L., Morino, I., Park, S., Robinson, J., Roehl, C. M., Sawa, Y., Sherlock, V., Sweeney, C., Tanaka, T., and Zondlo, M. A.: Calibration of the Total Carbon Column Observing Network using aircraft profile data, Atmospheric Measurement Techniques, 3(5), 1351-1362, doi:10.5194/amt-3-1351-2010.

Wunch, D., Toon, G. C., Sherlock, V., Deutscher, N. M., Liu X., Feist, D. G., and Wennberg, P. O.: The Total Carbon Column Observing Network's GGG2014 Data Version. doi:10.14291/tccon.ggg2014.documentation.R0/1221662, 2015.

Wunch, D., Wennberg, P.O.,, Osterman, G., Fisher, B., Naylor, B., Roehl, C. M., O'Dell, C., Mandrake, L.,Viatte, C., Griffith, D. W. T., Deutscher, N. M., Velazco, V. A., Notholt, J.,Warneke, T.,Petri, C., Maziere, M. De, Sha, M. K., Sussmann,R., Rettinger, M., Pollard, D., Robinson, J.,Morino, I., Uchino O., Hase, F., Blumenstock, T., Kiel, M., Feist, D. G., Arnold S.G., Strong, K., Mendonca, J., Kivi, R.,Heikkinen, P., Iraci, L., Podolske, J., Hillyard, P. W., Kawakami, S., Dubey, M. K., Parker, H. A., Sepulveda, E., Rodriguez, O. E. G., Te, Y., Jeseck, P., Gunson, M. R., Crisp, D., and Eldering A., Comparisons of the Orbiting Carbon Observatory-2 (OCO-2) XCO_2 measurements with TCCON, Atmos. Meas. Tech. Discuss., doi:10.5194/amt-2016-227, 2016.

Co-authors and TCCON member Second comment revision

Characteristics of Greenhouse Gas Concentrations Derived from Ground-based FTS Spectra at Anmyeondo, Korea

Young-Suk Oh[1,2*], Samuel Takele Kenea[1], Tae-Young Goo[1], Kyu-Sun Chung[2], Jae-Sang Rhee[1], Mi-Lim Ou[5], Young-Hwa Byun[1], Paul O. Wennberg[4,5], Matthäus Kiel[4], Voltaire A. Velazco[3] and David W. T. Griffith[3]

1. Climate Research Division, National Institute of Meteorological Sciences (NIMS), Jeju-do, Republic of Korea
2. Department of Electrical Eng. & Centre for Edge Plasma Science, Hanyang University, Seoul, Republic of Korea
3. School of Chemistry, University of Wollongong, Northfields Ave, Wollongong, NSW 2522, Australia
4. Division of Geological and Planetary Sciences, California Institute of Technology, 1200E. California Boulevard, Pasadena, CA, 91125, USA
5.Division of Engineering and Applied Science, California Institute of Technology, 1200E. California Boulevard, Pasadena, CA, 91125, USA
5. Climate Change Monitoring Division, Korea Meteorological Administration, Seoul, Republic of Korea

*Correspondence to: Young-Suk Oh (ysoh306@gmail.com)

Abstract.

Since the late 1990s, the meteorological observatory established in Anmyeondo (36.5382° N, 126.3311° E, and 30 m above mean sea level), has been monitoring several greenhouse gases such as CO_2, CH_4, N_2O, CFCs, and SF_6, as a part of the Global Atmosphere Watch (GAW) Program. A high resolution ground-based (g-b) Fourier Transform Spectrometer (FTS) was installed at this observation site in 2013, and has been operated within the framework of the Total Carbon Column Observing Network (TCCON) since August, 2014. The solar spectra recorded by the g-b FTS cover the spectral range 3,800 to 16,000 cm^{-1} at a resolution of 0.02 cm^{-1} during the measurement period between 2014 and the present. In this work, the GGG2014 version of the TCCON standard retrieval algorithm was used to retrieve total column average CO_2 mole fractions (XCO_2) from the FTS spectra. Spectral bands of CO_2 (at 6220.0 and 6339.5 cm^{-1} centre wavenumbers, CH_4 at xxx wavenumber, and O_2 near 7880 cm^{-1}) were used to derive the XCO_2 and XCH_4. In this paper, we provide comparisons of XCO_2 and XCH_4 between the aircraft observations and g-b FTS over Anmyeondo station. A comparison of 13 coincident observations of XCO_2 between g-b FTS and OCO-2 (Orbiting Carbon Observatory) satellite measurements are also presented for the measurement period between February 2014 and November 2017. OCO-2 exhibited a slight positive bias with respect to the g-b FTS, approximately 0.189 ppm with the standard deviation of 1.19 ppm, and revealed a strong correlation (R=0.94). Based on seasonal cycle comparisons, both instruments generally agreed in capturing seasonal variations of the target species with maximum and minimum values in spring and late summer, respectively. In the future, it is planned to further utilize the FTS measurements for the evaluation of satellite observations such as Greenhouse Gases Observing Satellite (GOSAT, GOSAT-2). This is the first report of the g-b FTS observations of XCO_2 species over the Anmyeondo station.

Key words: Aircraft**,** XCO_2, OCO-2, TCCON, Infrared spectra

1. Introduction

Monitoring of greenhouse gases (GHGs) is a crucial issue in the context of global climate change. Carbon dioxide (CO_2) is one of the key greenhouse gases and its global annual mean concentration has increased rapidly from 278 to 400 ppm since the preindustrial data of 1750 (WMO greenhouse gas bulletin, 2016). Radiative forcing due to changes in atmospheric CO_2 accounts for approximately 65 % of the total change in radiative forcing by long-lived GHGs (Ohyama et al., 2015 and reference therein). Human activities such as burning of fossil fuels and land use change are the primary drivers of the continuing increase in atmospheric greenhouse gases and the gases involved in their chemical production (Kiel et al., 2016 and reference therein). There is a global demand for accurate and precise long-term measurements of greenhouse gases.

In the field of remote sensing techniques, solar absorption infrared spectroscopy has been increasingly used to determine changes in atmospheric constituents. Today, a number of instruments deployed on various platforms (ground-based and space-borne) have been operated for measuring GHGs such as CO_2. Our g-b FTS at the Anmyeondo station has been measuring several atmospheric GHG and other gases such as CO_2, CH_4, CO, N_2O, and H_2O operated within the framework of the Total Carbon Column Observing Network (TCCON). XCO_2 retrievals from the g-b FTS have been reported at different TCCON sites (e.g, Ohyama et al., 2009; Deutscher et al., 2010; Messerschmidt et al., 2010, 2012; Miao et al., 2013; Kivi and Heikkinen, 2016). TCCON achieves accuracy and precision in measuring the column averaged dry air mole fraction of CO_2 (XCO_2), of about 0.25 %, or better than 1 ppm (Wunch et al., 2010), which is essential to retrieve information about sinks and sources, as well as validating satellite products (Rayner and O'Brien, 2001; Miller et al., 2007). Precision for XCO_2 of 0.1 % can be achieved during clear sky conditions (Messerschmidt et al., 2010; Deutscher et al., 2010). The network aims to improve global carbon cycle studies and supply the primary validation data of different atmospheric trace gases for space-based instruments, e.g., the Orbiting Carbon Observatory 2 (OCO-2), the Greenhouse Gases Observing Satellite (GOSAT, GOSAT-2) (Morino et al., 2011; Frankenberg et al., 2015).

This study is focused on the initial characteristics of XCO_2 retrievals from g-b FTS spectra over the Anmyeondo station, and comparison with in situ aircraft overflights and the OCO-2 satellite. The FTS spectra have been processed using the TCCON standard GGG2014 (Wunch et al.,

2015) retrieval software. One of the unique aspects in this work is a new homemade addition to our g-b FTS instrument that reduces the solar intensity variations from the 5% maximum allowed in TCCON to less than 2%. This paper presents an introduction to the instrumentation and measurement site, and provides initial results and discussion followed by conclusions.

2 Station and instrumentation

2.1 Station description

The g-b FTS observatory was established in 2013 at the Anmyeondo (AMY) station located at 36.32˚ N, 126.19˚ E, and 30 m above sea level. This station is situated on the west coast of the Korean Peninsula, 180 km SE of Seoul, the capital city of Republic of Korea. Figure 1 displays the Anmyeondo station. It is also a regional GAW (Global Atmosphere Watch) station that is operated by the Climate Change Monitoring Network of KMA (Korean Meteorological Administration). The AMY station has been monitoring various atmospheric parameters such as greenhouse gases, aerosols, ultraviolet radiation, ozone, and precipitation since 1999. The total area of the Anmyeondo island is estimated to be ~88 km^2 and approximately 1.25 million people reside on the island. Some of the residents over this area are engaged in agricultural activities. Vegetated areas consisting of mainly pine trees are located in and around the FTS observatory. The topographic feature of the area is one of low level hills, on average about 100 m above sea level. The minimum temperature in winter is on average 2.7 ˚C, and the maximum temperature is about 25.6 ˚C during summer. Average annual precipitation amount is 1,155 mm with snow winter. The site has been formally designated as a provisional TCCON site since August 2014. Full acceptance requires calibration via overflights with WMO-calibrated in situ vertical profiles, as described in this paper. The AMY Station's TCCON wiki page can be found at: [https://tccon-wiki.Anmyeondo.edu]

메모 [Office1]: ??

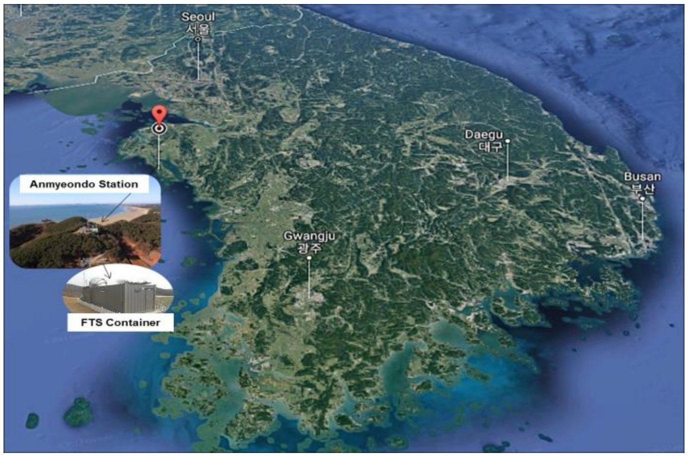

Figure 1. Anmyeodo (AMY) g-b FTS station

2.2 G-b FTS instrument

Solar spectra are acquired using a Bruker IFS 125HR spectrometer (Bruker Optics, Germany) under the guidelines set by TCCON. Currently, our g-b FTS instrument operation is semi-automated for taking the routine measurements under clear sky conditions. It is planned to make an FTS operation mode fully automated by 2018. The solar tracker (A547, Bruker Optics, Germany) is mounted inside a remotely controlled protective dome. The tracking ranges in azimuthal and elevation angles are about 0 to 315 and -10 to 85 degrees, respectively, while the tracking speed is about 2 degrees per second. The tracking accuracy of ±4 minutes of arc is achieved by the Camtracker mode which centres an image of the sun onto the spectrometer's input field stop. Under clear sky conditions, the dome is opened and set to an automatic tracking mode, in which the mirrors are initially moved to the calculated solar position, then. the camtracker control is activated in such a way that the mirrors are finely and continuously controlled to fix the beam onto the entrance stop of the spectrometer. Figure 2 displays an overview of the general data acquisition system. This ensures that all spectra are recorded under clear weather conditions.

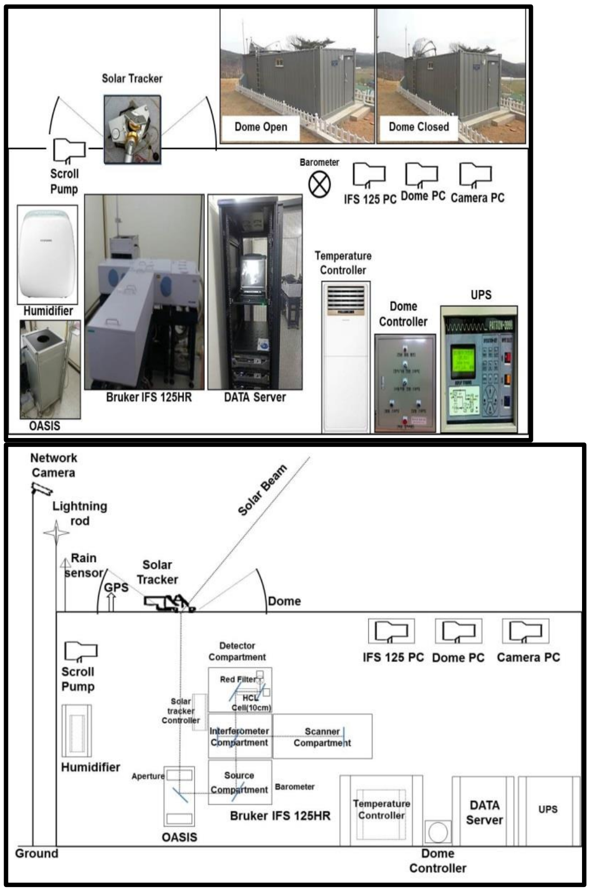

Figure 2. Photographs of the automated FTS laboratory. The Bruker Solar Tracker type A547 is mounted in the custom made dome. A servo controlled solar tracker directs the solar beam through a CaF_2 window to the FTS (125HR) in the laboratory. The server computer is used for data acquisition. PC1 and PC2 are used for controlling the spectrometer, solar tracker, dome, camera, pump, GPS satellite time, and humidity sensor.

The spectrometer is equipped with two room temperature detectors; an Indium-Gallium-Arsenide (InGaAs) detector, which covers the spectral region from 3,800 to 12,800 cm^{-1}, and Silicon (Si) diode detector (9,000 – 25,000 cm^{-1}) used in a dual-acquisition mode with a dichroic optic (Omega Optical, 10,000 cm^{-1} cut-on). A red longpass filter (Oriel Instruments 59523; 15,500 cm^{-1} cut-on) prior to the Si diode detector blocks visible light, which would otherwise be aliased into the near-infrared spectral domain. TCCON measurements are routinely recorded at a maximum optical path difference (OPD_{max}) of 45 cm leading to a spectral resolution of 0.02 cm^{-1} (0.9/max OPD). Two scans, one forward and one backward, are performed and individual forward-backward interferograms are recorded. As an example, Figure 3 shows a single spectrum recorded on 4 October 2014 with a resolution of 0.02 cm^{-1}. A single forward-backward scan in one measurement takes about 112 s. Measurement setting for the Anmyeondo g-b FTS spectrometer of the Bruker 125HR model is summarized in Table 1. The pressure inside the FTS is kept at 0.1 to 0.2 hPa with an oil-free vacuum pump to maintain the stability of the system and to ensure clean and dry conditions.

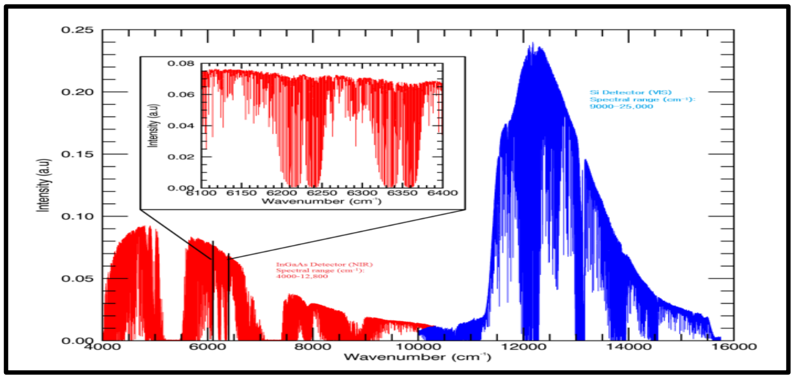

Figure 3. Single spectrum recorded on 4 October 2014 with a resolution of 0.02 cm^{-1}. A typical example for the spectrum of XCO_2 is shown in the inset.

Table 1. Measurement setting for the Anmyeondo g-b FTS spectrometer of the Bruker 125HR model.

Item	Setting
Aperture (field stop)	0.8 mm
Detectors	RT-Si Diode DC, RT-InGaAs DC
Beamsplitters	CaF_2
Scanner velocity	10 kHz
Low pass filter	10 kHz
High folding limit	15798.007
Spectral Resolution	0.02 cm^{-1}
Optical path difference	45 cm
Acquisition mode	Single sided, forward backward
Sample scan	2 scans, forward, backward
Sample scan time	~110 s

2.3 Characterization of FTS-instrumental line shapes

For the accurate retrieval of total column amounts of the species of interest, a good alignment of the g-b FTS is essential. The instrument line shape (ILS) retrieved from the regular HCl cell measurements is an important indicator of the status of the FTS's alignment (Hase et al., 1999). The analyses of the measurements were performed using a spectrum fitting algorithm (LINEFIT14 software) (Hase et al., 2013). In Figure 4 we show time series of the modulation efficiency (lift panel) and phase error (rad) (right panel) from the HCl cell measurement in the period of October 2013 to September 2017 using a tungsten lamp as light source. Modulation amplitudes for TCCON-acceptable alignment should be within 5 % of the ideal case (100%) at the maximum optical path difference (Wunch et al., 2011). In our g-b FTS measurements, it is found that the maximum loss of modulation efficiency is within 1 %, close to the ideal value. The phase errors are less than ± 0.0001 rad. Hase et al. (2013) reported that this level of small disturbances from the ideal value of the modulation efficiency is common to all well-aligned instruments. This result confirmed that the g-b FTS instrument is well aligned and has remained stable during the whole operation period.

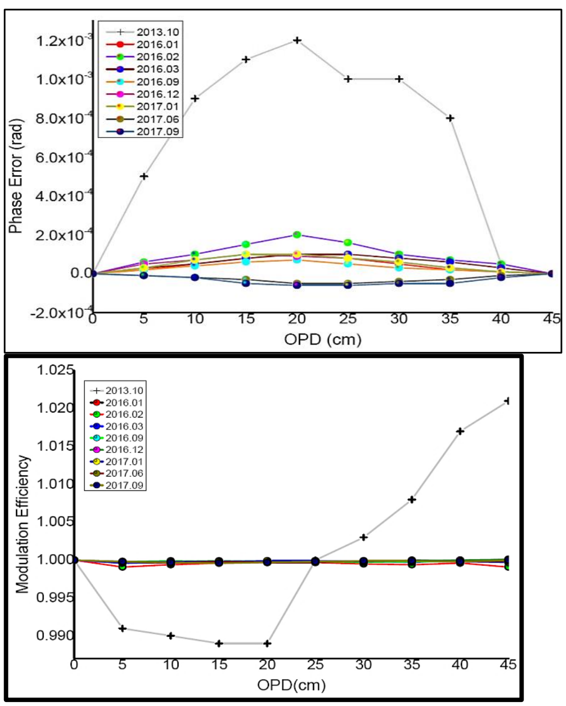

Figure 4. Modulation efficiency (left panel) and Phase error (rad) (right panel) of HCl measurements from the g-b FTS are displayed in the period from October 2013 to September 2017. Resolution = 0.02 cm^{-1}, Aperture = 0.8 mm.

We also confirmed that the ILS was not affected by the variable aperture (OASIS) during the operation of this system (see section 2.5) The modulation efficiency and phase error were estimated to be 99.98 % and 0.0001 rad. Sun et al. (2017) reported the detailed characteristics of the ILS with respect to applications of different optical attenuators to FTIR spectrometers within the TCCON and NDACC networks. They used both lamp and sun as light sources for the cell measurements, which were conducted after the insertion of five different attenuators in front of and behind the interferometer. In Sun et al. (2017).

2.4 Data processing

Using the TCCON standard retrieval strategy, we have derived the column-averaged dry-air mole fraction CO_2 (XCO_2) and other atmospheric gases (O_2, CO, CH_4, N_2O, and H_2O) using the GFIT algorithm and software. The spectral windows used for the retrieval of CO_2 and O_2 are given in Table 2. The TCCON standard GGG2014 (version 4.8.6) retrieval software was used to obtain the abundance of the species from FTS spectra (Wunch et al., 2015). XCO_2 is derived from the ratio of retrieved CO_2 column to retrieved O_2 column,

, (1)

메모 [Office2]: doesn't render in my word version.

Computing the ratio using Eq. (1) minimizes systematic and correlated errors such as errors in solar zenith angle pointing error, surface pressure, and instrumental line shape that may exist in the retrieved CO_2 and O_2 columns (Washenfelder et al., 2006, Messerschmidt et al., 2012). The top panel of Figure 5 depicts the time series of laser sampling error (LSE) obtained from InGaAs spectra at the Anmyeondo FTS station in the measurement period of February 2014 to December 2016. LSE is due to inaccuracies in the laser sample timing, which have been reduced to acceptable levels by the instrument manufacturer. In the AMY FTS, the LSE is small and centered around zero. Slightly large LSE values were shown on 10 March, 2014 (see top panel of Fig. 5). On this date, we conducted the laser adjustment in FTS.

Table 2. Spectral windows used for the retrievals of the columns of CO_2 and O_2

Gas	**Center of spectral window (cm^{-1})**	Width (cm^{-1})	Interfering gas
O_2	7885.0	240.0	H_2O, HF, CO_2
CO_2	6220.0	80.0	H_2O ,HDO, CH_4
CO_2	6339.5	85.0	H_2O ,HDO

X_{air} is the ratio of atmospheric pressure to total column O_2, scaled such that for a perfect measurement X_{air} = 1.0. X_{air} is a useful indicator of the quality of measurements and the instrument performance. Due to spectroscopic limitations there is a TCCON-wide bias (X_{air} ~ 0.98) and small solar zenith angle (SZA) dependence. The retrieval of X_{air} deviating more than 1% from the TCCON-wide mean value of 0.98 would suggest a systematic error. The time series of X_{air} is shown in the bottom panel of Figure 5. The X_{air} record reveals that the instrument has been stable during the measurement period. It shows that the values of X_{air} fluctuate between 0.974 and 0.985, and the mean value is 0.982 with a standard deviation of 0.0015 in which the scatter for X_{air} is about 0.15 %. The low variability in time series of X_{air} indicates the stability of the measurements.

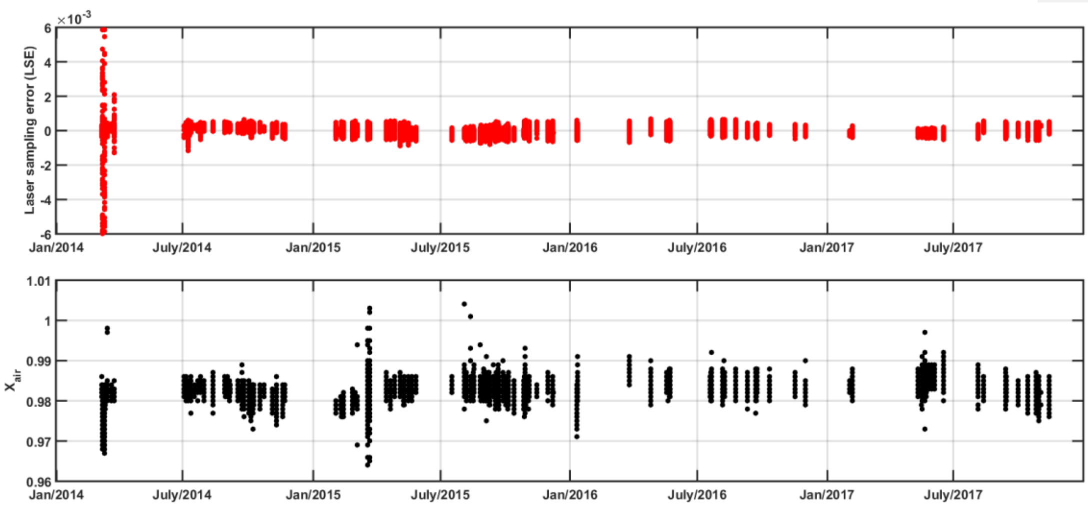

Figure 5. Time series of LSE (top panel) and X_{air} (bottom panel) from the g-b FTS during 2014- 2017 is shown. Each marker represents a single measurement.

2.5 Operational Automatic System for the Intensity of Sunray (OASIS) effect on the retrieval results

The OASIS system was developed for improving the quality of the spectra recorded by the spectrometer by maintaining a constant signal level. OASIS is beneficial for minimizing the variability that may be induced in the spectra due to intensity fluctuations of the incoming solar radiation that reaches the instrument. The main function of the OASIS is to control an aperture diameter in the parallel-inlet beam to the interferometer. This aperture is placed inside the OASIS system, in the parallel input solar beam external to the FTS**.** The fundamental purpose of this system is to optimize the measurement of solar spectra by reducing the effect of the fluctuations of the intensity of the incoming light due to changes in thin clouds along the line of sight over the measurement site. The maximum threshold value of the solar intensity variation (SIV) is 5 %, the TCCON standard value (Ohyama et al., 2015). This value has been reduced to ≤ 2 % in our case by introducing the OASIS system to our g-b FTS since December 2014.

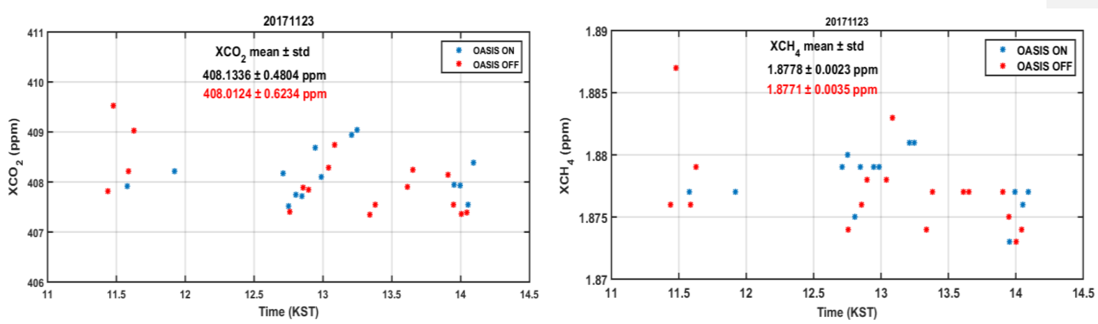

Figure 6. G-b FTS XCO_2 (left panel) and XCH_4 (right panel) values as function of time in KST (Korean Standard time, UTC+9) taken October 23, 2017 with OASIS system on (operating) and off (without operating) positions are shown. Each marker represents a single measurement.

In order to assess the impact of OASIS system on the retrieval results of XCO_2 and XCH_4, we have conducted experiments on recording alternate FTS spectra with and without operation of this system under clear sky conditions. As an example, Figure 6 depicts the retrieval results of XCO_2 (left panel) and XCH_4 (right panel) as a function of time (KST, UTC+9), taken November 23, 2017 with OASIS on (blue) and off (red) positions. Mean differences of 0.12 ppm for XCO_2 and 7.0×10^{-4} ppm for XCH_4 were found between OASIS on and off position (i.e., with and without operating of OASIS system). This suggests that the impact of OASIS system on the retrieval is negligible.

메모 [VV3]: Already defined

메모 [VV4]: Convert to parts per billion (ppb)

2.6 Aircraft observation campaigns over Anmyeondo station

2.6.1 Aircraft instrumentation

In this section, we discuss a preliminary comparison between aircraft in situ observations and g-b

FTS column measurements over the Anmyeondo station. In situ profiles were conducted over Anmyeondo station by the National Institute of Meteorological Sciences (NIMS) and as part of the KORUS-AQ from NASA's DC8 .

메모 [Office5]: What kind of airplane?

For the NIMS profiles, the flight take-off and landing was carried out from Hanseo University which is approximately 5 km away from Anmyeondo FTS station. The aircraft was equipped with a Wavelength Scanned Cavity Ring Down Spectrometer (CRDS; Picarro, G2401-m) (see Fig. 7) providing mixing ratio data recorded at 0.3 Hz intervals. The position of the aircraft was monitored by GPS, and information on the outside temperature, static pressure, and ground speed was provided by the aircraft's instruments. The temperature and pressure of the gas sample have to be tightly controlled at 45 ℃ and 140 Torr in the CRDS, which leads to highly stable spectroscopic features (Chen et al., 2010). Any deviations from these values cause a reduction of the instrument's precision. Data recorded beyond these range of variations in cavity pressure and temperature were discarded in this analysis. Variance of the cavity pressure and temperature in flight result in variance in the CO_2 and CH_4 mixing ratios. The Picarro CRDS instrument has been regularly calibrated with respect to the standard gases within the error range recommend by World Meteorological Organization (CO_2 is 380.23 ± 0.1 ppm, CH_4 is 1.825 ± 0.001 ppm). Measurements were made in wet air, and dry air mixing ratio were derived following method of Chen et al. (2010). [I assume that water was measured and you correctly accounted for water in the column integration?]

메모 [DG6]: You should say what range of pressure and temperature was acceptable

메모 [DG7]: The meaning of these numbers is not clear – are these values for single calibration tanks?

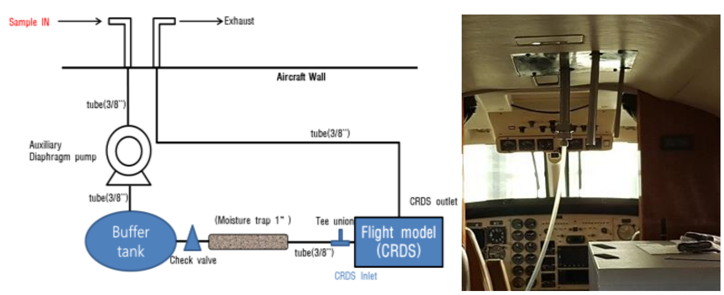

Figure 7. CRDS instrument on board of the aircraft.

On NASA’s DC8, CO2 was measured by xx instrument with yy precision and accuracy. CH4 was measured by zz, and water was measured by zz. The aircraft static pressure and altitude were recorded using zz. As with the NIMS profiles, the vertical profiles of CO_2 and CH_4 mixing ratio were obtained during an upward and a downward spiral flight centred on the Anmyeondo

메모 [DG8]: Needs to be completed, after contacting the KORUS in situ team.

2.6.2 Aircraft CO_2 and CH_4 data

The vertical profiles of CO_2 and CH_4 mixing ratio were obtained by NIMS during upward and a downward spiral flights centred on the Anmyeondo FTS station, on 29 October and 12 November, 2017. As an example, the flight trajectory on 29 October, 2017 is shown in the left panel of Figure 8 while the profiles of CO_2 and CH_4 from flight during the ascent and descent are depicted in the middle and right panels. All flights occurred under clear sky conditions,. The campaign measurements were performed over 2 hours. Specifically, the respective measurements were taken from 11:00:37 to 12:03:25 KST (UTC+9) and from 13:58:58 to 15:19:40 KST on 29 October, 2017 and similarly from 11:12:20 to 12:13:00 KST and from 14:14:46 to 15:14:46 KST on 12 November, 2017. Thealtitude ranges of the aircraft measurements were limited to approximately from 0.1 to a maximum of 9.1 km., we constructed the complete CO_2 and CH_4 profiles in a similar way to that of by Deutscher et al. 2010; Miyamoto et al. (2013); Ohyama et al. (2015). For both CO_2 and CH_4 profiles, we extend the lowermost observations of aircraft profiles to the surface level, and above the aircraft ceiling, the mole fractions throughout the altitude range between the uppermost aircraft and the tropopause is assumed to be the same as at the highest aircraft measurement level because we have no other information. This extrapolation produces the largest uncertainty in the in situ column estimate. For this analysis, the tropopause height was derived from NOAA National Centers for Environmental Prediction/National Center

메모 [Office9]: Does the surface in situ measurement at Anmyeondo agree with the lowest aircraft point? Why don’t you use these?

for Atmospheric Research Reanalysis datasets which are provided in every 6 hours interval (0:00, 06:00, 12:00, and 18:00 UTC) with a horizontal resolution of 2.5 by 2.5 degrees. The measurements of surface pressure were available at the FTS stations, which we have used for calculating the XCO_2 and XCH_4. Above the tropopause height, GFIT a priori profiles were utilized., the completed aircraft profiles based on those assumptions were transformed into a total column XCO_2 and XCH_4 by pressure weighting functions. For this comparison, we considered only the FTS averaged XCO_2 and XCH_4 retrieval values for the corresponding aircraft measurement time. Details about the aircraft XCO_2 and XCH_4 values during ascending and descending aircraft flight duration and the corresponding FTS averaged XCO_2 and XCH_4 retrieval values are also provided in Table 3. the vertically resolved FTS column-averaging kernels were taken into account for smoothing the aircraft profiles. The XCO_2 and XCH_4 for the aircraft in situ profile weighted by the column averaging kernel a (Rodgers and Connor, 2003) is computed as follows: ?]

where is the column-averaged dry air mole fraction for the apriori profile (CO_2 or CH_4), is the aircraft profile and is the pressure weighting function.

We estimated the uncertainty of the XCO_2 and XCH_4 columns derived from the extended aircraft profile by assigning uncertainties. Uncertainty at the surface was assumed to be same as the uncertainty in the lowest measurements. For the stratosphere, we used the method suggested by Wunch et al. (2010). This method shifts the stratospheric values up and down by 1 km to calculate the difference in column, which is used as an estimate of the uncertainty in the location of the tropopause and therefore for the stratospheric contribution. We estimated the stratospheric errors in aircraft integrated amount of XCO_2 and XCH_4 by shifting the apriori profile by 1 km (Ohyama et al. 2015). It was found to be 0.08 ppm for XCO_2 and 6 ppb for XCH_4.

Tor the NASA DC8 measurements, the in situ profiles extended from xx to yy meters. We extrapolated from the lowest measurements to the surface using ??? and from the highest point to the tropopause (estimated by NCEP to be at zz km).

Figure 9 illustrates the results of XCO_2 and XCH_4 comparisons between the aircraft observation

메모 [DG10]: Were they scaled to be the same as the tropospheric profile at the tropopause?

메모 [Office11]: Here is where the water is needed, because you need to weight by the dry pressure.

메모 [Office12]: Please double check this – it seems far too small (see Matt's figures for our estimates of this uncertainty).

and TCCON sites data. In the bottom panels, light blue diamond marks show for Anmyeondo station. Our results laid within the indicated linear regression curves as with other TCCON sites.

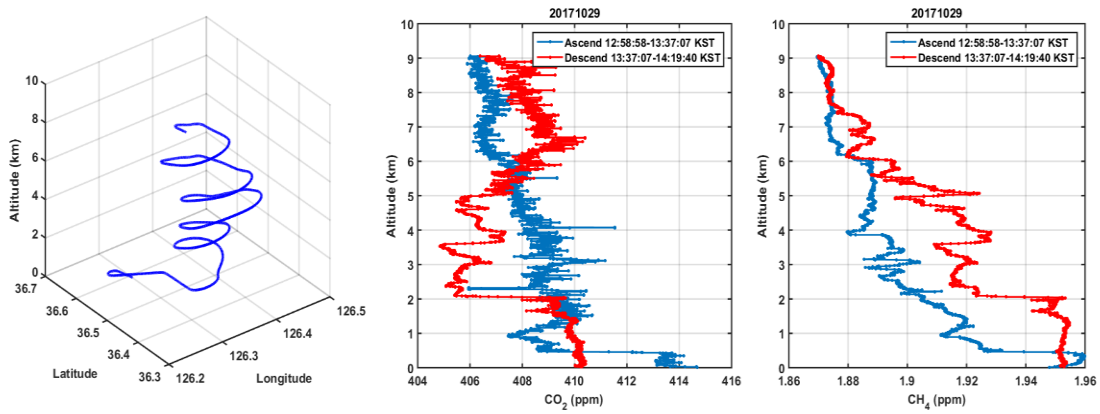

Figure 8. Typical flight path (left panel) and CO_2 (middle panel) and CH_4 (right panel) VMR profiles during ascending and descending of the aircraft over Anmyeondo on October 29, 2017 are shown.

Table 3. Summary of the column average dry-air mole fractions obtained during the inter-comparison between the in-situ instrument on board the aircraft and the g-b FTS at the Anmyeondo station. A and D represent ascending and descending, respectively. Note that FTS values given below are without removing TCCON common scale factor.

Date of measurements (hours in KST)	**Aircraft NIMS XCO_2 (ppm)**	**g-b FTS XCO_2 (ppm)**	**Aircraft NIMS XCH_4 (ppm)**	**g-b FTS XCH_4 (ppm)**
2017-10-29				
09:59:16-10:31:08 (A)	409.179(409.428)	408.408	1.8895(1.8904)	1.8904
10:31:09-11:03:24 (D)	409.008(409.201)	408.039	1.8849(1.8850)	1.8898
12:58:58-13:37:07 (A)	406.979(407.073)	405.184	1.8554(1.8551)	1.8705
13:37:07-14:19:40 (D)	406.664(406.842)	404.665	1.8715(1.8715)	1.8688
2017-11-12				
11:12:20-11:38:01 (A)	405.996(406.099)	405.980	1.8509(1.8513)	1.8660
11:38:02-12:13:00 (D)	406.420(406.540)	406.072	1.8514(1.8515)	1.8658
14:14:46-14:45:55 (A)	406.776(406.962)	405.730	1.8474(1.8482)	1.8639
14:45:56-15:23:47 (D)	407.424(407.798)	405.610	1.8498(1.8511)	1.8629
Mean ± std	**407.3061 ±1.178**	**406.211± 1.3244**	**1.862± 0.0169**	**1.8723± 0.0113**
	KORUS	**TCCON**	**KORUS**	**TCCON**
2016-05-22	405.80 ± 0.42	401.91 ± 0.57	1.8641± 0.0132	1.8100±0.002

Difference in XCO_2 (FTS-CRDS) = 406.0243 - 406.6458 = -0.625 ppm

Difference in XCH_4 (FTS-CRDS) = 1.8658 – 1.8613 = 0.0045 ppm

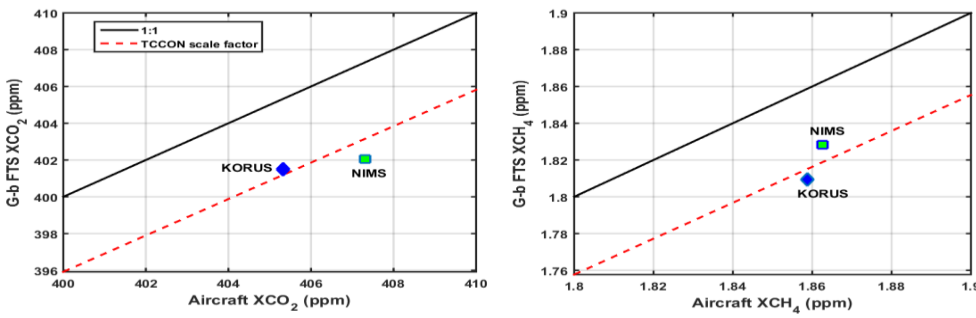

Figure 9. The comparisons of XCO_2 and XCH_4 between the aircraft observation and g-b FTS data over Anmyeondo station are shown. The diamond symbol represents for the aircraft campaign conducted by KORUS (May, 2016), whereas square symbol indicates for the aircraft campaign operated by NIMS (2017). Note that FTS values shown in the figure are after removing TCCON common scale factor.

메모 [Office13]: Add error bars

2.7 Comparison with OCO-2 measurements

The Orbiting Carbon Observatory-2 (OCO-2) is NASA's first Earth-orbiting satellite dedicated to greenhouse gas measurement, it was successfully launched on July 2, 2014 into low-Earth orbit. It is devoted to observing atmospheric carbon dioxide (CO_2) to provide improved insight into the carbon cycle. The primary mission is to measure carbon dioxide with high precision and accuracy in order to characterize its sources and sinks at different spatial and temporal scales (Boland et al., 2009; Crisp, 2008, 2015). The instrument measures the near infrared spectra (NIR) of sunlight reflected off the Earth's surface. Atmospheric abundances of carbon dioxide and related atmospheric parameters are retrieved from the spectra in nadir, sun glint and target modes. Detailed information about the instrument is available in, for example (Connor et al., 2008; O'Dell et al., 2012). In this work, we used the OCO-2 version 7Br bias corrected data. The comparisons are discussed in section 3.4.

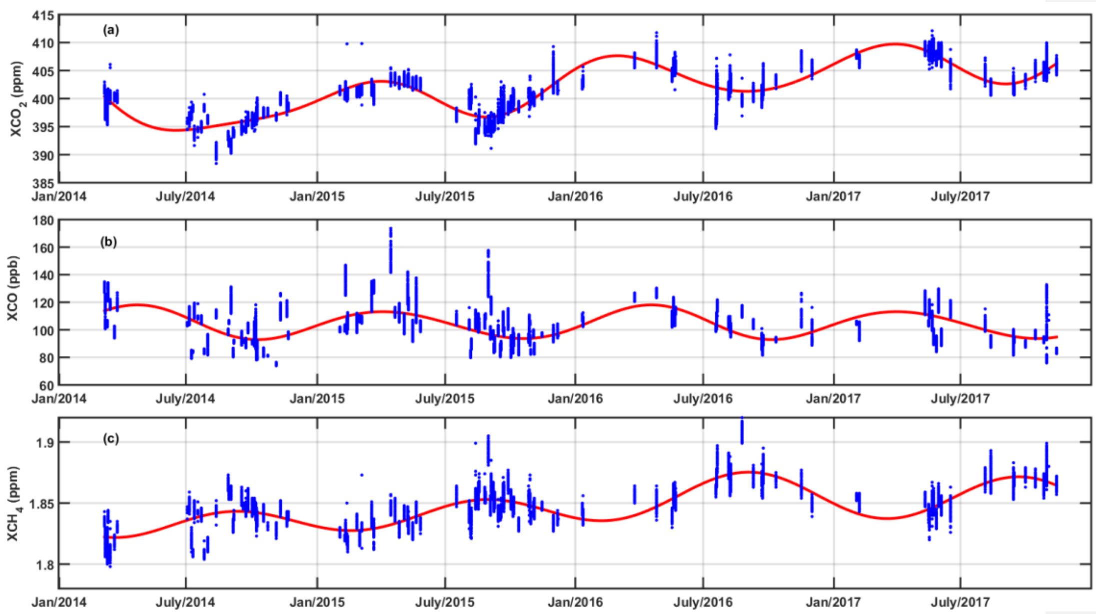

Figure 10. Time series of XCO_2, XCO, and XCH_4 from top to bottom panels (a-c), respectively in the period between February 2014 and November 2017 is given. Each marker indicates a single retrieval. Fitting curves (red solid lines) are also displayed.

Table 4. Annual mean of XCO_2, XCO, and XCH_4 from Anmyeondo g-b FTS from February 2014 to November 2017 is given.

	Annual mean ± standard deviation			
Gases	**2014**	**2015**	**2016**	**2017**
XCO_2 (ppm)	**396.91 ± 2.55**	**399.32 ± 2.96**	**402.97 ± 2.74**	**406.04 ± 2.38**
XCO (ppb)	**99.42 ± 14.71**	**102.73 ± 14.91**	**105.39 ± 10.68**	**100.14 ± 10.3**
XCH_4 (ppm)	**1.837 ± 0.014**	**1.844 ± 0.015**	**1.864 ± 0.015**	**1.859 ± 0.013**

3 Results and discussion

3.1 Time series of g-b FTS XCO_2, seasonal and annual cycle

The time series of XCO_2 along with retrievals of other trace gases such as XCO and XCH_4 from g-b FTS is presented in Figure 10 (panel a-c) for the period from February 2014 to November 2017. In these time series plots, each marker represents a single retrieval, and the fitting curves of the retrieved values are also depicted (red solid line). We show the seasonal cycle of XCO_2, XCO, and XCH_4 in the time series using a fitting procedure described by Thoning et al. (1989). Standard deviations of the differences between the retrieved values and the fitting curves are 1.64 ppm, 11.34 ppb, and 10.1 ppb for XCO_2, XCO, and XCH_4, respectively. It is evident that all species have a seasonal cycle feature. Year to year variability of XCO_2 is highest in spring and lowest during the growing season in June to September. Moreover, the behavior of the seasonal cycle of XCO_2 at our site was compared with that of XCO_2 at Saga, Japan, which is discussed in a later section. The atmospheric increase of XCO_2 from 2015 to 2016 was 3.65 ppm, which is larger than the increase from 2014 to 2015. For the case of XCH_4, its increase from 2015 to 2016 was 0.02 ppm, which is higher than the increase from 2014 to 2015, whereas in XCO the rate of increment from year to year was found to be slightly decreased (see Table 4).

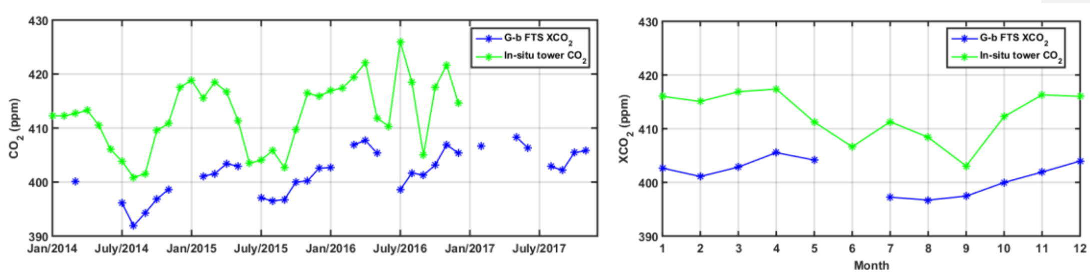

Figure 11. Left panel shows the time series of FTS XCO_2 and in-situ tower CO_2 on monthly mean basis, whereas right panel depicts annual cycle (2014-2016).

메모 [DG14]: The Yaxes should have the same label, one is CO2 and one is XCO2

The seasonal and annual cycles of XCO_2 derived from the g-b FTS were compared with in-situ tower observations of CO_2 over the Anmyeondo station, which are presented in Figure 11. Regarding in-situ data, samples were collected using flasks and analysed using non-dispersive infrared (NDIR) spectroscopy at the altitude of 77 meters above sea level (details about in situ data are available at http://ds.data.jma.go.jp/jmd/wdcgg/). Nearly 97 % of in-situ data in Figure 11 were taken during day time between 04:00 – 08:40 UTC (13:00 – 17:40 Korea Standard Time (KST)) so that the early morning and night time enhancements of CO_2 were mostly excluded. In-situ CO_2 monthly means are generated by first averaging all valid event measurements with a unique sample date and time. The values are then extracted at weekly intervals from a smooth curve (Thoning et al., 1989) fitted to the averaged data and then these weekly values are averaged for each month. As can be seen in Figure 10, the overall patterns of seasonal and annual cycle of FTS XCO_2 tend to be similar with those of in-situ tower CO_2.

3.2 Correlations between XCO_2 and XCO

CO is co-emitted with CO_2 from combustion sources, leading to a significant positive correlation between them when combustion is a significant source of observed CO_2. The midday peaks for each gas reflect the influence of anthropogenic emissions. To examine this effect, we have determined the correlations between ΔXCO and ΔXCO_2 at our station. In order to compute the correlations, first we have selected hourly averaged data for both XCO and XCO_2 that were recorded between 06:00 and 07:00 UTC (i.e., 15:00 and 16:00 LST, local standard time), and then calculated the anomalies by subtracting the hourly averaged data from the mean of the selected data during the measurement period of February 2014 to November 2017. Figure 12 depicts the relationship between hourly CO_2 and CO means of anomalies at Anmyeondo during the whole measurement period, excluding summer data. CO_2 and CO had a correlation coefficient (R^2) of 0.33, and this suggests that there is small influence of combustion emissions on CO_2. However, in a summer season, a negative relationship between CO and CO_2 was identified at this site, with the small magnitude of correlation R= -0.22, and a correlation slope of R= -0.84. Ohyama et al., (2015) derived the correlation coefficients and slopes of $\Delta XCO/\Delta XCO_2$ and $\Delta XCH_4/\Delta XCO$ in order to understand the short term variations of XCO_2, XCO, and XCH_4 in summer seasons during July 2011 and December 2014 at Saga, Japan. The trajectories for the summer season were classified into three types, depending on the origin of the air masses. The trajectories for types I, II, and III relate to transport of air masses from the Asian continent (China), Southeast Asia, and the Pacific Ocean, respectively. The negative slope of the $\Delta XCO/\Delta XCO_2$ ratio for the type I (slope was -3.15 ppb ppm^{-1}) gentler than for the type II (slope was -14.3 ppb ppm^{-1}), which was due to the transport of the air masses that experience the strong biospheric uptake of CO_2 over the Asia. This argument could support our analysis at Anmyeondo station. The slope that we obtained in our station is close to the slope reported in type III case in Ohyama et al., (2015) paper.

메모 [Office15]: I strongly suggest you remove this section. Your method produces a simple seasonal correlation diagram for co2:co and has little to do with their sources – especially the local sources. To get at the source CO:CO2 you have to use a method such as Debra used for the Los Angeles study where you look at daily/short term anomalies.

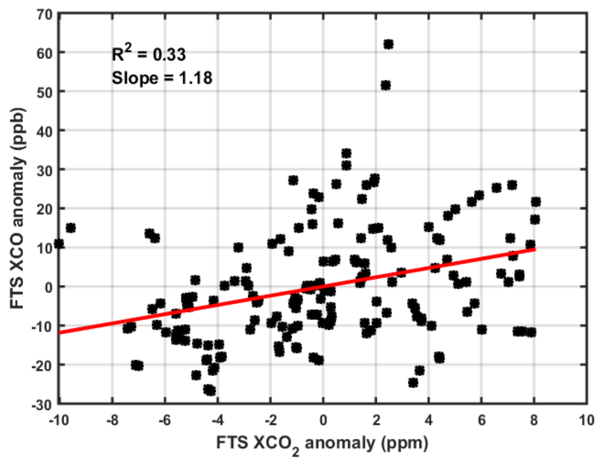

Figure 12. Correlation between XCO_2 versus XCO anomalies at Anmyeondo FTS station between February 2014 and November 2017, excluding summer data, is depicted.

In Wang et al (2010), the diurnal cycles of CO_2 signal was dominated by the biospheric activity from May to September, with a maximum drawdown of 39 ppmv in daily CO_2 in the summer at rural station near Beijing. Biospheric activity, however, has little impact on CO except for the CO source from in situ oxidation of biogenic hydrocarbons. Wang et al (2010) found insignificant correlation between CO_2 and CO in summer. The correlation slope gives the emission ratio of CO to CO_2, which fluctuates with the sources of CO_2, depending on different combustion types and biospheric activity. In our case, the correlation slope of CO to CO_2 was found to be 1.18 ppb ppm^{-1} during the whole measurement period excluding summer, which is smaller than the correlation slope reported in Hefei FTS station where it was estimated to be 5.66 ppb ppm^{-1} (Wang et al., 2017 and references therein). Our result is primarily attributed to the smaller emissions of CO near our coastal, rural site.

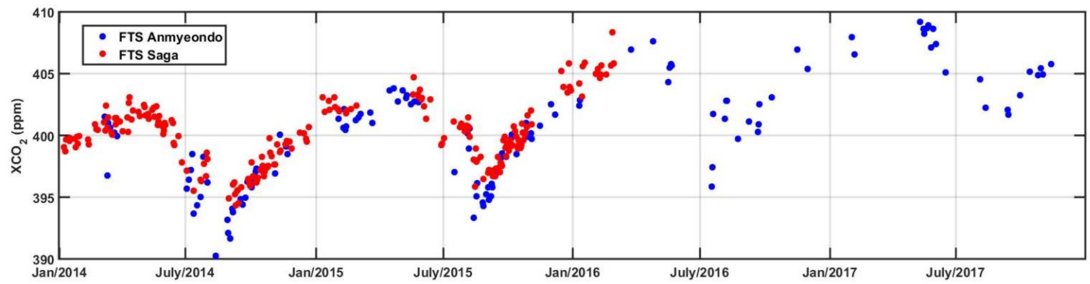

Figure 13. Time series of daily averaged XCO_2 retrieval from Anmyeondo FTS and Saga FTS in the period of February 2014 to November 2017 is depicted.

3.3 Comparison of Anmyeondo XCO_2 with nearby TCCON station

In Figure 13, we present the comparison of our FTS XCO_2 data with a similar ground-based high resolution TCCON FTS observation at Saga station (33.26 N, 130.29 E) in Japan, which is the closest TCCON station to our site. Among nearby TCCON stations, Rikubetsu, Tsukuba, and Saga are located in Japan (Morino et al., 2011, Ohyama et al., 2009, 2015) and Hefei is located in China (Wang et al., 2017). To demonstrate the comparison between them, we have shown the daily averaged XCO_2 of two stations during the period of 2014 to 2017 in Figure 13. As can be seen, variations of XCO_2 at the Saga station agreed well with Anmyeondo station. The daily averaged XCO_2 revealed the same seasonal cycle as that of our station. The lowest XCO_2 appeared in late summer (August and September), and the highest value was in spring (April).

Ohyama et al., (2015) studied the time series of XCO_2 at Saga, Japan during the period from July 2011 to December 2014. They showed seasonal and interannual variations. The peak-to-peak seasonal amplitude of XCO_2 was 6.9 ppm over Saga during July 2011 and December 2014, with a seasonal maximum and minimum in the average seasonal cycle during May and September, respectively. In recent findings of Wang et al. (2017), the g-b FTS temporal distributions of XCO_2 at Hefei, China were reported. The FTS observations in 2014 to 2016 had a clear and similar seasonal cycle, i.e. XCO_2 reaches a minimum in late summer, and then slowly increases to the highest value in spring. The daily average of XCO_2 ranges from 392.33 ± 0.86 to 411.62 ± 0.90 ppm, and the monthly average value shows a seasonal amplitude of 8.31 and 13.56 ppm from 2014 to 2015 and from 2015 to 2016, respectively. The seasonal cycle was mainly driven by large scale (hemispheric) biosphere–atmosphere exchange. Butz et al., (2011) reported that the observations from GOSAT and the co-located ground-based measurements agreed well in capturing the seasonal cycle of XCO_2 with the late summer minimum and the spring maximum for four TCCON stations (Bialystok, Orleans, Park Falls, and Lamont) in the Northern Hemisphere. We infer that the variation of XCO_2 over Anmyeondo station is in harmony with the variation pattern in mid-latitude Northern Hemisphere.

3.4 Comparison of XCO_2 between the g-b FTS and OCO-2

In this section, we present a comparison of XCO_2 between the g-b FTS and OCO-2 version 7Br data (bias corrected data) over Anmyeondo station during the period between 2014 and 2017. For making a direct comparison of the g-b FTS measurements against OCO-2, we applied the spatial coincidence criteria for the OCO-2 data within 3° latitude/longitude of the FTS station, as well as setting up a time window of 3 hours (maximum 3 hours mismatch between satellite and g-b FTS observations). Based on the coincidence criteria, we obtained 13 coincident measurements, which were not sufficient to infer a robust conclusion, but do provide a preliminary result. The comparison of the time series of XCO_2 concentrations derived from the g-b FTS and OCO-2 on daily median basis is demonstrated during the measurement period between 2014 and 2017, depicted in Figure 14. As can be seen in the plot, the g-b FTS measurement exhibits some gaps which occurred due to bad weather conditions, instrument failures, and absences of an instrument operator. In the present analysis, the XCO_2 concentrations from FTS were considered only when retrieval error was below 1.50 ppm (not shown), which is the sum of all error components such as laser sampling error, zero level offsets, ILS error, smoothing error, atmospheric a-priori temperature, atmospheric a-priori pressure, surface pressure, and random noise. Wunch et al. (2016) reported that the comparison of XCO_2 derived from the OCO-2 version 7Br data against co-located ground-based TCCON data that indicates the median differences between the OCO-2 and TCCON data were less than 0.50 ppm and corresponding RMS differences of less than 1.50 ppm. The overall results of our comparisons were comparable with the report of Wunch et al. (2016). The OCO-2 product of XCO_2 was biased (satellite minus g-b FTS) with respect to the g-b FTS, which was slightly higher by 0.18 ppm with a standard deviation of 1.19 ppm, a corresponding RMS difference of 1.16 ppm. This bias could be attributed to the instrument uncertainty. In addition to that, we also obtained a strong correlation between the two datasets, which was quantified as a correlation coefficient of 0.94 (see Table 5 and Figure 14).

Table 5. Summary of the statistics of XCO_2 comparisons between OCO-2 and the g-b FTS from 2014 to 2017 are presented. N - coincident number of data, R - Pearson correlation coefficient, RMS - Root Mean Squares differences.

N	Mean Absolute. diff. (ppm)	Mean Relative diff (%)	R	RMS (ppm)
13	0.18±1.19	0.04±0.29	0.94	1.16

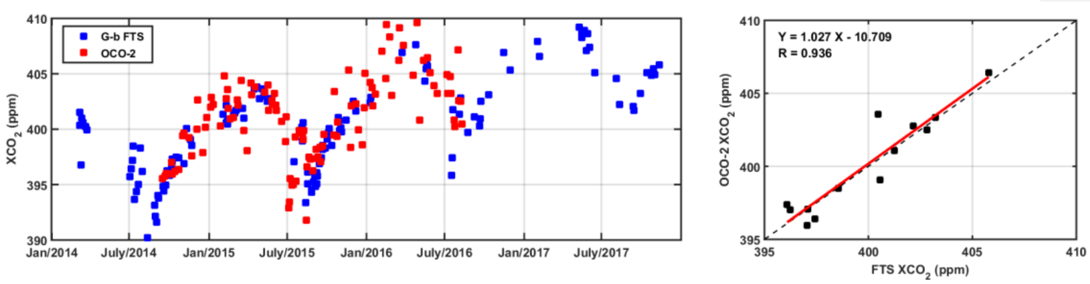

Figure 14. Left panel: The time series of XCO_2 from the g-b FTS (blue square) and OCO-2 (red square) over the Anmyeondo station from February 2014 to November 2017 are shown. Right panel: The linear regression curve between FTS and OCO-2 is shown. All results are given on daily medians basis.

Table 6. Seasonal mean and standard deviations of XCO_2 from the g-b FTS and OCO-2 in the period between 2014 and 2016 are given below.

Season	g−b FTS XCO_2 mean ± std (ppm)	OCO−2 XCO_2 mean ± std (ppm)
Winter	401.52 ± 0.85	402.67 ± 2.67
Spring	402.72 ± 2.79	403.96 ± 2.77
Summer	396.92 ± 3.28	399.68 ± 3.77
Autumn	398.01 ± 2.83	398.48 ± 2.41

Both instruments generally agreed in capturing the seasonal variability of XCO_2 at the measurement station. As can be seen clearly from the temporal distribution of FTS XCO_2, the maximum and minimum values are discernible in spring and late summer seasons, respectively. It was found that mean values in spring and summer were 402.72 and 396.92 ppm, respectively (see Table 6). This is because the seasonal variation of XCO_2 is most likely to be controlled by the imbalance of the terrestrial ecosystem exchange, and this could explain the larger XCO_2 values in the northern hemisphere in late April (Schneising et al. 2008, and references therein).

The minimum value of XCO_2 occurs in August, which is most likely due to uptake of carbon into the biosphere associated with the period of plant growth. Furthermore, both instruments showed high standard deviations during summer, about 3.28 ppm in FTS and 3.77 ppm in OCO-2, and this suggests that the variability reflects strong sources and sink signals.

4 Conclusions

Monitoring of greenhouse gases is an essential issue in the context of global climate change. Accurate and precise continuous long-term measurements of greenhouse gases (GHGs) are substantial for investigating their sources and sinks. Today, several remote sensing instruments operated on different platforms are dedicated for measuring GHGs. Total column measurements of greenhouse gases such as XCO_2, XCH_4, XH_2O, XN_2O have been made using the g-b FTS at the Anmyeondo station since 2013. In this work, we focused on the measurements taken during the period of February 2014 to November 2017. The instrument has been operated in a semi-automated mode since then. The FTS instrument has been stable during the whole measurement period. Regular instrument alignment checks using the HCl cell measurements are performed. The TCCON standard GGG2014 retrieval software was used to retrieve XCO_2, XCO, and others GHG gases from the g-b FTS spectra.

In this work, the g-b FTS retrieval of XCO_2 and XCH_4 were compared with aircraft measurements that were conducted over Anmyeondo station on 22 May 2016, 29 October and 12 November, 2017. The mean absolute difference between FTS and aircraft XCO_2 we obtained were found to be -1.129 ± 1.989 ppm, corresponding to a mean relative difference of -0.280 ± 0.491 %, while the mean absolute difference for XCH_4 is -0.010 ± 0.0273 ppm, corresponding to a mean relative difference of -0.542 ± 1.468 %. These differences appeared in both species and were consistent with the combined instrument errors. The preliminary comparison results of XCO_2 between FTS and OCO-2 were also presented over the Anmyeondo station. The mean absolute difference of XCO_2 between FTS and OCO-2 was calculated on daily median basis, and it was estimated to be 0.18 ppm with a standard deviation of 0.19 with respect to the g-b FTS. This bias could be attributed to instrument uncertainty. Based on the seasonal cycle comparison, both the g-b FTS and OCO-2 showed a consistent pattern in capturing the seasonal variability of XCO_2, with maximum in spring and minimum in summer.

메모 [DG16]: Is this after scaling the TCCON measurments by the network-wide scaling factors (0.99, 0.98 for CO2, CH4)?

5 Acknowledgements

This research was supported by the Research and Development for KMA Weather, Climate, and Earth system Services (NIMS-2016-3100). D.W.T.G. and V.A.V. would like to acknowledge financial support from the Australian Research Council (ARC) for TCCON activities (DP160101598, DP140101552, DP110103118). We would greatly acknowledge the two anonymous reviewers who helped us to improve this manuscript well.

References

메모 [Office17]: If you do not add the in situ PIs to the authorlist, please thank them personally here and include the URL where the data were obtained from.

Boland, S., Brown L. R., Burrows J. P., Ciais P., Connor B. J., Crisp D., Denning S., Doney S. C., Engelen R., Fung I. Y., Griffith P., Jacob D. J., Johnson B., Martin-Torres J., Michalak A. M., Miller C. E., Polonsky I., Potter C., Randerson J. T., Rayner P. J., Salawitch R. J., Santee M., Tans P. P., Wennberg P. O., Wunch D., Wofsy S. C., and Yung Y. L.: The Need for Atmospheric Carbon Dioxide Measurements from Space: Contributions from a Rapid Reflight of the Orbiting Carbon Observatory, 2009, http://www.nasa.gov/pdf/363474main_OCO_Reflight.pdf.

Brault, J. W.: New approach to high-precision Fourier transform spectrometer design. Appl. Opt. 35, 2891–2896, 1996.

Butz, A., Guerlet, S., Hasekamp, O., Schepers, D., Galli, A., Aben, I., Frankenberg, C., Hartmann, J.-M., Tran, H., Kuze, A., Keppel-Aleks, G., Toon, G., Wunch, D., Wennberg, P., Deutscher, N., Griffith, D., Macatangay, R., Messerschmidt, J., Notholt, J., and Warneke, T.: Toward accurate CO_2 and CH_4 observations from GOSAT, Geophys. Res. Lett., 38, L14812, https://doi.org/10.1029/2011GL047888, 2011.

Chen, H., Winderlich, J., Gerbig, C., Hoefer, A., Rella, C. W., Crosson, E. R., Van Pelt, A. D., Steinbach, J., Kolle, O., Beck, V., Daube, B. C., Gottlieb, E. W., Chow, V. Y., Santoni, G. W., and Wofsy, S. C: High-accuracy continuous airborne measurement of greenhouse gases (CO_2 and CH_4) using the cavity ring-down spectroscopy (CRDS) technique Atmos. Meas. Tech., 3, 375-386, 2010.

Connor B. J., Bösch H., Toon G., Sen B., Miller C. E., and Crisp D.: Orbiting carbon observatory: Inverse method and prospective error analysis, J. Geophys. Res., 113 doi: 10.1029/2006JD008336, 2008.

Crisp D., Miller C. E., DeCola P. L.: NASA Orbiting Carbon Observatory: measuring the column averaged carbon dioxide mole fraction from space. J. Appl. Remote Sens., 2, 023508, doi:10.1117/1.2898457, 2008.

Crisp D. for the OCO-2 Team: Measuring Atmospheric Carbon Dioxide from Space with the Orbiting Carbon Observatory-2 (OCO-2), Proc. SPIE 9607, Earth Observing Systems XX, 960702, doi: 10.1117/12.2187291, 2015.

Deutscher, N. M., Griffith, D. W. T., Bryant, G. W., Wennberg, P. O., Toon, G. C., Washenfelder, R. A., Keppel-Aleks, G., Wunch, D., Yavin, Y., Allen N. T., Blavier, J.-F., Jiménez R., Daube, B. C., Bright, A. V., Matross, D. M., Wofsy, S. C., and Park, S.: Total column CO_2 measurements at Darwin, Australia-site description and calibration against in situ aircraft profiles, Atmos. Meas. Tech., 3, 947-958, doi:10.5194/amt-3-947-2010, 2010.

Frankenberg, C., Pollock, R., Lee, R. A. M., Rosenberg, R., Blavier, J.-F., Crisp, D., O'Dell C. W., Osterman, G. B., Roehl, C., Wennberg, P. O., and Wunch, D.: The Orbiting Carbon Observatory (OCO-2): spectrometer performance evaluation using pre-launch direct sun measurements. Atmospheric Measurement Techniques, 8(1), 301–313. doi:10.5194/amt-8-301-2015, 2015.

Hase, F., Blumenstock, T., and Paton-Walsh, C.: Analysis of the instrumental line shape of high resolution Fourier transform IR spectrometers with gas cell measurements and new retrieval software, Appl. Optics, 38, 3417–3422, doi:10.1364/AO.38.003417,1999.

Hase, F., Drouin, B. J., Roehl, C. M., Toon, G. C., Wennberg, P. O., Wunch, D., Blumenstock, T., Desmet F., Feist, D. G., Heikkinen, P., De Mazière, M., Rettinger, M., Robinson, J., Schneider, M., Sherlock, V., Sussmann, R., Té Y., Warneke, T., and Weinzierl, C.: Calibration of sealed HCl cells used for TCCON instrumental line shape monitoring, Atmospheric Measurement Techniques, 6(12), 3527–3537, doi:10.5194/amt-6-3527-2013, 2013.

Kiel, M., Wunch, D., Wennberg, P. O., Toon, G. C., Hase, F., and Blumenstock, T.: Improved retrieval of gas abundances from near-infrared solar FTIR spectra measured at the Karlsruhe TCCON station, Atmos. Meas. Tech., 9(2), 669–682, doi:10.5194/amt-9-669-2016, 2016.

Kivi, R. and Heikkinen, P.: Fourier transform spectrometer measurements of column CO_2 at Sodankylä, Finland, Geosci. Instrum. Method. Data Syst., 5, 271–279, 2016.

Messerschmidt, J., Macatangay, R., Notholt, J., Petri C., Warneke, T., and Weinzierl, C.: Side by side measurements of CO_2 by ground-based Fourier transform spectrometry (FTS), Tellus B, 62(5), 749-758, doi:10.1111/j.1600-0889.2010.00491.x., 2010.

Messerschmidt, J., H. Chen, N. M. Deutscher, C. Gerbig, P. Grupe, K. Katrynski, F.-T. Koch, J.

V. Lavrič, J. Notholt, C. Rödenbeck, W. Ruhe, T. Warneke, and Weinzierl, C.: Automated ground-based remote sensing measurements of greenhouse gases at the Białystok site in comparison with collocated in situ measurements and model data, Atmospheric Chemistry and Physics, 12(15), 6741–6755, doi:10.5194/acp-12-6741-2012, 2012.

Miao, R., Lu N., Yao L., Zhu, Y., Wang, J., and Sun, J.: Multi-Year Comparison of Carbon Dioxide from Satellite Data with Ground-Based FTS Measurements (2003–2011), Remote Sensing, 5(7), 3431–3456, doi:10.3390/rs5073431, 2013.

Miller, C. E., Crisp, D. DeCola, P. L., Olsen, S. C., Randerson, J. T., Michalak, A. M., Alkhaled, A., Rayner, P., Jacob, D. J., Suntharalingam, P., Jones, D. B. A., Denning, A. S., Nicholls, M. E., Doney, S. C., Pawson, S., Boesch, H., Connor B. J., Fung I. Y., O'Brien, D., Salawitch, R. J., Sander, S. P., Sen, B., Tans, P., Toon, G. C., Wennberg, P. O., Wofsy, S. C., Yung, Y. L., and Law, R. M.: Precision requirements for space-based XCO_2 data, J. Geophys. Res-Atmos., 109, D02301, doi: 10.1029/2006JD007659, 2007.

Morino, I., Uchino, O., Inoue, M., Yoshida, Y., Yokota T., Wennberg, P. O., Toon, G. C., Wunch, D., Roehl, C. M., Notholt, J., Warneke, T., Messerschmidt, J., Griffith, D. W. T., Deutscher, N. M., Sherlock, V., Connor, B. J., Robinson, J., Sussmann, R., and Rettinger, M.: Preliminary validation of column-averaged volume mixing ratios of carbon dioxide and methane retrieved from GOSAT short-wavelength infrared spectra, Atmospheric Measurement Techniques, 4(6), 1061-1076, doi:10.5194/amt-4-1061-2011, 2011.

Miyamoto, Y., Inoue, M., Morino, I., Uchino, O., Yokota, T., Machida, T., Sawa, Y., Matsueda, H., Sweeney, C., Tans, P. P., Andrews, A. E., and Patra, P. K.: Atmospheric column-averaged mole fractions of carbon dioxide at 53 aircraft measurement sites, Atmos. Chem. Phys., 13, 52655275, 2013.

O'Dell, C. W., Connor, B., Bösch, H., O'Brien, D., Frankenberg C., Castano, R., Christi, M., Eldering, D., Fisher, B., Gunson, M., McDuffie, J., Miller, C. E., Natraj, V., Oyafuso, F., Polonsky, I., Smyth, M., Taylor, T., Toon, G. C., Wennberg, P. O., and Wunch, D.: The ACOS CO2 retrieval algorithm – Part 1: Description and validation against synthetic observations, Atmospheric Measurement Techniques, 5, 99–121, doi: 10.5194/amt-5-99-2012, http://www.atmos-meas-tech.net/5/99/2012/, 2012.

Ohyama, H., Morino, I., Nagahama, T., Machida, T., Suto H., Oguma, H., Sawa, Y., Matsueda, H., Sugimoto, N., Nakane, H., and Nakagawa, K.: Column-averaged volume mixing ratio of

CO_2 measured with ground-based Fourier transform spectrometer at Tsukuba, J. Geophys. Res., 114, D18303 doi:10.1029/2008JD011465, 2009.

Ohyama, H., Kawakami, S., Tanaka, T., Morino, Uchino, I., O., Inoue, M., Sakai, T., Nagai, T., Yamazaki, A., Uchiyama, A., Fukamachi, T., Sakashita, M., Kawasaki, T., Akaho, T., Arai, K., and Okumura, H.: Observations of XCO_2 and XCH_4 with ground-based high-resolution FTS at Saga, Japan, and comparisons with GOSAT products, Atmos. Meas. Tech., 8(12), 5263–5276, doi:10.5194/amt-8-5263-2015.

Rayner P. J., and O'Brien D. M.: The utility of remotely sensed CO_2 concentration data in surface source inversions, Geophys. Res. Lett., 28, 175–178, doi: 10.1029/2000GL011912, 2001.

Schneising O., Buchwitz M., Burrows J. P., Bovensmann, H., Reuter, M., Notholt, J., Macatangay, R., and Warneke, T.: Three years of greenhouse gas column-averaged dry air mole fractions retrieved from satellite-Part 1: Carbon dioxide, Atmos. Chem. Phys., 8, 3827-3853, 2008.

Sun, Y., Palm, M., Weinzierl, C., Peteri, C., Notholt, J., Wang, Y., and Liu, C.: Technical note: Sensitivity of instrumental line shape monitoring for the ground-based high-resolution FTIR spectrometer with respect to different optical attenuators, Atmos. Meas. Tech. Discuss., doi:10.5194/amt-10-989- 2017.

Thoning, K. W., Tans, P. P. and Komhyr, W. D.: Atmospheric carbon dioxide at Mauna Loa Observatory. Analysis of the NOAA GMCC Data, 1974-1985, J. Geophys. Res., 94, 8549-8565, 1989.

WMO (2016). The state of greenhouse gases in the atmosphere based on global observations through 2015, greenhouse gas. Greenhouse Gas Bulletin 2016. https://library.wmo.int/opac/doc_num.php.

Wang, W., Tian, Y., Liu, C., Sun, Y., Liu, W., Xie, P., Liu, J., Xu, J., Morino, I., Velazco, V., Griffith, D., Notholt, J., and Warneke, T.: Investigating the performance of a greenhouse gas observatory in Hefei, China, Atmos. Meas. Tech., 10, 2627–2643, 2017.

Wang, Y., Munger, J. W., Xu, S., McElroy, M. B., Hao, J., Nielsen, C. P., and Ma, H.: CO2 and its correlation with CO at a rural site near Beijing: implications for combustion efficiency in China, Atmos. Chem. Phys., 10, 8881–8897, https://doi.org/10.5194/acp-10-8881-2010, 2010.

Washenfelder R. A., Toon G. C., Blavier J-F., Yang Z., Allen N. T., Wennberg P. O., Vay S. A., Matross, D. M., and Daube B. C.: Carbon dioxide column abundances at the Wisconsin Tall Tower site, Journal of Geophysical Research, 2006, 111, doi:10.1029/2006JD00715, 2006. Warneke, T., Yang, Z., Olsen, S., Korner, S., Notholt J., Toon, G. C., Velazco, V., Schultz, A., and Schrems, O.: Seasonal and latitudinal variations of column averaged volume-mixing ratios of atmospheric CO_2, Geophysical Research Letters, 32(3), 2-5, doi:10.1029/2004GL021597, 2005.

Wunch, D., Toon G. C., Wennberg, P. O., Wofsy, S. C., Stephens, B., Fisher, M. L., Uchino O., Abshire, J. B., Bernath, P. F., Biraud, S. C., Blavier, J.-F. L., Boone, C. D., Bowman, K. P., Browell, E. V., Campos, T., Connor, B. J., Daube, B. C., Deutscher, N. M., Diao M., Elkins, J. W., Gerbig, C., Gottlieb, E., Griffith, D. W. T., Hurst, D. F., Jiménez, R., Keppel-Aleks, G., Kort, E. A., Macatangay, R., Machida, T., Matsueda, H., Moore, F. L., Morino, I., Park, S., Robinson, J., Roehl, C. M., Sawa, Y., Sherlock, V., Sweeney, C., Tanaka, T., and Zondlo, M. A.: Calibration of the Total Carbon Column Observing Network using aircraft profile data, Atmospheric Measurement Techniques, 3(5), 1351-1362, doi:10.5194/amt-3-1351-2010.

Wunch, D., Toon, G. C., Sherlock, V., Deutscher, N. M., Liu X., Feist, D. G., and Wennberg, P. O.: The Total Carbon Column Observing Network's GGG2014 Data Version. doi:10.14291/tccon.ggg2014.documentation.R0/1221662, 2015.

Wunch, D., Wennberg, P.O.,, Osterman, G., Fisher, B., Naylor, B., Roehl, C. M., O’Dell, C., Mandrake, L.,Viatte, C., Griffith, D. W. T., Deutscher, N. M., Velazco, V. A., Notholt, J.,Warneke, T.,Petri, C., Maziere, M. De, Sha, M. K., Sussmann,R., Rettinger, M., Pollard, D., Robinson, J.,Morino, I., Uchino O., Hase, F., Blumenstock, T., Kiel, M., Feist, D. G., Arnold S.G., Strong, K., Mendonca, J., Kivi, R.,Heikkinen, P., Iraci, L., Podolske, J., Hillyard, P. W., Kawakami, S., Dubey, M. K., Parker, H. A., Sepulveda, E., Rodriguez, O. E. G., Te, Y., Jeseck, P., Gunson, M. R., Crisp, D., and Eldering A., Comparisons of the Orbiting Carbon Observatory-2 (OCO-2) XCO_2 measurements with TCCON, Atmos. Meas. Tech. Discuss., doi:10.5194/amt-2016-227, 2016.

Co-authors and TCCON member Final comment revision

Characteristics of Greenhouse Gas Concentrations Derived from Ground-based FTS Spectra at Anmyeondo, Korea

Young-Suk Oh[1,2*], Samuel Takele Kenea[1], Tae-Young Goo[1], Kyu-Sun Chung[2], Jae-Sang Rhee[1], Mi-Lim Ou[5], Young-Hwa Byun[1], Paul O. Wennberg[4,5], Matthäus Kiel[4], Voltaire A. Velazco[3] and David W. T. Griffith[3]

1. Climate Research Division, National Institute of Meteorological Sciences (NIMS), Jeju-do, Republic of Korea
2. Department of Electrical Eng. & Centre for Edge Plasma Science, Hanyang University, Seoul, Republic of Korea
3. School of Chemistry, University of Wollongong, Northfields Ave, Wollongong, NSW 2522, Australia
4. Division of Geological and Planetary Sciences, California Institute of Technology, 1200E. California Boulevard, Pasadena, CA, 91125, USA
5. Division of Engineering and Applied Sciences, California Institute of Technology, 1200E. California Boulevard, Pasadena, CA, 91125, USA
6. Climate Change Monitoring Division, Korea Meteorological Administration, Seoul, Republic of Korea

*Correspondence to: Young-Suk Oh (ysoh306@gmail.com)

Abstract.

Since the late 1990s, the meteorological observatory established in Anmyeondo (36.5382˚ N, 126.3311˚ E, and 30 m above mean sea level), has been monitoring several greenhouse gases such as CO_2, CH_4, N_2O, CFCs, and SF_6, as a part of the Global Atmosphere Watch (GAW) Program. A high resolution ground-based (g-b) Fourier Transform Spectrometer (FTS) was installed at this observation site in 2013, and has been operated within the framework of the Total Carbon Column Observing Network (TCCON) since August, 2014. The solar spectra recorded by the g-b FTS cover the spectral range 3,800 to 16,000 cm^{-1} at a resolution of 0.02 cm^{-1}. In this work, the GGG2014 version of the TCCON standard retrieval algorithm was used to retrieve total column average CO_2 and CH4 dry mole fractions (XCO_2, XCH4) and from the FTS spectra. Spectral bands of CO_2 (at 6220.0 and 6339.5 cm^{-1} centre wavenumbers, CH_4 at 6002 cm^{-1} wavenumber, and O_2 near 7880 cm^{-1}) were used to derive the XCO_2 and XCH_4. In this paper, we provide comparisons of XCO_2 and XCH_4 between the aircraft observations and g-b FTS over Anmyeondo station. A comparison of 13 coincident observations of XCO_2 between g-b FTS and OCO-2 (Orbiting Carbon

Observatory) satellite measurements are also presented for the measurement period between February 2014 and November 2017. OCO-2 observations are highly correlated with the g-b FTS measurements (r2 = 0.94^2) and exhibited a small positive bias (0.189 ppm). Both data sets capture seasonal variations of the target species with maximum and minimum values in spring and late summer, respectively. In the future, it is planned to further utilize the FTS measurements for the evaluation of satellite observations such as Greenhouse Gases Observing Satellite (GOSAT, GOSAT-2). This is the first report of the g-b FTS observations of XCO_2 species over the Anmyeondo station.

Key words: Aircraft**,** XCO_2, OCO-2, TCCON, Infrared spectra

1. Introduction

Monitoring of greenhouse gases (GHGs) is a crucial issue in the context of global climate change. Carbon dioxide (CO_2) is one of the key greenhouse gases and its global annual mean concentration has increased rapidly from 278 to 400 ppm since the preindustrial data of 1750 (WMO greenhouse gas bulletin, 2016). Radiative forcing due to changes in atmospheric CO_2 accounts for approximately 65 % of the total change in radiative forcing by long-lived GHGs (Ohyama et al., 2015 and reference therein). Human activities such as burning of fossil fuels and land use change are the primary drivers of the continuing increase in atmospheric greenhouse gases and the gases involved in their chemical production (Kiel et al., 2016 and reference therein). There is a global demand for accurate and precise long-term measurements of greenhouse gases.

In the field of remote sensing techniques, solar absorption infrared spectroscopy has been increasingly used to determine changes in atmospheric constituents. Today, a number of instruments deployed on various platforms (ground-based and space-borne) have been operated for measuring GHGs such as CO_2. The g-b FTS at the Anmyeondo station has been measuring several atmospheric GHG and other gases such as CO_2, CH_4, CO, N_2O, and H_2O operated within the framework of the Total Carbon Column Observing Network (TCCON). XCO_2 retrievals from the g-b FTS have been reported at different TCCON sites (e.g, Ohyama et al., 2009; Deutscher et al., 2010; Messerschmidt et al., 2010, 2012; Miao et al., 2013; Kivi and Heikkinen, 2016). TCCON achieves accuracy and precision in measuring the column averaged dry air mole fraction of CO_2 (XCO_2), of about 0.25 %, or better than 1 ppm (Wunch et al., 2010), which is essential to retrieve information about sinks and sources, as well as validating satellite products (Rayner and O'Brien, 2001; Miller et al., 2007). Precision for XCO_2 of 0.1 % can be achieved during clear sky conditions (Messerschmidt et al., 2010; Deutscher et al., 2010). The network aims to improve global carbon cycle studies and supply the primary validation data of different atmospheric trace gases for space-based instruments, e.g., the Orbiting Carbon Observatory 2 (OCO-2), the Greenhouse Gases Observing Satellite (GOSAT, GOSAT-2) (Morino et al., 2011; Frankenberg et al., 2015).

This study is focused on the initial characteristics of XCO_2 retrievals from g-b FTS spectra over the Anmyeondo station, and comparison with in situ aircraft overflights and the OCO-2 satellite. The FTS spectra have been processed using the TCCON standard GGG2014 (Wunch et al., 2015) retrieval software. One of the unique aspects in this work is a new homemade addition to our g-b FTS instrument that reduces the solar intensity variations from the 5% maximum allowed in TCCON to less than 2%. This paper presents an introduction to the instrumentation and measurement site, and provides initial results and discussion followed by conclusions.

2 Station and instrumentation

2.1 Station description

The g-b FTS observatory was established in 2013 at the Anmyeondo (AMY) station, located at 36.32˚ N, 126.19˚ E, and 30 m above sea level. This station is situated on the west coast of the Korean Peninsula, 180 km SE of Seoul, the capital city of Republic of Korea. Figure 1 displays the Anmyeondo station. It is also a regional GAW (Global Atmosphere Watch) station that is operated by the Climate Change Monitoring Network of KMA (Korean Meteorological Administration). The AMY station has been monitoring various atmospheric parameters such as greenhouse gases, aerosols, ultraviolet radiation, ozone, and precipitation since 1999. The total area of the Anmyeondo island is estimated to be ~88 km^2 and approximately 1.25 million people reside on the island. Some of the residents over this area are engaged in agricultural activities. Vegetated areas consisting of mainly pine trees are located in and around the FTS observatory. The topographic feature of the area is one of low level hills, on average about 100 m above sea level. The minimum temperature in winter season is on average 2.7 ˚C, and the maximum temperature is about 25.6 ˚C during summer. Average annual precipitation amount is 1,155 mm; with snow winter. The site has been formally designated as a provisional TCCON site since August 2014. Full acceptance requires calibration via overflights with WMO-calibrated in situ vertical profiles, as described in this paper. The AMY Station’s TCCON wiki page can be found at: [https://tccon-wiki.Anmyeondo.edu]

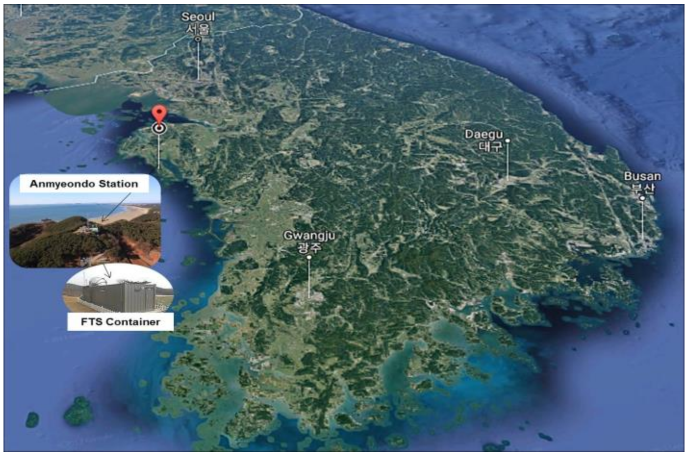

Figure 18. Anmyeodo (AMY) g-b FTS station

2.2 G-b FTS instrument

Solar spectra are acquired using a Bruker IFS 125HR spectrometer (Bruker Optics, Germany) under the guidelines set by TCCON. Currently, our g-b FTS instrument operation is semi-automated for taking the routine measurements under clear sky conditions. It is planned to make an FTS operation mode fully automated in 2018. The solar tracker (A547, Bruker Optics, Germany) is mounted inside a remotely controlled protective dome. The tracking ranges in azimuthal and elevation angles are about 0 to 315 and -10 to 85 degrees, respectively, while the tracking speed is about 2 degrees per second. The tracking accuracy of ±4 minutes of arc is achieved by the Camtracker mode which centres an image of the sun onto the spectrometer's input field stop. Under clear sky conditions, the dome is opened and set to an automatic tracking mode, in which the mirrors are initially moved to the calculated solar position, then. The camtracker control is activated in such a way that the mirrors are finely and continuously controlled to fix the beam onto the entrance stop of the spectrometer. Figure 2 displays an overview of the general data acquisition system. This ensures that all spectra are recorded under clear weather conditions.

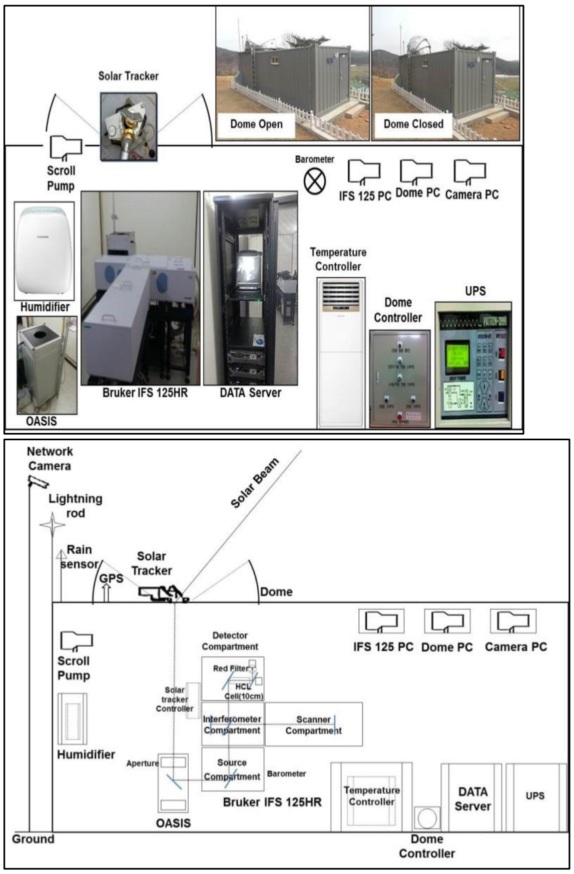

Figure 2. Photographs of the automated FTS laboratory. The Bruker Solar Tracker type A547 is mounted in the custom made dome. A servo controlled solar tracker directs the solar beam through a CaF_2 window to the FTS (125HR) in the laboratory. The server computer is used for data acquisition. PC1 and PC2 are used for controlling the spectrometer, solar tracker, dome, camera, pump, GPS satellite time, and humidity sensor.

The spectrometer is equipped with two room temperature detectors; an Indium-Gallium-Arsenide (InGaAs) detector, which covers the spectral region from 3,800 to 12,800 cm^{-1}, and Silicon (Si) diode detector (9,000 – 25,000 cm^{-1}) used in a dual-acquisition mode with a dichroic optic (Omega Optical, 10,000 cm^{-1} cut-on). A red longpass filter (Oriel Instruments 59523; 15,500 cm^{-1} cut-on) prior to the Si diode detector blocks visible light, which would otherwise be aliased into the near-infrared spectral domain. TCCON measurements are routinely recorded at a maximum optical path difference (OPD_{max}) of 45 cm leading to a spectral resolution of 0.02 cm^{-1} (0.9/max OPD). Two scans, one forward and one backward, are performed and individual forward-backward interferograms are recorded. As an example, Figure 3 shows a single spectrum recorded on 4 October 2014 with a resolution of 0.02 cm^{-1}. A single forward-backward scan in one measurement takes about 112 s. Measurement setting for the Anmyeondo g-b FTS spectrometer of the Bruker 125HR model is summarized in Table 1. The pressure inside the FTS is kept at 0.1 to 0.2 hPa with an oil-free vacuum pump to maintain the stability of the system and to ensure clean and dry conditions.

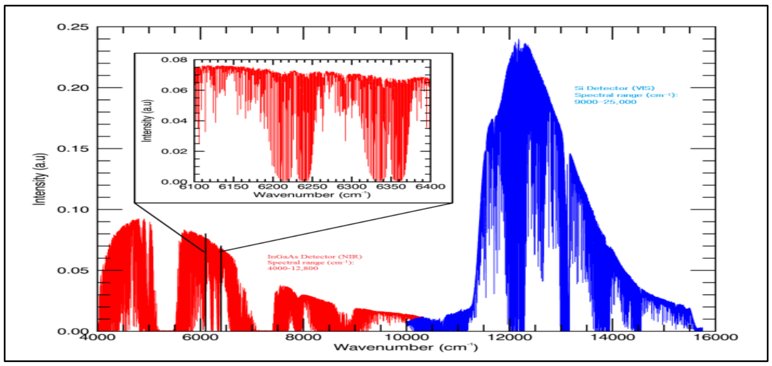

Figure 3. Single spectrum recorded on 4 October 2014 with a resolution of 0.02 cm^{-1}. A typical example for the spectrum of XCO_2 is shown in the inset.

Table 8. Measurement setting for the Anmyeondo g-b FTS spectrometer of the Bruker 125HR model.

Item	Setting
Aperture (field stop)	0.8 mm
Detectors	RT-Si Diode DC, RT-InGaAs DC
Beamsplitters	CaF_2
Scanner velocity	10 kHz
Low pass filter	10 kHz
High folding limit	15798.007
Spectral Resolution	0.02 cm^{-1}
Optical path difference	45 cm
Acquisition mode	Single sided, forward backward
Sample scan	2 scans, forward, backward
Sample scan time	~110 s

2.3 Characterization of FTS-instrumental line shapes

For the accurate retrieval of total column amounts of the species of interest, a good alignment of the g-b FTS is essential. The instrument line shape (ILS) retrieved from the regular HCl cell measurements is an important indicator of the status of the FTS's alignment (Hase et al., 1999). The analyses of the measurements were performed using a spectrum fitting algorithm (LINEFIT14 software) (Hase et al., 2013). In Figure 4 we show time series of the modulation efficiency (left panel) and phase error (rad) (right panel) from the HCl cell measurement in the

메모 [Office18]: Actually on right below.

period of October 2013 to September 2017 using a tungsten lamp as light source. Modulation amplitudes for TCCON-acceptable alignment should be within 5 % of the ideal case (100%) at the maximum optical path difference (Wunch et al., 2011). In our g-b FTS measurements, it is found that the maximum loss of modulation efficiency is within 1 %, close to the ideal value. The phase errors are less than ± 0.0001 rad. Hase et al. (2013) reported that this level of small disturbances from the ideal value of the modulation efficiency is common to all well-aligned instruments. This result confirmed that the g-b FTS instrument is well aligned and has remained stable during the whole operation period.

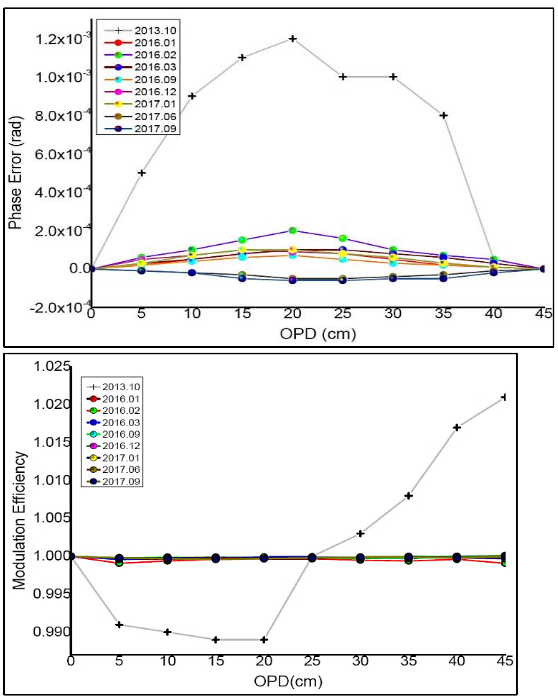

Figure 4. Modulation efficiency (left panel) and Phase error (rad) (right panel) of HCl measurements from the g-b FTS are displayed in the period from October 2013 to September 2017. Resolution = 0.02 cm^{-1}, Aperture = 0.8 mm.

We also confirmed that the ILS was not affected by the variable aperture (OASIS) during the operation of this system (see section 2.5). The modulation efficiency and phase error were estimated to be 99.98 % and 0.0001 rad. Sun et al. (2017) reported the detailed characteristics of the ILS with respect to applications of different optical attenuators to FTIR spectrometers within the TCCON and NDACC networks. They used both lamp and sun as light sources for the cell measurements, which were conducted after the insertion of five different attenuators in front of and behind the interferometer.

2.4 Data processing

Using the TCCON standard retrieval strategy, we have derived the column-averaged dry-air mole fraction CO_2 (XCO_2) and other atmospheric gases (O_2, CO, CH_4, N_2O, and H_2O) using the GFIT algorithm and software. The spectral windows used for the retrieval of CO_2 and O_2 are given in Table 2. The TCCON standard GGG2014 (version 4.8.6) retrieval software was used to obtain the abundance of the species from FTS spectra (Wunch et al., 2015). XCO_2 is derived from the ratio of retrieved CO_2 column to retrieved O_2 column,

$$\mathrm{XCO_2} = \frac{\mathrm{CO_{2\,column}}}{\mathrm{O_{2\,column}}} \times 0.2095\,, \tag{1}$$

Computing the ratio using Eq. (1) minimizes systematic and correlated errors such as errors in solar zenith angle pointing error, surface pressure, and instrumental line shape that may exist in the retrieved CO_2 and O_2 columns (Washenfelder et al., 2006, Messerschmidt et al., 2012). The top panel of Figure 5 depicts the time series of laser sampling error (LSE) obtained from InGaAs spectra at the Anmyeondo FTS station in the measurement period of February 2014 to December 2016. LSE is due to inaccuracies in the laser sample timing, which have been reduced to acceptable levels by the instrument manufacturer. In the AMY FTS, the LSE is small and centered around zero. Slightly large LSE values were shown on 10 March, 2014 (see top panel of Fig. 5). On this date, we conducted the laser adjustment in FTS.

Table 9. Spectral windows used for the retrievals of the columns of CO_2 and O_2

Gas	Center of spectral window (cm^{-1})	Width (cm^{-1})	Interfering gas
O_2	**7885.0**	**240.0**	**H_2O, HF, CO_2**
CO_2	**6220.0**	**80.0**	**H_2O ,HDO, CH_4**
CO_2	**6339.5**	**85.0**	**H_2O ,HDO**

X_{air} is the ratio of atmospheric pressure to total column O_2, scaled such that for a perfect measurement X_{air} = 1.0. X_{air} is a useful indicator of the quality of measurements and the instrument performance. Due to spectroscopic limitations there is a TCCON wide bias (X_{air} ~ 0.98) and small solar zenith angle (SZA) dependence. The retrieval of X_{air} deviating more than 1% from the TCCON-wide mean value of 0.98 would suggest a systematic error. The time series of X_{air} is shown in the bottom panel of Figure 5. The X_{air} record reveals that the

메모 [DG19]: Could you add a reference to the definition of Xair that any reader could use to follow exactly the calculation ?

instrument has been stable during the measurement period. It shows that the values of X_{air} fluctuate between 0.974 and 0.985, and the mean value is 0.982 with a standard deviation of 0.0015 in which the scatter for X_{air} is about 0.15 %. The low variability in time series of X_{air} indicates the stability of the measurements.

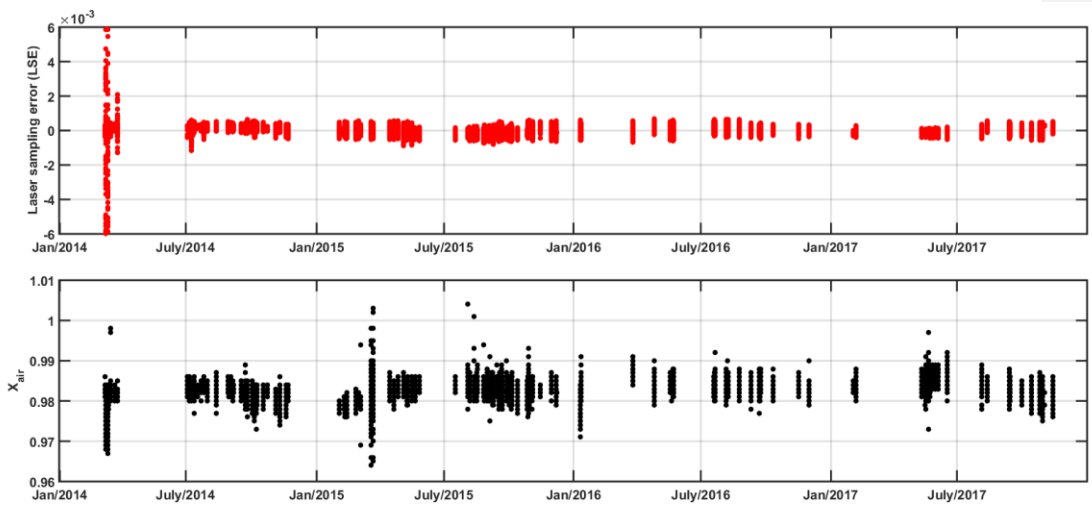

Figure 5. Time series of LSE (top panel) and X_{air} (bottom panel) from the g-b FTS during 2014- 2017 is shown. Each marker represents a single measurement.

2.5 Operational Automatic System for the Intensity of Sunray (OASIS) effect on the retrieval results

The OASIS system was developed for improving the quality of the spectra recorded by the spectrometer by maintaining a constant signal level. OASIS is beneficial for minimizing the variability that may be induced in the spectra due to intensity fluctuations of the incoming solar radiation that reaches the instrument. The main function of the OASIS is to control an aperture diameter in the parallel-inlet beam to the interferometer. This aperture is placed inside the OASIS system, in the parallel input solar beam external to the FTS. The fundamental purpose of this system is to optimize the measurement of solar spectra by reducing the effect of the fluctuations of the intensity of the incoming light due to changes in thin clouds along the line of sight over the measurement site. The maximum threshold value of the solar intensity variation

(SIV) is 5 %, the TCCON standard value (Ohyama et al., 2015). This value has been reduced to ≤ 2 % in our case by introducing the OASIS system to our g-b FTS since December 2014.

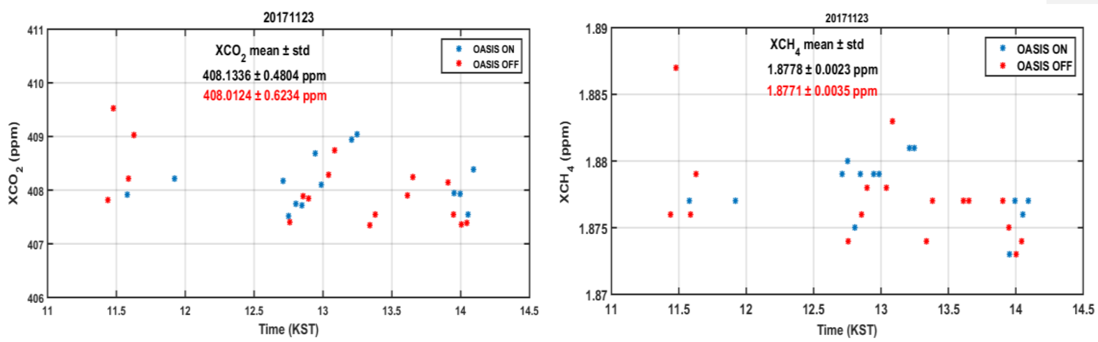

Figure 6. G-b FTS XCO_2 (left panel) and XCH_4 (right panel) values as function of time in KST (Korean Standard time, UTC+9) taken October 23, 2017 with OASIS system on (operating) and off (without operating) positions are shown. Each marker represents a single measurement.

In order to assess the impact of the OASIS system on the retrieval results of XCO_2 and XCH_4, we have conducted experiments on recording alternate FTS spectra with and without operation of this system under clear sky conditions. As an example, Figure 6 depicts the retrieval results of XCO_2 (left panel) and XCH_4 (right panel) as a function of time (KST, UTC+9), taken November 23, 2017 with OASIS on (blue) and off (red) positions. Mean differences of 0.12 ppm for XCO_2 and 7.0 x 10^{-4} ppm for XCH_4 were found between OASIS on and off position (i.e., with and without operating of OASIS system). This suggests that the impact of OASIS system on the retrieval is negligible.

2.6 Aircraft observation campaigns over Anmyeondo station

2.6.1 Aircraft instrumentation

In this section, we present a comparison between aircraft in-situ observations and g-b FTS column measurements over the Anmyeondo station. In situ profiles were conducted over the Anmyeondo station by the National Institute of Meteorological Sciences (King Air 350ER) and as part of the KORUS-AQ campaign from NASA's DC8. For the NIMS profiles, the flight take-off and landing was carried out from Hanseo University which is approximately 5 km away from the Anmyeondo FTS station. The aircraft was equipped with a Wavelength Scanned Cavity Ring Down Spectrometer (CRDS; Picarro, G2401-m), (see Fig. 7) providing mixing ratio data recorded

메모 [DG20]: Provide a reference to the KORU campaign for further information – publication (prefereably) or if not available, the web site.

at 0.3 Hz intervals. The position of the aircraft was monitored by GPS, and information on the outside temperature, static pressure, and ground speed was provided by instruments carried on the plane. The temperature and pressure of the gas sample have to be tightly controlled at 45 ℃ and 140 Torr in the CRDS, which leads to highly stable spectroscopic features (Chen et al., 2010). Any deviations from these values cause a reduction of the instrument's precision. Data recorded beyond the range of variations in cavity pressure and temperature were discarded in this analysis. Variance of the cavity pressure and temperature during flight results in variance in the CO_2 and CH_4 mixing ratios. The Picarro CRDS instrument has been regularly calibrated with respect to the standard gases within the error range recommend by World Meteorological Organization (CO_2 is 380.23 ± 0.1 ppm, CH_4 is 1.825 ± 0.001 ppm). Measurements were made in wet air, and dry air mixing ratios were derived following the method described in Chen et al. (2010). Water was measured and its effect was accounted for the column integration of CO_2 and CH_4

메모 [DG21]: The meaning of these numbers is not clear – are they the values for a single camibration gas used to calibrate the analyser? When was it calibrated before, during and after the flights.

On NASA's DC8, CO_2 was measured by a non-dispersive IR spectrometer instrument (LI-COR 6252) with an uncertainty of 0.25 ppm, and CH_4 was measured by a Diode Laser Spectrometer. The aircraft static pressure and altitude were recorded using radar altimeter and central air data computer (flight instruments). As with the NIMS profiles, the vertical profiles of CO_2 and CH_4 mixing ratio were obtained during an upward and a downward spiral flight centred on the Anmyeondo.

메모 [DG22]: Provide references (from KORUS partners?)

메모 [Office23]: Only downward.

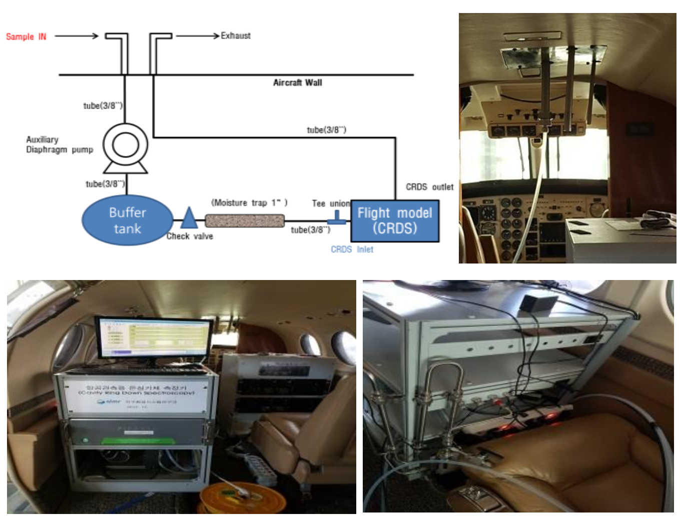

Figure 7. NIMS CRDS instrument on board of the King Air 350ER .

2.6.2 Aircraft CO_2 and CH_4 data

The NIMS vertical profiles of CO_2 and CH_4 mixing ratio were obtained during an upward and a d ownward spiral flights centred over the Anmyeondo FTS station, on 29 October and 12 Novemb er, 2017. As an example, the flight trajectory is shown in the left panel of Figure 8 while the pro files of CO_2 and CH_4 from flight during the ascent and descent on 29 October, 2017 are depicted in the middle and right panels of Figure 8, respectively. All flights were performed under clear s ky conditions. The campaign was performed for 2 hours on both days.

Specifically, the respective measurements were taken from 11:00:37 to 12:03:25 KST (UTC+9) and from 13:58:58 to 15:19:40 KST on 29 October, 2017 and similarly from 11:12:20 to 12:13:00 KST and from 14:14:46 to 15:14:46 KST on 12 November, 2017. The altitude range of the aircraf t measurements was limited to approximately 0.1 to 9.1 km. We constructed the complete CO_2 and CH_4 profiles in a similar way as performed by Deutscher et al. 2010; Miyamoto et al. (2013); Ohyama et al. (2015). For both CO_2 and CH_4 profiles, since we do not have in-situ surface data during the aircraft observation time , we extend the lowermost observations of the aircraft prof iles to the surface level, and above the aircraft ceiling, the mole fractions throughout the altitud e range between the uppermost aircraft and the tropopause is assumed to be the same as at th e highest aircraft measurement level because of lack of data. This extrapolation produces the largest uncertainty in the in situ column estimate. For this analysis, the tropopause height was derived from NOAA National Centers for Environmental Prediction/National Center for Atmosp heric Research Reanalysis datasets which are provided in 6 hour intervals (0:00, 06:00, 12:00, a nd 18:00 UTC) with a horizontal resolution of 2.5 by 2.5 degrees. The measurements of surface pressure were available at the FTS station, which we have used for calculating XCO_2 and XCH_4. A bove the tropopause height, GFIT apriori profiles were utilized to extrapolate the aircraft profile. Eventually, the completed aircraft profiles based on those assumptions were transformed into a total column XCO_2 and XCH_4 by pressure weighting functions. For this comparison, we consider ed only the FTS averaged XCO_2 and XCH_4 retrieval values for the corresponding aircraft measure ment time. Details about the aircraft XCO_2 and XCH_4 values during ascending and descending aircraft flight duration and the corresponding FTS averaged XCO_2 and XCH_4 retrieval values are also provided in Table 3. Note that the vertically resolved FTS column-averaging kernels were ta ken into account for smoothing the aircraft profiles. The XCO_2 and XCH_4 for the aircraft in situ profile weighted by the column averaging kernel a (Rodgers and Connor, 2003) is c omputed as follows:

메모 [DG24]: Why can't you use the data from the AMY GAW station? You have made a point earlier that you are co-located. See also Paul's comment below – same question.

$$X^{in-situ} = X^{a} + \sum_{j} h_j a_j (t_{in-situ} - t_a)_j$$

where X^{a} is the column-averaged dry air mole fraction for the apriori profile t_a (CO_2 or CH_4), $t_{in-situ}$ is the aircraft profile and h_j is the pressure weighting function.

We estimated the uncertainty of the XCO_2 and XCH_4 columns derived from the extended aircraft profiles by assigning uncertainties. Uncertainty at the surface was assumed to be same as the uncertainty in the lowest measurements. For the stratosphere, we used the method suggested by Wunch et al. (2010). This method shifts the stratospheric values up and down by 1 km to calculate the difference in the total column, which is used as an estimate of the uncertainty in the location of the tropopause and therefore for the stratospheric contribution. We estimated the stratospheric errors in aircraft integrated amount of XCO_2 and XCH_4 by shifting the apriori profile by 1 km (Ohyama et al. 2015). For KORUS-AQ, it was found to be 0.42 ppm for XCO_2 and 13.26 ppb for XCH_4.

메모 **[Office25]:** I believe I asked this earlier – why don't you use the GAW CO2 and CH4 measurements for the surface?

For NASA's DC8 measurements, the in-situ profiles covered the altitude range of approximately 0.17 to 9.0 km, we extended the lowest measurements to the surface and from the highest point to the tropopause which is estimated by NCEP to be at 139.0 hPa. Figure 9 illustrates the results of XCO_2 and XCH_4 comparisons between the aircraft observation and TCCON site data. In this plot, blue represents the KORUS-AQ campaign, whereas green indicates the NIMS campaign. KORUS-AQ data lie on the best line which is derived using TCCON stations where aircraft profiles are available. This shows that TCCON Anmyeondo data is consistent with other TCCON stations.

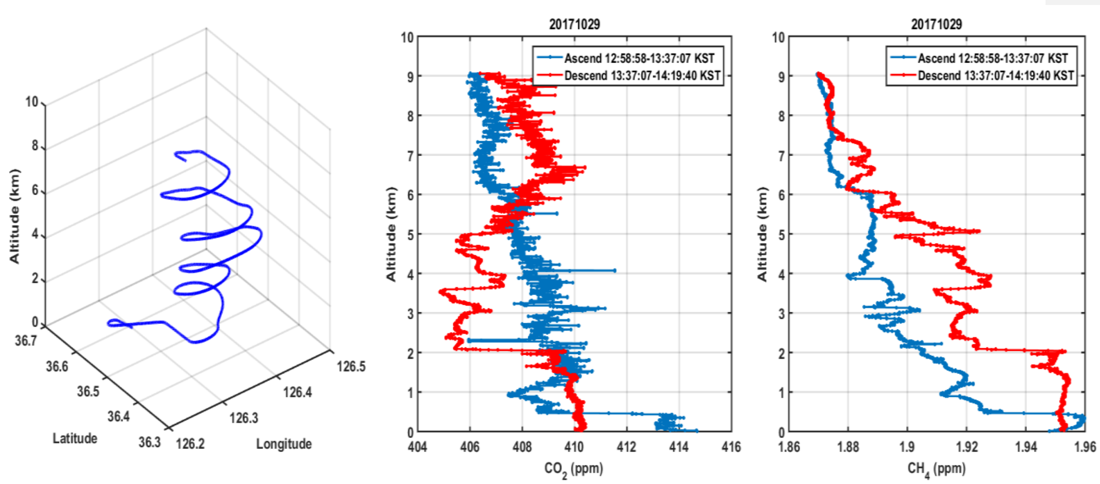

Figure 8. Typical flight path (left panel) and CO_2 (middle panel) and CH_4 (right panel) VMR profiles during ascending and descending of the aircraft over Anmyeondo on October 29, 2017 are shown.

Table 3. Summary of the column averaged dry-air mole fractions obtained during the inter-comparison between the in-situ instrument on board of the aircrafts and the g-b FTS at the Anmyeondo station. A and D represent ascending and descending, respectively. Note that FTS values given below are without TCCON common scale factor and FTS column averaging kernels are applied to the aircraft data.

Date of measurements (hours in KST)	**Aircraft NIMS XCO_2 (ppm)**	**g-b FTS XCO_2 (ppm)**	**Aircraft NIMS XCH_4 (ppm)**	**g-b FTS XCH_4 (ppm)**
2017-10-29				
09:59:16-10:31:08 (A)	409.428	404.242	1.8904	1.8460
10:31:09-11:03:24 (D)	409.201	403.877	1.8850	1.8454
12:58:58-13:37:07 (A)	407.073	401.051	1.8551	1.8265
13:37:07-14:19:40 (D)	406.842	400.537	1.8715	1.8249
2017-11-12				
11:12:20-11:38:01 (A)	406.099	401.839	1.8513	1.8221
	406.540	401.930	1.8515	1.8220

11:38:02-12:13:00 (D)	406.962	401.592	1.8482	1.8201
14:14:46-14:45:55 (A)	407.798	401.473	1.8511	1.8191
14:45:56-15:23:47 (D)				
Mean ± std	**407.3061 ±1.178**	**402.068± 1.311**	**1.8630± 0.0169**	**1.8283± 0.011**

	KORUS	TCCON	KORUS	TCCON
2016-05-22	405.80 ± 0.42	401.91 ± 0.57	1.8641± 0.0132	1.8100±0.002

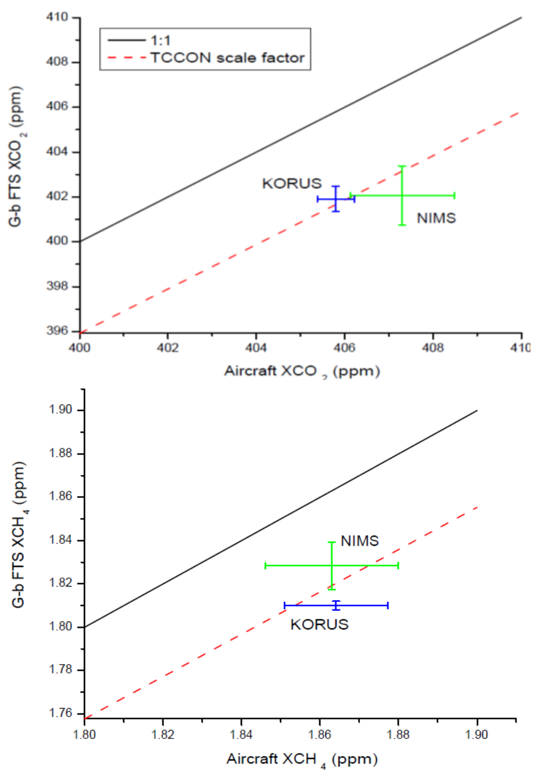

Figure 9. The comparisons of XCO_2 and XCH_4 between the aircraft observations and g-b FTS data over Anmyeondo station are shown. The diamond symbol represents for the aircraft campaign conducted by KORUS-AQ (May, 2016), whereas square symbol indicates for the aircraft campaign operated by NIMS (2017). Note that FTS values shown in the figure are after removing TCCON common scale factor.

메모 [Office26]: There are no diamond nor square symbols in the figure.

메모 [DG27]: 1.It would be more informative to plot two points for the two NIMS campaigns than a single average point
2.2. The meaning and explanation of the dotted line is ambiguous – I assume your data have NOT been corrected by the TCCON-wide scaling factors, and therefore should lie on the uncorrected line - shown by the dotted line. I think you discussed this with Matt Kiel earlier.

2.7 Comparison with OCO-2 measurements

The Orbiting Carbon Observatory-2 (OCO-2) is NASA's first Earth-orbiting satellite dedicated to greenhouse gas measurement, it was successfully launched on July 2, 2014 into low-Earth orbit. It is devoted to observing atmospheric carbon dioxide (CO_2) to provide improved insight into the carbon cycle. The primary mission is to measure carbon dioxide with high precision and accuracy in order to characterize its sources and sinks at different spatial and temporal scales (Boland et al., 2009; Crisp, 2008, 2015). The instrument measures the near infrared spectra (NIR) of sunlight reflected off the Earth's surface. Atmospheric abundances of carbon dioxide and related atmospheric parameters are retrieved from the spectra in nadir, sun glint and target modes. Detailed information about the instrument is available in, for example (Connor et al., 2008; O'Dell et al., 2012). In this work, we used the OCO-2 version 7Br bias corrected data. The comparisons are discussed in section 3.3.

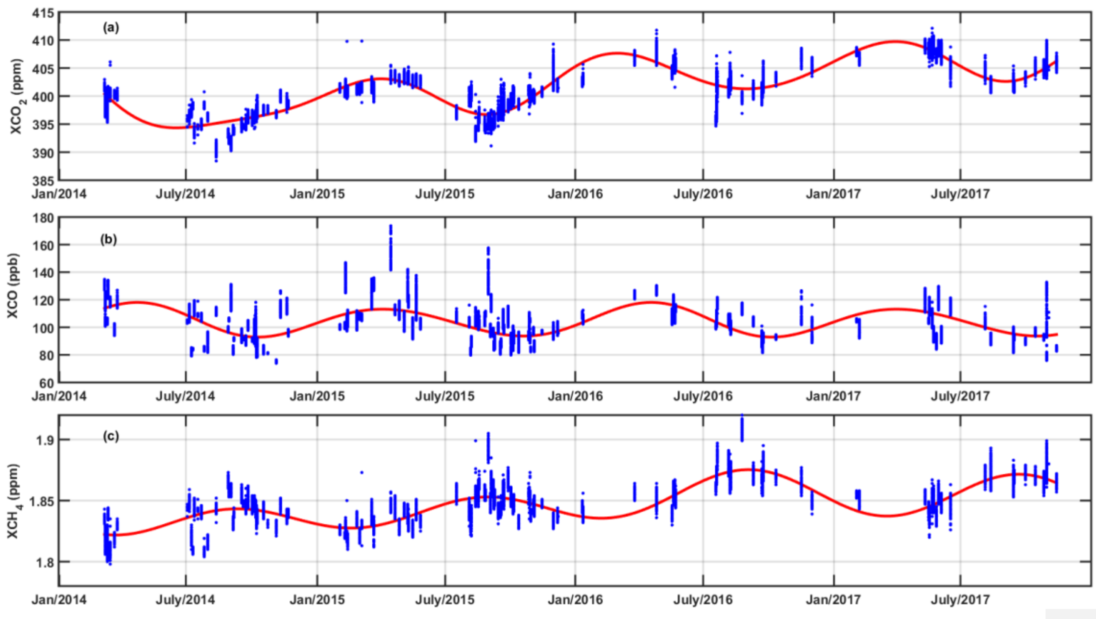

Figure 10. Time series of XCO_2, XCO, and XCH_4 from top to bottom panels (a-c), respectively in the period between February 2014 and November 2017 is given. Each marker indicates a single retrieval. Fitting curves (red solid lines) are also displayed.

Table 4. Annual mean of XCO_2, XCO, and XCH_4 from Anmyeondo g-b FTS from February 2014 to November 2017 is given.

	Annual mean ± standard deviation			
Gases	2014	2015	2016	2017
XCO_2 (ppm)	396.91 ± 2.55	399.32 ± 2.96	402.97 ± 2.74	406.04 ± 2.38
XCO (ppb)	99.42 ± 14.71	102.73 ± 14.91	105.39 ± 10.68	100.14 ± 10.3
XCH_4 (ppm)	1.837 ± 0.014	1.844 ± 0.015	1.864 ± 0.015	1.859 ± 0.013

3 Results and discussion

3.1 Time series of g-b FTS XCO_2, seasonal and annual cycle

The time series of XCO_2 along with retrievals of other trace gases such as XCO and XCH_4 from g-b FTS is presented in Figure 10 (panel a-c) for the period from February 2014 to November 2017. In these time series plots, each marker represents a single retrieval, and the fitting curves of the retrieved values are also depicted (red solid line). We show the seasonal cycle of XCO_2, XCO, and XCH_4 in the time series using a fitting procedure described by Thoning et al. (1989). Standard deviations of the differences between the retrieved values and the fitting curves are 1.64 ppm, 11.34 ppb, and 10.1 ppb for XCO_2, XCO, and XCH_4, respectively. It is evident that all species have a seasonal cycle feature. Year to year variability of XCO_2 is highest in spring and lowest during the growing season in June to September. Moreover, the behavior of the seasonal cycle of XCO_2 at our site was compared with that of XCO_2 at Saga, Japan, which is discussed in a later section. The atmospheric increase of XCO_2 from 2015 to 2016 was 3.65 ppm, which is larger than the increase from 2014 to 2015. For the case of XCH_4, its increase from 2015 to 2016 was 0.02 ppm, which is higher than the increase from 2014 to 2015, whereas in XCO the rate of increment from year to year was found to be slightly decreased (see Table 4).

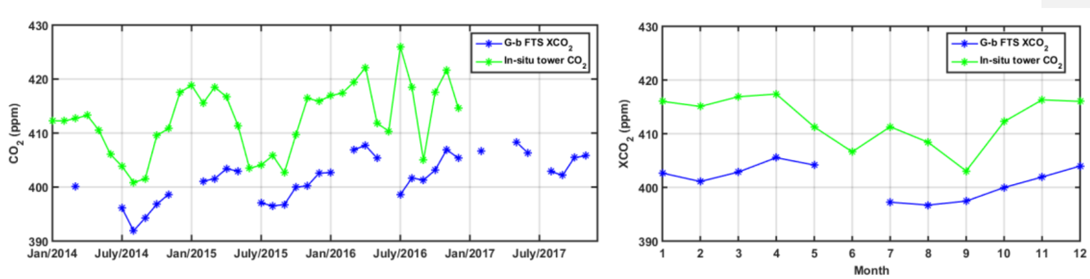

Figure 11. Left panel shows the time series of FTS XCO_2 and in-situ tower CO_2 on monthly mean basis, whereas right panel depicts annual cycle (2014-2016).

The seasonal and annual cycles of XCO_2 derived from the g-b FTS were compared with in-situ tower observations of CO_2 over the Anmyeondo station, which are presented in Figure 11. Regarding in-situ data, samples were collected using flasks and analysed using non-dispersive infrared (NDIR) spectroscopy at the altitude of 77 meters above sea level (details about in situ data are available at http://ds.data.jma.go.jp/jmd/wdcgg/). Nearly 97 % of in-situ data in Figure 11 were taken during day time between 04:00 – 08:40 UTC (13:00 – 17:40 Korea Standard Time (KST)) so that the early morning and night time enhancements of CO_2 were mostly excluded. In-situ CO_2 monthly means are generated by first averaging all valid event measurements with a unique sample date and time. The values are then extracted at weekly intervals from a smooth curve (Thoning et al., 1989) fitted to the averaged data and then these weekly values are averaged for each month. As can be seen in Figure 10, the overall patterns of seasonal and annual cycle of FTS XCO_2 tend to be similar with those of in-situ tower CO_2.

3.2 Comparison of Anmyeondo XCO_2 with nearby TCCON station

In Figure 12, we present the comparison of our FTS XCO_2 data with a similar ground-based high resolution TCCON FTS observation at Saga station (33.26 N, 130.29 E) in Japan, which is the closest TCCON station to our site. Among nearby TCCON stations, Rikubetsu, Tsukuba, and Saga are located in Japan (Morino et al., 2011, Ohyama et al., 2009, 2015) and Hefei is located in China (Wang et al., 2017). To demonstrate the comparison between them, we have shown the daily averaged XCO_2 of two stations during the period of 2014 to 2017 in Figure 12. As can be seen, variations of XCO_2 at the Saga station agreed well with Anmyeondo station. The daily averaged XCO_2 revealed the same seasonal cycle as that of our station. The lowest XCO_2 appeared in late summer (August and September), and the highest value was in spring (April).

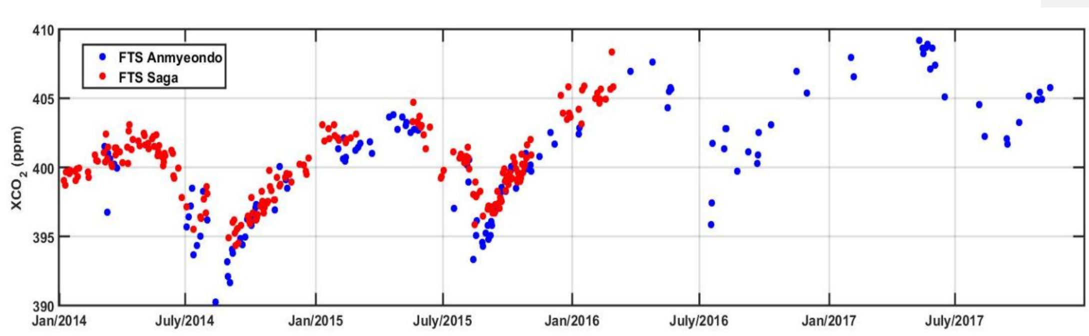

Figure 12. Time series of daily averaged XCO_2 retrieval from Anmyeondo FTS and Saga FTS in the period of February 2014 to November 2017 is depicted.

Ohyama et al., (2015) studied the time series of XCO_2 at Saga, Japan during the period from July 2011 to December 2014. They showed seasonal and interannual variations. The peak-to-peak seasonal amplitude of XCO_2 was 6.9 ppm over Saga during July 2011 and December 2014, with a seasonal maximum and minimum in the average seasonal cycle during May and September, respectively. In recent findings of Wang et al. (2017), the g-b FTS temporal distributions of XCO_2 at Hefei, China were reported. The FTS observations in 2014 to 2016 had a clear and similar seasonal cycle, i.e. XCO_2 reaches a minimum in late summer, and then slowly increases to the highest value in spring. The daily average of XCO_2 ranges from 392.33 $\pm$ 0.86 to 411.62 $\pm$ 0.90 ppm, and the monthly average value shows a seasonal amplitude of 8.31 and 13.56 ppm from 2014 to 2015 and from 2015 to 2016, respectively. The seasonal cycle was mainly driven by large scale (hemispheric) biosphere–atmosphere exchange. Butz et al., (2011) reported that the observations from GOSAT and the co-located ground-based measurements agreed well in capturing the seasonal cycle of XCO_2 with the late summer minimum and the spring maximum for four TCCON stations (Bialystok, Orleans, Park Falls, and Lamont) in the Northern Hemisphere. We infer that the variation of XCO_2 over Anmyeondo station is in harmony with the variation pattern in mid-latitude Northern Hemisphere.

3.3 Comparison of XCO_2 between the g-b FTS and OCO-2

In this section, we present a comparison of XCO_2 between the g-b FTS and OCO-2 version 7Br data (bias corrected data) over Anmyeondo station during the period between 2014 and 2017. For making a direct comparison of the g-b FTS measurements against OCO-2, we applied the spatial coincidence criteria for the OCO-2 data within 3° latitude/longitude of the FTS station, as well as setting up a time window of 3 hours (maximum 3 hours mismatch between satellite and g-b FTS observations). Based on the coincidence criteria, we obtained 13 coincident measurements, which were not sufficient to infer a robust conclusion, but do provide a preliminary result. The comparison of the time series of XCO_2 concentrations derived from the g-b FTS and OCO-2 on daily median basis is demonstrated during the measurement period between 2014 and 2017, depicted in Figure 13. As can be seen in the plot, the g-b FTS measurement exhibits some gaps which occurred due to bad weather conditions, instrument failures, and absences of an instrument operator. In the present analysis, the XCO_2 concentrations from FTS were considered only when retrieval error was below 1.50 ppm (not shown), which is the sum of all error components such as laser sampling error, zero level offsets, ILS error, smoothing error, atmospheric a-priori temperature, atmospheric a-priori pressure, surface pressure, and random noise. Wunch et al. (2016) reported that the comparison of XCO_2 derived from the OCO-2 version 7Br data against co-located ground-based TCCON data that indicates the median differences between the OCO-2 and TCCON data were less than 0.50 ppm, and corresponding RMS differences of less than 1.50 ppm. The overall results of our comparisons were comparable with the report of Wunch et al. (2016). The OCO-2 product of XCO_2 was biased (satellite minus g-b FTS) with respect to the g-b FTS, which was slightly higher by 0.18 ppm with a standard deviation of 1.19 ppm, a corresponding RMS difference of 1.16

ppm. This bias could be attributed to the instrument uncertainty. In addition to that, we also obtained a strong correlation between the two datasets, which was quantified as a correlation coefficient of 0.94 (see Table 5 and Figure 13).

Table 5. Summary of the statistics of XCO_2 comparisons between OCO-2 and the g-b FTS from 2014 to 2017 are presented. N - coincident number of data, R - Pearson correlation coefficient, RMS - Root Mean Squares differences.

N	Mean Absolute.diff. (ppm)	Mean Relative diff (%)	R	RMS (ppm)
13	0.18±1.19	0.04±0.29	0.94	1.16

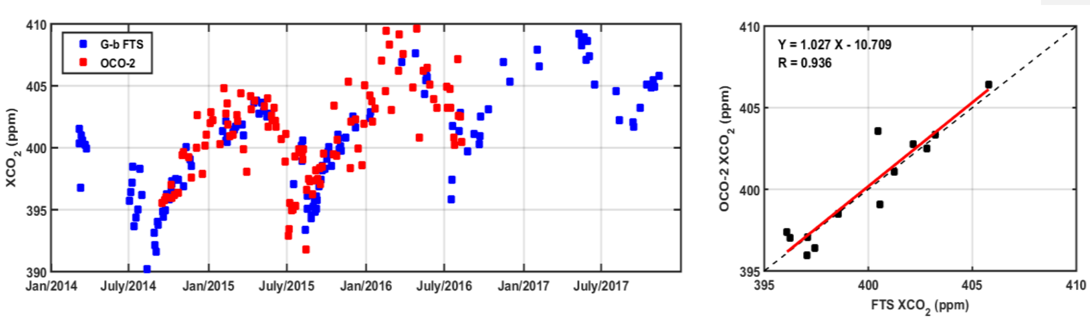

Figure 13. Left panel: The time series of XCO_2 from the g-b FTS (blue square) and OCO-2 (red square) over the Anmyeondo station from February 2014 to November 2017 are shown. Right panel: The linear regression curve between FTS and OCO-2 is shown. All results are given on daily medians basis.

Table 6. Seasonal mean and standard deviations of XCO_2 from the g-b FTS and OCO-2 in the period between 2014 and 2016 are given below.

Season	g-b FTS XCO_2 mean ± std (ppm)	OCO-2 XCO_2 mean ± std (ppm)
Winter	401.52 ± 0.85	402.67 ± 2.67
Spring	402.72 ± 2.79	403.96 ± 2.77
Summer	396.92 ± 3.28	399.68 ± 3.77
Autumn	398.01 ± 2.83	398.48 ± 2.41

Both measurements capture the seasonal variability of XCO_2. As can be seen clearly from the temporal distribution of FTS XCO_2, the maximum and minimum values are discernible in spring and late summer seasons, respectively. The mean values in spring and summer were 402.72 and 396.92 ppm, respectively (see Table 6). This is because the seasonal variation of XCO_2 is most likely to be controlled by the imbalance of the terrestrial ecosystem exchange, and this could explain the larger XCO_2 values in the northern hemisphere in late April (Schneising et al.

2008, and references therein). The minimum value of XCO_2 occurs in August, which is most likely due to uptake of carbon into the biosphere associated with the period of plant growth. Furthermore, both instruments showed high standard deviations during summer, about 3.28 ppm in FTS and 3.77 ppm in OCO-2, and this suggests that the variability reflects strong sources and sink signals.

4 Conclusions

Monitoring of greenhouse gases is an essential issue in the context of global climate change. Accurate and precise continuous long-term measurements of greenhouse gases (GHGs) are substantial for investigating their sources and sinks. Today, several remote sensing instruments operated on different platforms are dedicated for measuring GHGs. Total column measurements of greenhouse gases such as XCO_2, XCH_4, XH_2O, XN_2O have been made using the g-b FTS at the Anmyeondo station since 2013. In this work, we focused on the measurements taken during the period of February 2014 to November 2017. The instrument has been operated in a semi-automated mode since then. The FTS instrument has been stable during the whole measurement period. Regular instrument alignment checks using the HCl cell measurements are performed. The TCCON standard GGG2014 retrieval software was used to retrieve XCO_2, XCO, and others GHG gases from the g-b FTS spectra.

In this work, the g-b FTS retrieval of XCO_2 and XCH_4 were compared with aircraft measurements that were conducted over Anmyeondo station on 22 May 2016, 29 October and 12 November, 2017. The mean absolute difference between FTS and aircraft XCO_2 we obtained were found to be -1.129 ± 1.989 ppm, corresponding to a mean relative difference of -0.280 ± 0.491 % for XCO_2, while the mean absolute difference for XCH_4 is -0.010 ± 0.0273 ppm, corresponding to a mean relative difference of -0.542 ± 1.468 %. These differences appeared in both species and were consistent with the combined instrument errors. The preliminary comparison results of XCO_2 between FTS and OCO-2 were also presented over the Anmyeondo station. The mean absolute difference of XCO_2 between FTS and OCO-2 was calculated on daily median basis, and it was estimated to be 0.18 ppm with a standard deviation of 0.19 with respect to the g-b FTS. This bias could be attributed to instrument uncertainty. Based on the seasonal cycle comparison, both the g-b FTS and OCO-2 showed a consistent pattern in capturing the seasonal variability of XCO_2, with maximum in spring and minimum in summer.

5 Acknowledgements

This research was supported by the Research and Development for KMA Weather, Climate, and Earth system Services (NIMS-2016-3100). D.W.T.G and V.A.V. would like to acknowledge financial support from the Australian Research Council (ARC) for TCCON activities (DP160101598, DP140101552, DP110103118). We would like to thank all the NASA's KORUS campaign team, in-situ tower station team (WDCGG), and TCCON community for the provision of data. We also greatly acknowledge the two anonymous reviewers who helped us to improve this manuscript well.

메모 [Office28]: As I asked earlier, have you shared this with these investigators? Is this an adequate acknowledgement? Generally, the investigators should be thanked by name if you have agreed with them that they are not interested in being co-authors.

References

Boland, S., Brown L. R., Burrows J. P., Ciais P., Connor B. J., Crisp D., Denning S., Doney S. C., Engelen R., Fung I. Y., Griffith P., Jacob D. J., Johnson B., Martin-Torres J., Michalak A. M., Miller C. E., Polonsky I., Potter C., Randerson J. T., Rayner P. J., Salawitch R. J., Santee M., Tans P. P., Wennberg P. O., Wunch D., Wofsy S. C., and Yung Y. L.: The Need for Atmospheric Carbon Dioxide Measurements from Space: Contributions from a Rapid Reflight of the Orbiting Carbon Observatory, 2009, http://www.nasa.gov/pdf/363474main_OCO_Reflight.pdf.

Brault, J. W.: New approach to high-precision Fourier transform spectrometer design. Appl. Opt. 35, 2891–2896, 1996.

Butz, A., Guerlet, S., Hasekamp, O., Schepers, D., Galli, A., Aben, I., Frankenberg, C., Hartmann, J.-M., Tran, H., Kuze, A., Keppel-Aleks, G., Toon, G., Wunch, D., Wennberg, P., Deutscher, N., Griffith, D., Macatangay, R., Messerschmidt, J., Notholt, J., and Warneke, T.: Toward accurate CO_2 and CH_4 observations from GOSAT, Geophys. Res. Lett., 38, L14812, https://doi.org/10.1029/2011GL047888, 2011.

Chen, H., Winderlich, J., Gerbig, C., Hoefer, A., Rella, C. W., Crosson, E. R., Van Pelt, A. D., Steinbach, J., Kolle, O., Beck, V., Daube, B. C., Gottlieb, E. W., Chow, V. Y., Santoni, G. W., and Wofsy, S. C: High-accuracy continuous airborne measurement of greenhouse gases (CO_2 and CH_4) using the cavity ring-down spectroscopy (CRDS) technique Atmos. Meas. Tech., 3, 375-386, 2010.

Connor B. J., Bösch H., Toon G., Sen B., Miller C. E., and Crisp D.: Orbiting carbon observatory: Inverse method and prospective error analysis, J. Geophys. Res., 113 doi: 10.1029/2006JD008336, 2008.

Crisp D., Miller C. E., DeCola P. L.: NASA Orbiting Carbon Observatory: measuring the column averaged carbon dioxide mole fraction from space. J. Appl. Remote Sens., 2, 023508, doi:10.1117/1.2898457, 2008.

Crisp D. for the OCO-2 Team: Measuring Atmospheric Carbon Dioxide from Space with the Orbiting Carbon Observatory-2 (OCO-2), Proc. SPIE 9607, Earth Observing Systems XX, 960702, doi: 10.1117/12.2187291, 2015.

Deutscher, N. M., Griffith, D. W. T., Bryant, G. W., Wennberg, P. O., Toon, G. C., Washenfelder, R. A., Keppel-Aleks, G., Wunch, D., Yavin, Y., Allen N. T., Blavier, J.-F., Jiménez R., Daube, B. C., Bright, A. V., Matross, D. M., Wofsy, S. C., and Park, S.: Total column CO_2 measurements at Darwin, Australia-site description and calibration against in situ aircraft profiles, Atmos. Meas. Tech., 3, 947-958, doi:10.5194/amt-3-947-2010, 2010.

Frankenberg, C., Pollock, R., Lee, R. A. M., Rosenberg, R., Blavier, J.-F., Crisp, D., O'Dell C. W., Osterman, G. B., Roehl, C., Wennberg, P. O., and Wunch, D.: The Orbiting Carbon Observatory (OCO-2): spectrometer performance evaluation using pre-launch direct sun measurements. Atmospheric Measurement Techniques, 8(1), 301–313. doi:10.5194/amt-8-301-2015, 2015.

Hase, F., Blumenstock, T., and Paton-Walsh, C.: Analysis of the instrumental line shape of high resolution Fourier transform IR spectrometers with gas cell measurements and new retrieval software, Appl. Optics, 38, 3417–3422, doi:10.1364/AO.38.003417,1999.

Hase, F., Drouin, B. J., Roehl, C. M., Toon, G. C., Wennberg, P. O., Wunch, D., Blumenstock, T., Desmet F., Feist, D. G., Heikkinen, P., De Mazière, M., Rettinger, M., Robinson, J., Schneider, M., Sherlock, V., Sussmann, R., Té Y., Warneke, T., and Weinzierl, C.: Calibration of sealed HCl cells used for TCCON instrumental line shape monitoring, Atmospheric Measurement Techniques, 6(12), 3527–3537, doi:10.5194/amt-6-3527-2013, 2013.

Kiel, M., Wunch, D., Wennberg, P. O., Toon, G. C., Hase, F., and Blumenstock, T.: Improved retrieval of gas abundances from near-infrared solar FTIR spectra measured at the Karlsruhe TCCON station, Atmos. Meas. Tech., 9(2), 669–682, doi:10.5194/amt-9-669-2016, 2016.

Kivi, R. and Heikkinen, P.: Fourier transform spectrometer measurements of column CO_2 at Sodankylä, Finland, Geosci. Instrum. Method. Data Syst., 5, 271–279, 2016.

Messerschmidt, J., Macatangay, R., Notholt, J., Petri C., Warneke, T., and Weinzierl, C.: Side by side measurements of CO_2 by ground-based Fourier transform spectrometry (FTS), Tellus B, 62(5), 749-758, doi:10.1111/j.1600-0889.2010.00491.x., 2010.

Messerschmidt, J., H. Chen, N. M. Deutscher, C. Gerbig, P. Grupe, K. Katrynski, F.-T. Koch, J. V. Lavrič, J. Notholt, C. Rödenbeck, W. Ruhe, T. Warneke, and Weinzierl, C.: Automated ground-based remote sensing measurements of greenhouse gases at the Białystok site in comparison with collocated in situ measurements and model data, Atmospheric Chemistry and Physics, 12(15), 6741–6755, doi:10.5194/acp-12-6741-2012, 2012.

Miao, R., Lu N., Yao L., Zhu, Y., Wang, J., and Sun, J.: Multi-Year Comparison of Carbon Dioxide from Satellite Data with Ground-Based FTS Measurements (2003–2011), Remote Sensing, 5(7), 3431–3456, doi:10.3390/rs5073431, 2013.

Miller, C. E., Crisp, D. DeCola, P. L., Olsen, S. C., Randerson, J. T., Michalak, A. M., Alkhaled, A., Rayner, P., Jacob, D. J., Suntharalingam, P., Jones, D. B. A., Denning, A. S., Nicholls, M. E., Doney, S. C., Pawson, S., Boesch, H., Connor B. J., Fung I. Y., O'Brien, D., Salawitch, R. J., Sander, S. P., Sen, B., Tans, P., Toon, G. C., Wennberg, P. O., Wofsy, S. C., Yung, Y. L., and Law, R. M.: Precision requirements for space-based XCO_2 data, J. Geophys. Res-Atmos., 109, D02301, doi: 10.1029/2006JD007659, 2007.

Morino, I., Uchino, O., Inoue, M., Yoshida, Y., Yokota T., Wennberg, P. O., Toon, G. C., Wunch, D., Roehl, C. M., Notholt, J., Warneke, T., Messerschmidt, J., Griffith, D. W. T., Deutscher, N. M., Sherlock, V., Connor, B. J., Robinson, J., Sussmann, R., and Rettinger, M.: Preliminary validation of column-averaged volume mixing ratios of carbon dioxide and methane retrieved from GOSAT short-wavelength infrared spectra, Atmospheric Measurement Techniques, 4(6), 1061-1076, doi:10.5194/amt-4-1061-2011, 2011.

Miyamoto, Y., Inoue, M., Morino, I., Uchino, O., Yokota, T., Machida, T., Sawa, Y., Matsueda, H., Sweeney, C., Tans, P. P., Andrews, A. E., and Patra, P. K.: Atmospheric column-averaged mole fractions of carbon dioxide at 53 aircraft measurement sites, Atmos. Chem. Phys., 13, 52655275, 2013.

O'Dell, C. W., Connor, B., Bösch, H., O'Brien, D., Frankenberg C., Castano, R., Christi, M., Eldering, D., Fisher, B., Gunson, M., McDuffie, J., Miller, C. E., Natraj, V., Oyafuso, F., Polonsky, I., Smyth, M., Taylor, T., Toon, G. C., Wennberg, P. O., and Wunch, D.: The ACOS CO2 retrieval algorithm – Part 1: Description and validation against synthetic observations, Atmospheric Measurement Techniques, 5, 99–121, doi: 10.5194/amt-5-99-2012, http://www.atmos-meas-tech.net/5/99/2012/, 2012.

Ohyama, H., Morino, I., Nagahama, T., Machida, T., Suto H., Oguma, H., Sawa, Y., Matsueda, H., Sugimoto, N., Nakane, H., and Nakagawa, K.: Column-averaged volume mixing ratio of CO_2 measured with ground-based Fourier transform spectrometer at Tsukuba, J. Geophys. Res., 114, D18303 doi:10.1029/2008JD011465, 2009.

Ohyama, H., Kawakami, S., Tanaka, T., Morino, Uchino, I., O., Inoue, M., Sakai, T., Nagai, T., Yamazaki, A., Uchiyama, A., Fukamachi, T., Sakashita, M., Kawasaki, T., Akaho, T., Arai, K., and Okumura, H.: Observations of XCO_2 and XCH_4 with ground-based high-resolution FTS at Saga, Japan, and comparisons with GOSAT products, Atmos. Meas. Tech., 8(12), 5263–5276, doi:10.5194/amt-8-5263-2015.

Rayner P. J., and O'Brien D. M.: The utility of remotely sensed CO_2 concentration data in surface source inversions, Geophys. Res. Lett., 28, 175–178, doi: 10.1029/2000GL011912, 2001.

Schneising O., Buchwitz M., Burrows J. P., Bovensmann, H., Reuter, M., Notholt, J., Macatangay, R., and Warneke, T.: Three years of greenhouse gas column-averaged dry air mole fractions retrieved from satellite-Part 1: Carbon dioxide, Atmos. Chem. Phys., 8, 3827-3853, 2008.

Sun, Y., Palm, M., Weinzierl, C., Peteri, C., Notholt, J., Wang, Y., and Liu, C.: Technical note: Sensitivity of instrumental line shape monitoring for the ground-based high-resolution FTIR spectrometer with respect to different optical attenuators, Atmos. Meas. Tech. Discuss., doi:10.5194/amt-10-989- 2017.

Thoning, K. W., Tans, P. P. and Komhyr, W. D.: Atmospheric carbon dioxide at Mauna Loa Observatory. Analysis of the NOAA GMCC Data, 1974-1985, J. Geophys. Res., 94, 8549-8565, 1989.

WMO (2016). The state of greenhouse gases in the atmosphere based on global observations through 2015, greenhouse gas. Greenhouse Gas Bulletin 2016. https://library.wmo.int/opac/doc_num.php.

Wang, W., Tian, Y., Liu, C., Sun, Y., Liu, W., Xie, P., Liu, J., Xu, J., Morino, I., Velazco, V., Griffith, D., Notholt, J., and Warneke, T.: Investigating the performance of a greenhouse gas observatory in Hefei, China, Atmos. Meas. Tech., 10, 2627–2643, 2017.

Wang, Y., Munger, J. W., Xu, S., McElroy, M. B., Hao, J., Nielsen, C. P., and Ma, H.: CO2 and its correlation with CO at a rural site near Beijing: implications for combustion efficiency in China, Atmos. Chem. Phys., 10, 8881–8897, https://doi.org/10.5194/acp-10-8881-2010, 2010.

Washenfelder R. A., Toon G. C., Blavier J-F., Yang Z., Allen N. T., Wennberg P. O., Vay S. A., Matross, D. M., and Daube B. C.: Carbon dioxide column abundances at the Wisconsin Tall Tower site, Journal of Geophysical Research, 2006, 111, doi:10.1029/2006JD00715, 2006.

Warneke, T., Yang, Z., Olsen, S., Korner, S., Notholt J., Toon, G. C., Velazco, V., Schultz, A., and Schrems, O.: Seasonal and latitudinal variations of column averaged volume-mixing ratios of atmospheric CO_2, Geophysical Research Letters, 32(3), 2-5, doi:10.1029/2004GL021597, 2005.

Wunch, D., Toon G. C., Wennberg, P. O., Wofsy, S. C., Stephens, B., Fisher, M. L., Uchino O., Abshire, J. B., Bernath, P. F., Biraud, S. C., Blavier, J.-F. L., Boone, C. D., Bowman, K. P., Browell, E. V., Campos, T., Connor, B. J., Daube, B. C., Deutscher, N. M., Diao M., Elkins, J. W., Gerbig, C., Gottlieb, E., Griffith, D. W. T., Hurst, D. F., Jiménez, R., Keppel-Aleks, G., Kort, E. A., Macatangay, R., Machida, T., Matsueda, H., Moore, F. L., Morino, I., Park, S., Robinson, J., Roehl, C. M., Sawa, Y., Sherlock, V., Sweeney, C., Tanaka, T., and Zondlo, M. A.: Calibration of the Total Carbon Column Observing Network using aircraft profile data, Atmospheric Measurement Techniques, 3(5), 1351-1362, doi:10.5194/amt-3-1351-2010.

Wunch, D., Toon, G. C., Sherlock, V., Deutscher, N. M., Liu X., Feist, D. G., and Wennberg, P. O.: The Total Carbon Column Observing Network's GGG2014 Data Version. doi:10.14291/tccon.ggg2014.documentation.R0/1221662, 2015.

Wunch, D., Wennberg, P.O.,, Osterman, G., Fisher, B., Naylor, B., Roehl, C. M., O'Dell, C., Mandrake, L.,Viatte, C., Griffith, D. W. T., Deutscher, N. M., Velazco, V. A., Notholt, J.,Warneke, T.,Petri, C., Maziere, M. De, Sha, M. K., Sussmann,R., Rettinger, M., Pollard, D., Robinson, J.,Morino, I., Uchino O., Hase, F., Blumenstock, T., Kiel, M., Feist, D. G., Arnold S.G., Strong, K., Mendonca, J., Kivi, R.,Heikkinen, P., Iraci, L., Podolske, J., Hillyard, P. W., Kawakami, S., Dubey, M. K., Parker, H. A., Sepulveda, E., Rodriguez, O. E. G., Te, Y., Jeseck, P., Gunson, M. R., Crisp, D., and Eldering A., Comparisons of the Orbiting Carbon Observatory-2 (OCO-2) XCO_2 measurements with TCCON, Atmos. Meas. Tech. Discuss., doi:10.5194/amt-2016-227, 2016.

Final Version agreed with Co-authors .

Characteristics of Greenhouse Gas Concentrations Derived from Ground-based FTS Spectra at Anmyeondo, Korea

Young-Suk Oh[1,2*], Samuel Takele Kenea[1], Tae-Young Goo[1], Kyu-Sun Chung[2], Jae-Sang Rhee[1], Mi-Lim Ou[6], Young-Hwa Byun[1], Paul O. Wennberg[4,5], Matthäus Kiel[4], Joshua P. DiGangi[7], Glenn S. Diskin[7], Voltaire A. Velazco[3] and David W. T. Griffith[3]

1. Climate Research Division, National Institute of Meteorological Sciences (NIMS), Jeju-do, Republic of Korea
2. Department of Electrical Eng. & Centre for Edge Plasma Science, Hanyang University, Seoul, Republic of Korea
3. School of Chemistry, University of Wollongong, Northfields Ave, Wollongong, NSW 2522, Australia
4. Division of Geological and Planetary Sciences, California Institute of Technology, 1200E. California Boulevard, Pasadena, CA, 91125, USA
5. Division of Engineering and Applied Sciences, California Institute of Technology, 1200E. California Boulevard, Pasadena, CA, 91125, USA
6. Climate Change Monitoring Division, Korea Meteorological Administration, Seoul, Republic of Korea
7. NASA Langley Research Center Building 1250, Mail Stop 401A Hampton, VA 23681 United States

*Correspondence to: Young-Suk Oh (ysoh306@gmail.com)

Abstract.

Since the late 1990s, the meteorological observatory established in Anmyeondo (36.5382˚ N, 126.3311˚ E, and 30 m above mean sea level), has been monitoring several greenhouse gases such as CO_2, CH_4, N_2O, CFCs, and SF_6, as a part of the Global Atmosphere Watch (GAW) Program. A high resolution ground-based (g-b) Fourier Transform Spectrometer (FTS) was installed at this observation site in 2013, and has been operated within the frame work of the Total Carbon Column Observing Network (TCCON) since August, 2014. The solar spectra recorded by the g-b FTS cover the spectral range 3,800 to 16,000 cm^{-1} at a resolution of 0.02 cm^{-1}. In this work, the GGG2014 version of the TCCON standard retrieval algorithm was used to retrieve total column average CO_2 and CH_4 dry mole fractions (XCO_2, XCH_4) and from the FTS spectra. Spectral bands of CO_2 (at 6220.0 and 6339.5 cm^{-1} centre wavenumbers, CH_4 at 6002 cm^{-1} wavenumber, and O_2 near 7880 cm^{-1}) were used to derive the XCO_2 and XCH_4. In this paper, we provide comparisons of XCO_2 and XCH_4 between the aircraft observations and g-b FTS over Anmyeondo station. A comparison of 13 coincident observations of XCO_2 between g-b FTS and OCO-2 (Orbiting Carbon Observatory) satellite measurements are also presented for the measurement period between February 2014 and November 2017. OCO-2 observations are highly correlated with the g-b FTS measurements (r^2=0.884) and exhibited a small positive bias (0.189 ppm). Both data set capture seasonal variations of the target species with maximum and minimum values in spring and late summer, respectively. In the future, it is planned to further utilize the FTS measurements for the evaluation of satellite observations such as Greenhouse Gases Observing Satellite (GOSAT, GOSAT-2). This is the first report of the g-b FTS observations of XCO_2 species over the Anmyeondo station.

Key words: Aircraft**,** XCO_2, OCO-2, TCCON, Infrared spectra

1. Introduction

Monitoring of greenhouse gases (GHGs) is a crucial issue in the context of global climate change. Carbon dioxide (CO_2) is one of the key greenhouse gases and its global annual mean concentration has increased rapidly from 278 to 400 ppm since the preindustrial data of 1750 (WMO greenhouse gas bulletin, 2016). Radiative forcing due to changes in atmospheric CO_2 accounts for approximately 65 % of the total change in radiative forcing by long-lived GHGs (Ohyama et al., 2015 and reference therein). Human activities such as burning of fossil fuels and land use change are the primary drivers of the continuing increase in atmospheric greenhouse gases and the gases involved in their chemical production (Kiel et al., 2016 and reference therein). There is a global demand for accurate and precise long-term measurements of greenhouse gases.

In the field of remote sensing techniques, solar absorption infrared spectroscopy has been increasingly used to determine changes in atmospheric constituents. Today, a number of instruments deployed on various platforms (ground-based and space-borne) have been operated for measuring GHGs such as CO_2. The g-b FTS at the Anmyeondo station has been measuring several atmospheric GHG and other gases such as CO_2, CH_4, CO, N_2O, and H_2O operated within the framework of the Total Carbon Column Observing Network (TCCON). XCO_2 retrievals from the g-b FTS have been reported at different TCCON sites (e.g, Ohyama et al., 2009; Deutscher et al., 2010; Messerschmidt et al., 2010, 2012; Miao et al., 2013; Kivi and Heikkinen, 2016, Velazco et al. 2017). TCCON achieves accuracy and precision in measuring the column averaged dry air mole fraction of CO_2 (XCO_2), of about 0.25 %, or better than 1 ppm (Wunch et al., 2010), which is essential to retrieve information about sinks and sources, as well as validating satellite products (Rayner and O'Brien, 2001; Miller et al., 2007). Precision for XCO_2 of 0.1 % can be achieved during clear sky conditions (Messerschmidt et al., 2010; Deutscher et al., 2010). The network aims to improve global carbon cycle studies and supply the primary validation data of different atmospheric trace gases for space-based instruments, e.g., the Orbiting Carbon Observatory 2 (OCO-2), the Greenhouse Gases Observing Satellite (GOSAT, GOSAT-2) (Morino et al., 2011; Frankenberg et al., 2015).

This study is focused on the initial characteristics of XCO_2 retrievals from g-b FTS spectra over the Anmyeondo station, and comparison with in situ aircraft overflights and the OCO-2 satellite. The FTS spectra have been processed using the TCCON standard GGG2014 (Wunch et al., 2015) retrieval software. One of the unique aspects in this work is a new homemade addition to our g-b FTS instrument that reduces the solar intensity variations from the 5% maximum allowed in TCCON to less than 2%. This paper presents an introduction to the instrumentation and measurement site, and provides initial results and discussion followed by conclusions.

2 Station and instrumentation

2.1 Station description

The g-b FTS observatory was established in 2013 at the Anmyeondo (AMY) station, located at 36.32˚ N, 126.19˚ E, and 30 m above sea level. This station is situated on the west coast of the Korean Peninsula, 180 km SE of Seoul, the capital city of Republic of Korea. Figure 1 displays the Anmyeondo station. It is also a regional GAW (Global Atmosphere Watch) station that is operated by the Climate Change Monitoring Network of KMA (Korean Meteorological Administration). The AMY station has been monitoring various atmospheric parameters such as greenhouse gases, aerosols, ultraviolet radiation, ozone, and precipitation since 1999. The total area of the Anmyeondo island is estimated to be ~88 km^2 and approximately 1.25 million people reside on the island. Some of the residents over this area are engaged in agricultural activities. Vegetated areas consisting of mainly pine trees are located in and around the FTS observatory. The topographic feature of the area is one of low level hills, on average about 100 m above sea level. The minimum temperature in winter season is on average 2.7 ˚C, and the maximum temperature is about 25.6 ˚C during summer. Average annual precipitation amount is 1,155 mm; with snow in winter. The site has been formally designated as a provisional TCCON site since August 2014. Full acceptance requires calibration via overflights with WMO-calibrated in situ vertical profiles, as described in this paper. The AMY Station's TCCON wiki page can be found at: [https://tccon-wiki.Anmyeondo.edu]

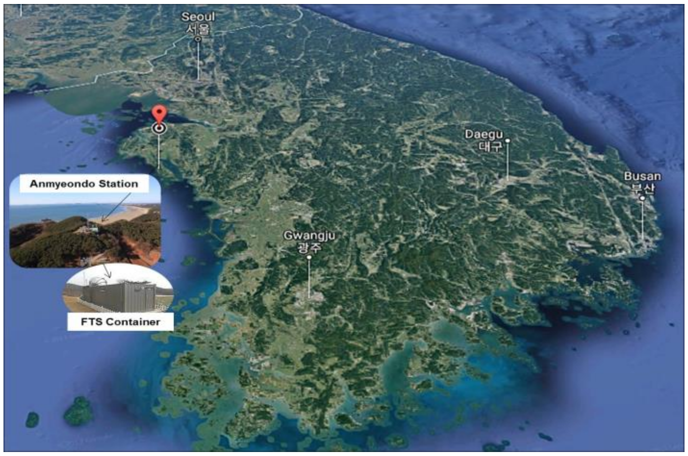

Figure 19. Anmyeodo (AMY) g-b FTS station

2.2 G-b FTS instrument

Solar spectra are acquired using a Bruker IFS 125HR spectrometer (Bruker Optics, Germany) under the guidelines set by TCCON. Currently, our g-b FTS instrument operation is semi-automated for taking the routine measurements under clear sky conditions. It is planned to make an FTS operation mode fully automated in 2018. The solar tracker (A547, Bruker Optics, Germany) is mounted inside a remotely controlled protective dome. The tracking ranges in azimuthal and elevation angles are about 0 to 315 and -10 to 85 degrees, respectively, while the tracking speed is about 2 degrees per second. The tracking accuracy of ±4 minutes of arc is achieved by the Camtracker mode which centres an image of the sun onto the spectrometer's input field stop. Under clear sky conditions, the dome is opened and set to an automatic tracking mode, in which the mirrors are initially moved to the calculated solar position, then. The camtracker control is activated in such a way that the mirrors are finely and continuously controlled to fix the beam onto the entrance stop of the spectrometer. Figure 2 displays an overview of the general data acquisition system. This ensures that all spectra are recorded under clear weather conditions.

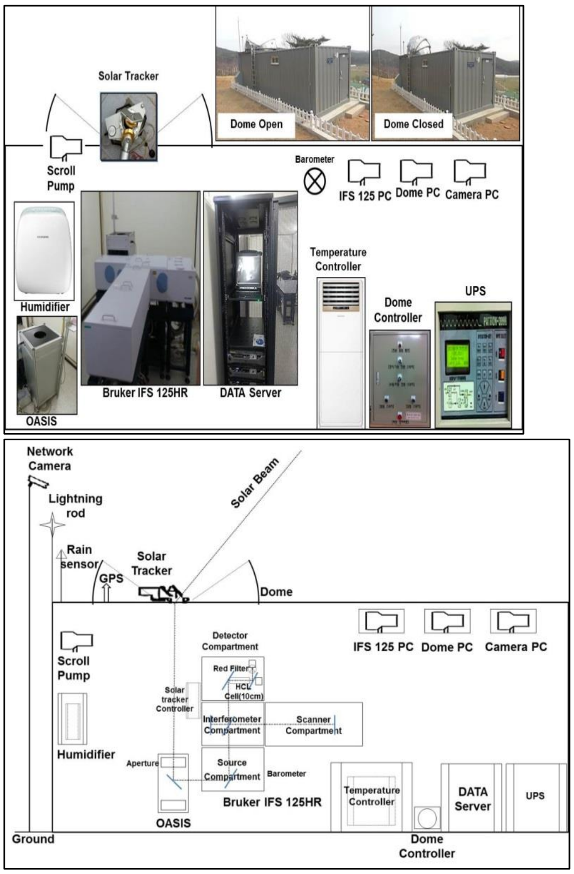

Figure 2. Photographs of the automated FTS laboratory. The Bruker Solar Tracker type A547 is mounted in the custom made dome. A servo controlled solar tracker directs the solar beam through a CaF_2 window to the FTS (125HR) in the laboratory. The server computer is used for data acquisition. PC1 and PC2 are used for controlling the spectrometer, solar tracker, dome, camera, pump, GPS satellite time, and humidity sensor.

The spectrometer is equipped with two room temperature detectors; an Indium-Gallium-Arsenide (InGaAs) detector, which covers the spectral region from 3,800 to 12,800 cm^{-1}, and Silicon (Si) diode detector (9,000 – 25,000 cm^{-1}) used in a dual-acquisition mode with a dichroic optic (Omega Optical, 10,000 cm^{-1} cut-on). A red longpass filter (Oriel Instruments 59523; 15,500 cm^{-1} cut-on) prior to the Si diode detector blocks visible light, which would otherwise be aliased into the near-infrared spectral domain. TCCON measurements are routinely recorded at a maximum optical path difference (OPD_{max}) of 45 cm leading to a spectral resolution of 0.02 cm^{-1} (0.9/max OPD). Two scans, one forward and one backward, are performed and individual forward-backward interferograms are recorded. As an example, Figure 3 shows a single spectrum recorded on 4 October 2014 with a resolution of 0.02 cm^{-1}. A single forward-backward scan in one measurement takes about 112 s. Measurement setting for the Anmyeondo g-b FTS spectrometer of the Bruker 125HR model is summarized in Table 1. The pressure inside the FTS is kept at 0.1 to 0.2 hPa with an oil-free vacuum pump to maintain the stability of the system and to ensure clean and dry conditions.

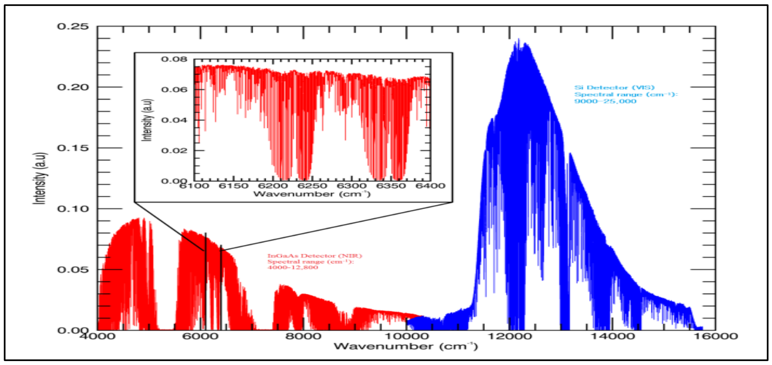

Figure 3. Single spectrum recorded on 4 October 2014 with a resolution of 0.02 cm^{-1}. A typical example for the spectrum of -XCO_2 is shown in the inset.

Table 10. Measurement setting for the Anmyeondo g-b FTS spectrometer of the Bruker 125HR model.

Item	Setting
Aperture (field stop)	0.8 mm
Detectors	RT-Si Diode DC, RT-InGaAs DC
Beamsplitters	CaF_2
Scanner velocity	10 kHz
Low pass filter	10 kHz
High folding limit	15798.007
Spectral Resolution	0.02 cm^{-1}
Optical path difference	45 cm
Acquisition mode	Single sided, forward backward
Sample scan	2 scans, forward, backward
Sample scan time	~110 s

2.3 Characterization of FTS-instrumental line shapes

For the accurate retrieval of total column amounts of the species of interest, a good alignment of the g-b FTS is essential. The instrument line shape (ILS) retrieved from the regular HCl cell measurements is an important indicator of the status of the FTS's alignment (Hase et al., 1999). The analyses of the measurements were performed using a spectrum fitting algorithm (LINEFIT14 software) (Hase et al., 2013). In Figure 4 we show time series of the modulation efficiency (right panel) and phase error (rad) (left panel) from the HCl cell measurement in the period of October 2013 to September 2017 using a tungsten lamp as light source. Modulation amplitudes for TCCON-acceptable alignment should be within 5 % of the ideal case (100%) at the maximum optical path difference (Wunch et al., 2011). In our g-b FTS measurements, it is found that the maximum loss of modulation efficiency is within 1 %, close to the ideal value. The phase errors are less than ± 0.0001 rad. Hase et al. (2013) reported that this level of small disturbances from the ideal value of the modulation efficiency is common to all well-aligned instruments. This result confirmed that the g-b FTS instrument is well aligned and has remained stable during the whole operation period.

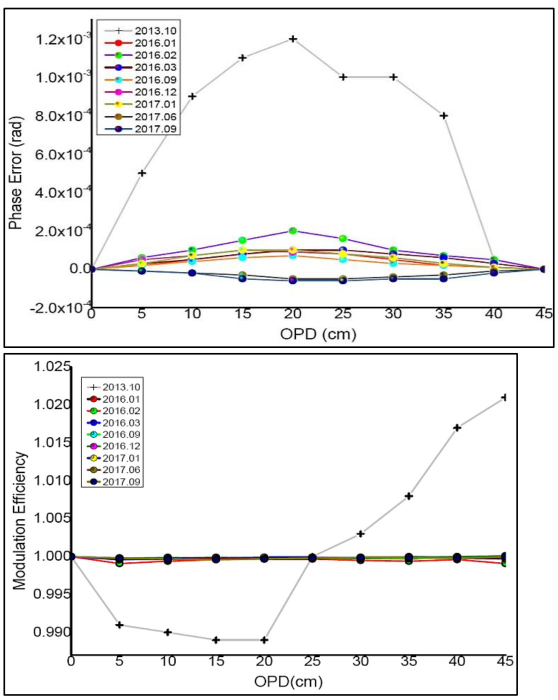

Figure 4. Modulation efficiency (right panel) and Phase error (rad) (left panel) of HCl measurements from the g-b FTS are displayed in the period from October 2013 to September 2017. Resolution = 0.02 cm^{-1}, Aperture = 0.8 mm.

We also confirmed that the ILS was not affected by the variable aperture (OASIS) during the operation of this system (see section 2.5). The modulation efficiency and phase error were estimated to be 99.98 % and 0.0001 rad. Sun et al. (2017) reported the detailed characteristics of the ILS with respect to applications of different optical attenuators to FTIR spectrometers within the TCCON and NDACC networks. They used both lamp and sun as light sources for the cell measurements, which were conducted after the insertion of five different attenuators in front of and behind the interferometer.

2.4 Data processing

Using the TCCON standard retrieval strategy, we have derived the column-averaged dry-air mole fractions CO_2 (XCO_2) and other atmospheric gases (O_2, CO, CH_4, N_2O, and H_2O) using the GFIT algorithm and software. The spectral windows used for the retrieval of CO_2 and O_2 are given in Table 2. The TCCON standard GGG2014 (version 4.8.6) retrieval software was used to obtain the abundance of the species from FTS spectra (Wunch et al., 2015). XCO_2 is derived from the ratio of retrieved CO_2 column to retrieved O_2 column,

$$XCO_2 = \frac{CO_{2\ \mathrm{column}}}{O_{2\ \mathrm{column}}} \times 0.2095\,, \qquad (1)$$

Computing the ratio using Eq. (1) minimizes systematic and correlated errors such as errors in solar zenith angle pointing error, surface pressure, and instrumental line shape that may exist in the retrieved CO_2 and O_2 columns (Washenfelder et al., 2006, Messerschmidt et al., 2012). The top panel of Figure 5 depicts the time series of laser sampling error (LSE) obtained from InGaAs spectra at the Anmyeondo FTS station in the measurement period of February 2014 to December 2016. LSE is due to inaccuracies in the laser sample timing, which have been reduced to acceptable levels by the instrument manufacturer. In the AMY FTS, the LSE is small and centered around zero. Slightly large LSE values were shown on 10 March, 2014 (see top panel of Fig. 5). On this date, we conducted the laser adjustment in FTS.

Table 11. Spectral windows used for the retrievals of the columns of CO_2 and O_2

Gas	Center of spectral window (cm^{-1})	Width (cm^{-1})	Interfering gas
O_2	7885.0	240.0	H_2O, HF, CO_2
CO_2	6220.0	80.0	H_2O ,HDO, CH_4
CO_2	6339.5	85.0	H_2O ,HDO

X_{air} is the ratio of atmospheric pressure to total column O_2, scaled such that for a perfect measurement X_{air} = 1.0. X_{air} is a useful indicator of the quality of measurements and the instrument performance (Wunch et al., 2015). Due to spectroscopic limitations there is a TCCON wide bias (X_{air} ~ 0.98) and small solar zenith angle (SZA) dependence. The retrieval of X_{air} deviating more than 1% from the TCCON-wide mean value of 0.98 would suggest a systematic error. The time series of X_{air} is shown in the bottom panel of Figure 5. The X_{air}

record reveals that the instrument has been stable during the measurement period. It shows that the values of X_{air} fluctuate between 0.974 and 0.985, and the mean value is 0.982 with a standard deviation of 0.0015 in which the scatter for X_{air} is about 0.15 %. The low variability in time series of X_{air} indicates the stability of the measurements.

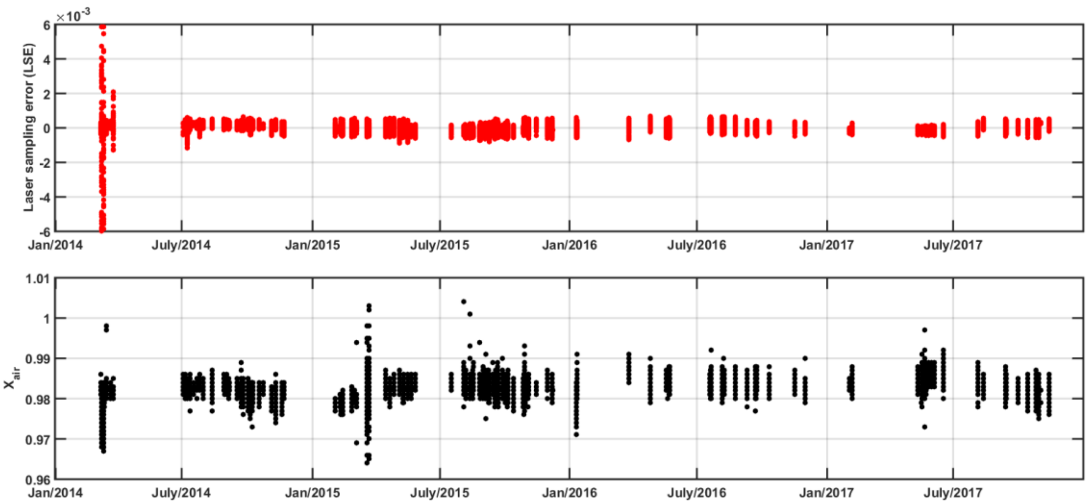

Figure 5. Time series of LSE (top panel) and X_{air} (bottom panel) from the g-b FTS during 2014- 2017 is shown. Each marker represents a single measurement.

2.5 Operational Automatic System for the Intensity of Sunray (OASIS) effect on the retrieval results

The OASIS system was developed for improving the quality of the spectra recorded by the spectrometer by maintaining a constant signal level. OASIS is beneficial for minimizing the variability that may be induced in the spectra due to intensity fluctuations of the incoming solar radiation that reaches the instrument. The main function of the OASIS is to control an aperture diameter in the parallel-inlet beam to the interferometer. This aperture is placed inside the OASIS system, in the parallel input solar beam external to the FTS. The fundamental purpose of this system is to optimize the measurement of solar spectra by reducing the effect of the fluctuations of the intensity of the incoming light due to changes in thin clouds along the line of sight over the measurement site. The maximum threshold value of the solar intensity variation

(SIV) is 5 %, the TCCON standard value (Ohyama et al., 2015). This value has been reduced to ≤ 2 % in our case by introducing the OASIS system to our g-b FTS since December 2014.

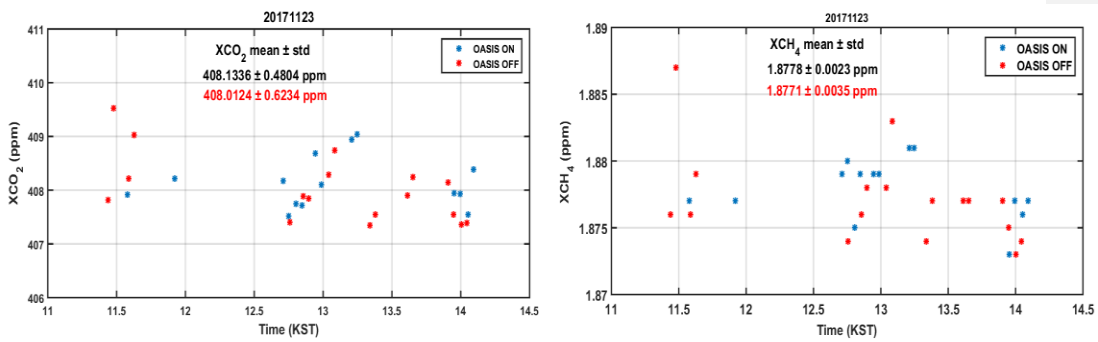

Figure 6. G-b FTS XCO_2 (left panel) and XCH_4 (right panel) values as function of time in KST (Korean Standard time, UTC+9) taken October 23, 2017 with OASIS system on (operating) and off (without operating) positions are shown. Each marker represents a single measurement.

In order to assess the impact of the OASIS system on the retrieval results of XCO_2 and XCH_4, we have conducted experiments on recording alternate FTS spectra with and without operation of this system under clear sky conditions. As an example, Figure 6 depicts the retrieval results of XCO_2 (left panel) and XCH_4 (right panel) as a function of time (KST, UTC+9), taken November 23, 2017 with OASIS on (blue) and off (red) positions. Mean differences of 0.12 ppm for XCO_2 and 7.0 x 10^{-4} ppm for XCH_4 were found between OASIS on and off position (i.e., with and without operating of OASIS system). This suggests that the impact of OASIS system on the retrieval is negligible.

2.6 Aircraft observation campaigns over Anmyeondo station

2.6.1 Aircraft instrumentation

In this section, we present a comparison between aircraft in-situ observations and g-b FTS column measurements over the Anmyeondo station. In situ profiles were conducted over Anmyeondo station by the National Institute of Meteorological Sciences (King Air C90) and as part of the KORUS-AQ campaign from NASA's DC8 (https://www-air.larc.nasa.gov/missinns/korus-aq). For the NIMS profiles, the flight take-off and landing was carried out from Hanseo University which is approximately 5 km away from the Anmyeondo FTS station. The aircraft was equipped with a Wavelength Scanned Cavity Ring Down Spectrometer (CRDS; Picarro, G2401-m), (see Fig. 7) providing mixing ratio data recorded at 0.3 Hz intervals. The position of the aircraft was monitored by GPS, and information on the outside temperature, static pressure, and ground speed was provided by instruments carried on the plane. The temperature and pressure of the gas sample have to be tightly controlled at 45 ℃ and 140 Torr in the CRDS, which leads to highly stable spectroscopic features (Chen et al., 2010). Any deviations from these values cause a reduction of the instrument's precision. Data recorded beyond the range of variations in cavity pressure and temperature were discarded in this analysis. Variance of the cavity pressure and temperature during flight results in variance in the CO_2 and CH_4 mixing ratios. The Picarro CRDS instrument has been regularly calibrated with respect to the standard gases within the error range recommended by the World Meteorological Organization. Measurements were made in wet air, and dry air mixing ratios were derived following the method described in Chen et al. (2010). Water was measured and its effect was accounted for in the column integration of CO_2 and CH_4

On NASA's DC8, CO_2 was measured by the Atmospheric Vertical Observations of CO_2 in the Earth's troposphere (AVOCET) instrument, a non-dispersive IR spectrometer (Vay et al., 2009) with an uncertainty of 0.25 ppm, CH_4 was measured by the Differential Absorption of CO Measurement (DACOM) instrument, a mid-IR absorption sensor (Sachse at al., 1987) with an accuracy of 1% and a precision of 1 ppb. Both instruments were calibrated in-flight with standard gases traceable to the respective World Meteorological scales. The aircraft static pressure and altitude were recorded via a pressure transducer and radar altimeter, respectively, recorded by the aircraft data system. As with the NIMS profiles, the vertical profiles of CO_2 and CH_4 mixing ratio were obtained during a downward flight centred on the Anmyeondo.

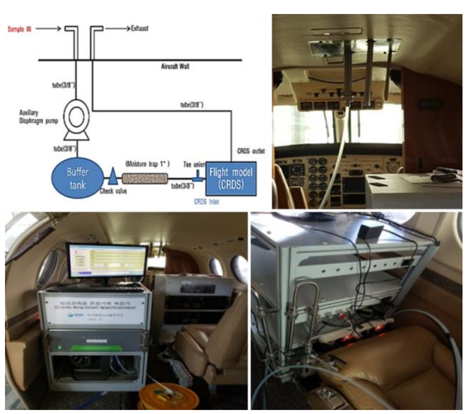

Figure 7. NIMS CRDS instrument on board the King Air 90C.

2.6.2 Aircraft CO_2 and CH_4 data

The NIMS vertical profiles of CO_2 and CH_4 mixing ratio were obtained during a downward spiral flight centred over the Anmyeondo FTS station, on 29 October and 12 November, 2017. As an example, the flight trajectory is shown in the left panel of Figure 8 while the profiles of CO_2 and CH_4 from flight dur-ing the ascent and descent on 29 October, 2017 are depicted in the middle and right panels of Figure 8, respectively. All flights were performed under clear sky conditions. The campaign was p-erformed for 2 hours on both days. Specifically, the respective measureme nts were taken from 11:00:37 to 12:03:25 KST (UTC+9) and from 13:58:58 to 15:19:40 KST on 2 9 October, 2017 and similarly from 11:12:20 to 12:13:00 KST and from 14:14:46 to 15:14:46 KST on 12 November, 2017. The altitude range of the aircraft measurements was limited to approxi mately 0.1 to a 9.1 km. We constructed the complete CO_2 and CH_4 profiles in a similar way as p erformed by Deutscher et al. 2010; Miyamoto et al. (2013); Ohyama et al. (2015).

For both CO_2 and CH_4 profiles, we have used in-situ surface data (AMY GAW station) to comple ment the aircraft profiles close to surface level, and above the aircraft ceiling, the mole fraction s throughout the altitude range between the uppermost aircraft and the tropopause is assumed to be the same as at the highest aircraft measurement level because of lack of data. This extrapolation produces the largest uncertainty in the in situ column estimate. For this analysis, the tropopause height was derived from NOAA National Centers for Environmental Prediction/ National Center for Atmospheric Research Reanalysis datasets which are provided in 6-hour int ervals (0:00, 06:00, 12:00, and 18:00 UTC) with a horizontal resolution of 2.5 by 2.5 degrees. Th e measurements of surface pressure were available at the FTS station, which we have used for c alculating XCO_2 and XCH_4. Above the tropopause height, GFIT apriori profiles were utilized to extrapolate the aircraft profile. Eventually, the completed aircraft profiles based on those assu mptions were transformed into a total column XCO_2 and XCH_4 by pressure weighting functions. For this comparison, we considered only the FTS averaged XCO_2 and XCH_4 retrieval values for th e corresponding aircraft measurement time. Details about the aircraft XCO_2 and XCH_4 values du ring ascending and descending aircraft flight duration and the corresponding FTS averaged XCO_2 and XCH_4 retrieval values are also provided in Table 3. Note that the vertically resolved FTS column-averaging kernels were taken into account for smoothing the aircraft profiles. The XCO_2 and XCH_4 for the aircraft in situ profile weighted by the column averaging kernel a (Rodge rs and Connor, 2003) is computed as follows:

$$X^{in-situ} = X^{a} + \sum_{j} h_j a_j (t_{in-situ} - t_a)_j$$

where X^a is the column-averaged dry air mole fraction for the apriori profile t_a (CO_2 or CH_4), $t_{in-situ}$ is the aircraft profile and h_j is the pressure weighting function.

We estimated the uncertainty of the XCO_2 and XCH_4 columns derived from the extended aircraft profiles by assigning uncertainties. Uncertainty at the surface was assumed to be same as the uncertainty in the lowest measurements. For the stratosphere, we used the method suggested by Wunch et al. (2010). This method shifts the stratospheric values up and down by 1 km to calculate the difference in the total column, which is used as an estimate of the uncertainty in the location of the tropopause and therefore for the stratospheric contribution. We estimated the stratospheric errors in aircraft integrated amount of XCO_2 and XCH_4 by shifting the apriori profile by 1 km (Ohyama et al. 2015). For KORUS-AQ, it was found to be 0.42 ppm for XCO_2 and 13.26 ppb for XCH_4.

For NASA's DC8 measurements, the in-situ profiles covered the altitude range of approximately 0.17 to 9.0 km, in-situ surface data were utilized near the surface to complement the aircraft profiles and extended the aircraft ceiling point of measurements to the tropopause which is estimated by NCEP to be at 139.0 hPa. Figure 9 illustrates the results of XCO_2 and XCH_4 comparisons between the aircraft observation and TCCON site data. In this plot, blue represents the KORUS-AQ campaign, whereas green indicates the NIMS campaign. KORUS-AQ data lie on the best line which is derived using TCCON stations where aircraft profiles are available. This shows that TCCON Anmyeondo data is consistent with other TCCON stations.

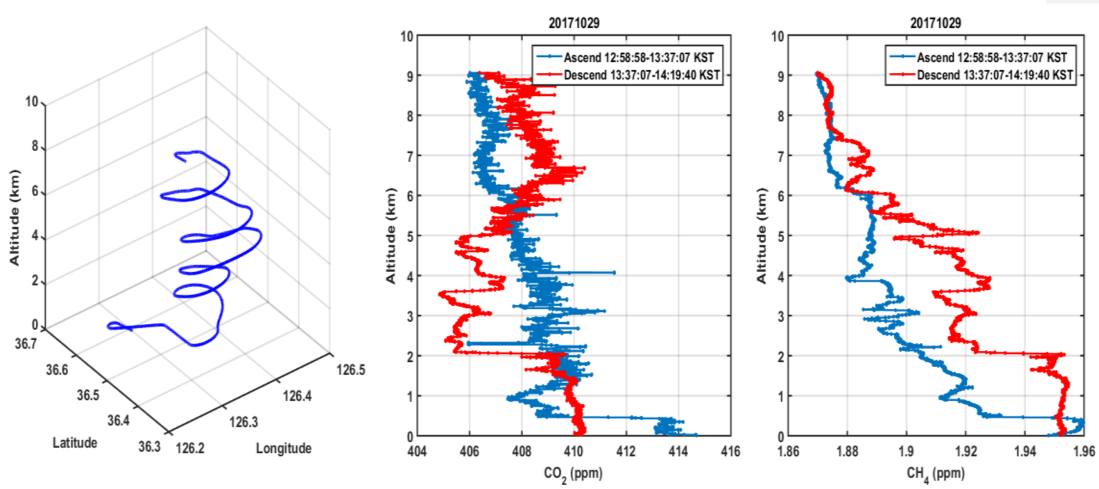

Figure 8. Typical flight path (left panel), CO_2 (middle panel) and CH_4 (right panel) VMR profiles during ascent and descent of the aircraft over Anmyeondo on October 29, 2017 are shown.

Table 3. Summary of the column averaged dry-air mole fractions obtained during the inter-comparison between the in-situ instrument on board the aircrafts and the g-b FTS at the Anmyeondo station. A and D represent ascending and descending, respectively. Note that FTS values given below are without TCCON common scale factor and FTS column averaging kernels are applied to the aircraft data.

Date of measurements (hours in KST)	Aircraft NIMS XCO_2 (ppm)	g-b FTS XCO_2 (ppm)	Aircraft NIMS XCH_4 (ppm)	g-b FTS XCH_4 (ppm)
2017-10-29				
09:59:16-10:31:08 (A)	409.152	404.242	1.8900	1.8460
10:31:09-11:03:24 (D)	409.336	403.877	1.8854	1.8454
12:58:58-13:37:07 (A)	407.011	401.051	1.8562	1.8265
13:37:07-14:19:40 (D)	406.898	400.537	1.8720	1.8249
2017-11-12				
11:12:20-11:38:01 (A)	406.541	401.839	1.8513	1.8221
11:38:02-12:13:00 (D)	406.839	401.930	1.8512	1.8220
14:14:46-14:45:55 (A)	406.517	401.592	1.8479	1.8201
14:45:56-15:23:47 (D)	407.628	401.473	1.8504	1.8191
Mean ± std	**407.491 ±1.137**	**402.068± 1.311**	**1.8630± 0.0170**	**1.8283± 0.011**
	KORUS	**TCCON**	**KORUS**	**TCCON**
2016-05-22	405.80 ± 0.42	401.91 ± 0.57	1.8641± 0.0132	1.8100±0.002

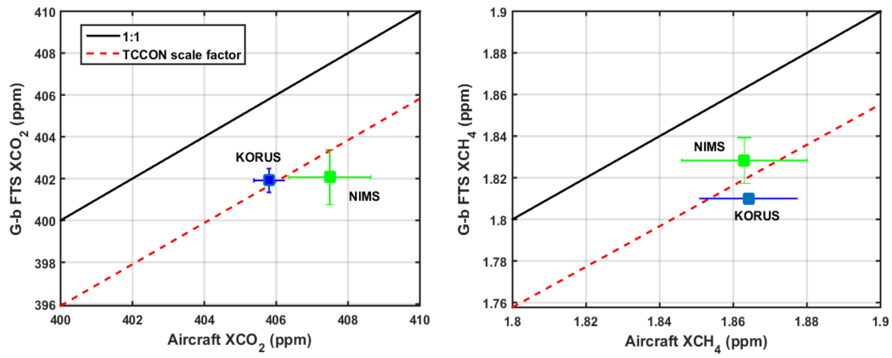

Figure 9. The comparisons of XCO_2 and XCH_4 between the aircraft observation and g-b FTS data over Anmyeondo station are shown. The blue square symbol represents for the aircraft campaign conducted by KORUS-AQ (May, 2016), whereas green square symbol indicates for the aircraft campaign operated by NIMS (2017). Note that FTS values shown in the figure are after removing TCCON common scale factor.

2.7 Comparison with OCO-2 measurements

The Orbiting Carbon Observatory-2 (OCO-2) is NASA's first Earth-orbiting satellite dedicated to greenhouse gas measurement, it was successfully launched on July 2, 2014 into low-Earth orbit. It is devoted to observing atmospheric carbon dioxide (CO_2) to provide improved insight into the carbon cycle. The primary mission is to measure carbon dioxide with high precision and accuracy in order to characterize its sources and sinks at different spatial and temporal scales (Boland et al., 2009; Crisp, 2008, 2015). The instrument measures the near infrared spectra (NIR) of sunlight reflected off the Earth's surface. Atmospheric abundances of carbon dioxide and related atmospheric parameters are retrieved from the spectra in nadir, sun glint and target modes. Detailed information about the instrument is available in, for example (Connor et al., 2008; O'Dell et al., 2012). In this work, we used the OCO-2 version 7Br bias corrected data. The comparisons are discussed in section 3.3.

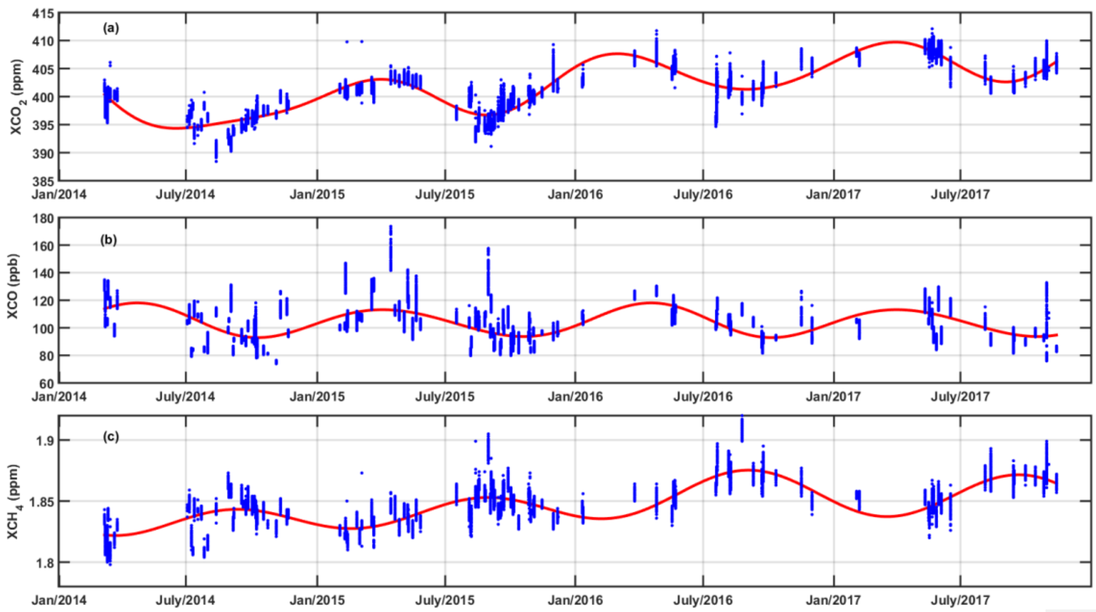

Figure 10. Time series of XCO_2, XCO, and XCH_4 from top to bottom panels (a-c), respectively in the period between February 2014 and November 2017 is given. Each marker indicates a single retrieval. Fitting curves (red solid lines) are also displayed.

Table 4. Annual mean of XCO_2, XCO, and XCH_4 from Anmyeondo g-b FTS from February 2014 to November 2017 is given.

	Annual mean ± standard deviation			
Gases	**2014**	**2015**	**2016**	**2017**
XCO_2 (ppm)	**396.91 ± 2.55**	**399.32 ± 2.96**	**402.97 ± 2.74**	**406.04 ± 2.38**
XCO (ppb)	**99.42 ± 14.71**	**102.73 ± 14.91**	**105.39 ± 10.68**	**100.14 ± 10.3**
XCH_4 (ppm)	**1.837 ± 0.014**	**1.844 ± 0.015**	**1.864 ± 0.015**	**1.859 ± 0.013**

3 Results and discussion

3.1 Time series of g-b FTS XCO_2, seasonal and annual cycle

The time series of XCO_2 along with retrievals of other trace gases such as XCO and XCH_4 from g-b FTS is presented in Figure 10 (panel a-c) for the period from February 2014 to November 2017. In these time series plots, each marker represents a single retrieval, and the fitting curves of the retrieved values are also depicted (red solid line). We show the seasonal cycle of XCO_2, XCO, and XCH_4 in the time series using a fitting procedure described by

Thoning et al. (1989). Standard deviations of the differences between the retrieved values and the fitting curves are 1.64 ppm, 11.34 ppb, and 10.1 ppb for XCO_2, XCO, and XCH_4, respectively. It is evident that all species have a seasonal cycle feature. Year to year variability of XCO_2 is highest in spring and lowest during the growing season in June to September. Moreover, the behavior of the seasonal cycle of XCO_2 at our site was compared with that of XCO_2 at Saga, Japan, which is discussed in a later section. The atmospheric increase of XCO_2 from 2015 to 2016 was 3.65 ppm, which is larger than the increase from 2014 to 2015. For the case of XCH_4, its increase from 2015 to 2016 was 0.02 ppm, which is higher than the increase from 2014 to 2015, whereas in XCO the rate of increment from year to year was found to be slightly decreased (see Table 4).

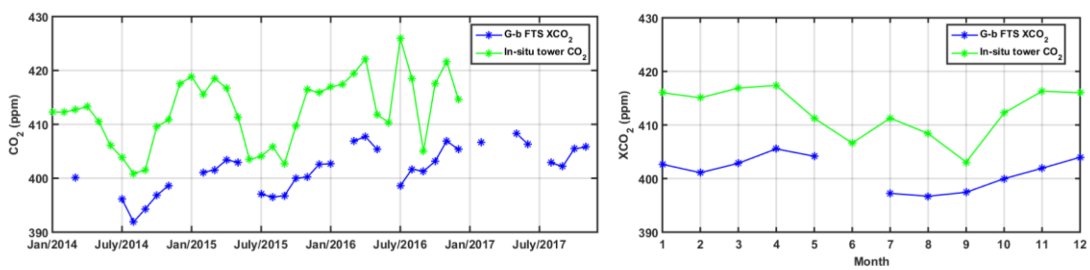

Figure 11. Left panel shows the time series of FTS XCO_2 and in-situ tower CO_2 on monthly mean basis, whereas right panel depicts annual cycle (2014-2016).

The seasonal and annual cycles of XCO_2 derived from the g-b FTS were compared with in-situ tower observations of CO_2 over the Anmyeondo station, which are presented in Figure 11. Regarding in-situ data, samples were collected using flasks and analysed using non-dispersive infrared (NDIR) spectroscopy at the altitude of 77 meters above sea level (details about in situ data are available at http://ds.data.jma.go.jp/jmd/wdcgg/). Nearly 97 % of in-situ data in Figure 11 were taken during day time between 04:00 – 08:40 UTC (13:00 – 17:40 Korea Standard Time (KST)) so that the early morning and night time enhancements of CO_2 were mostly excluded. In-situ CO_2 monthly means are generated by first averaging all valid event measurements with a unique sample date and time. The values are then extracted at weekly intervals from a smooth curve (Thoning et al., 1989) fitted to the averaged data and then these weekly values are averaged for each month. As can be seen in Figure 10, the overall patterns of seasonal and annual cycle of FTS XCO_2 tend to be similar with those of in-situ tower CO_2.

3.2 Comparison of Anmyeondo XCO_2 with nearby TCCON station

In Figure 12, we present the comparison of our FTS XCO_2 data with a similar ground-based high resolution TCCON FTS observation at Saga station (33.26 N, 130.29 E) in Japan, which is the closest TCCON station to our site. Among nearby TCCON stations, Rikubetsu, Tsukuba, and Saga are located in Japan (Morino et al., 2011, Ohyama et al., 2009, 2015) and Hefei is located in China (Wang et al., 2017). To demonstrate the comparison between them, we have shown the daily averaged XCO_2 of two stations during the period of 2014 to 2017 in Figure 12. As can be seen, variations of XCO_2 at the Saga station agreed well with Anmyeondo station. The daily averaged XCO_2 revealed the same seasonal cycle as that of our station. The lowest XCO_2 appeared in late summer (August and September), and the highest value was in spring (April).

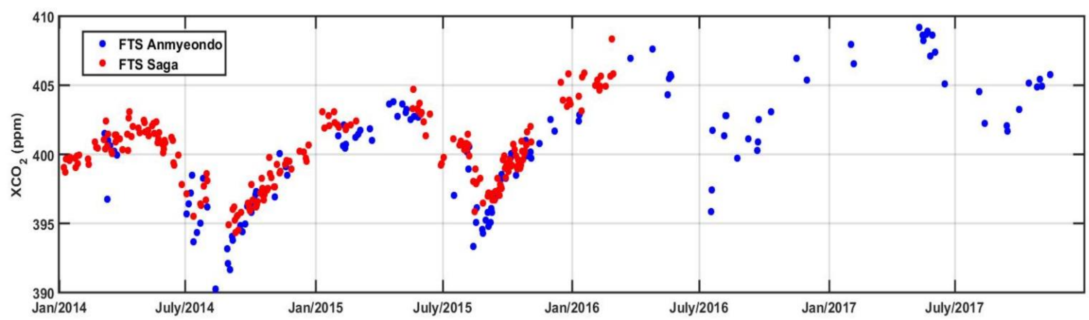

Figure 12. Time series of daily averaged XCO_2 retrieval from Anmyeondo FTS and Saga FTS in the period of February 2014 to November 2017 is depicted.

Ohyama et al., (2015) studied the time series of XCO_2 at Saga, Japan during the period from July 2011 to December 2014. They showed seasonal and interannual variations. The peak-to-peak seasonal amplitude of XCO_2 was 6.9 ppm over Saga during July 2011 and December 2014, with a seasonal maximum and minimum in the average seasonal cycle during May and September, respectively. In recent findings of Wang et al. (2017), the g-b FTS temporal distributions of XCO_2 at Hefei, China were reported. The FTS observations in 2014 to 2016 had a clear and similar seasonal cycle, i.e. XCO_2 reaches a minimum in late summer, and then slowly increases to the highest value in spring. The daily average of XCO_2 ranges from 392.33 ± 0.86 to 411.62 ± 0.90 ppm, and the monthly average value shows a seasonal amplitude of 8.31 and 13.56 ppm from 2014 to 2015 and from 2015 to 2016, respectively. The seasonal cycle was mainly driven by large scale (hemispheric) biosphere–atmosphere exchange. Butz et al., (2011) reported that the observations from GOSAT and the co-located ground-based measurements agreed well in capturing the seasonal cycle of XCO_2 with the late summer minimum and the spring maximum for four TCCON stations (Bialystok, Orleans, Park Falls, and Lamont) in the Northern Hemisphere. We infer that the variation of XCO_2 over Anmyeondo station is in harmony with the variation pattern in mid-latitude Northern Hemisphere.

3.3 Comparison of XCO_2 between the g-b FTS and OCO-2

In this section, we present a comparison of XCO_2 between the g-b FTS and OCO-2 version 7Br data (bias corrected data) over Anmyeondo station during the period between 2014 and 2017. For making a direct comparison of the g-b FTS measurements against OCO-2, we applied the spatial coincidence criteria for the OCO-2 data within 3° latitude/longitude of the FTS station, as well as setting up a time window of 3 hours (maximum 3 hours mismatch between satellite and g-b FTS observations). Based on the coincidence criteria, we obtained 13 coincident measurements, which were not sufficient to infer a robust conclusion, but do provide a preliminary result. The comparison of the time series of XCO_2 concentrations derived from the g-b FTS and OCO-2 on daily median basis is demonstrated during the measurement period between 2014 and 2017, depicted in Figure 13. As can be seen in the plot, the g-b FTS measurement exhibits some gaps which occurred due to bad weather conditions, instrument failures, and absences of an instrument operator. In the present analysis, the XCO_2 concentrations from FTS were considered only when retrieval error was below 1.50 ppm (not shown), which is the sum of all error components such as laser sampling error, zero level offsets, ILS error, smoothing error, atmospheric a-priori temperature, atmospheric a-priori pressure, surface pressure, and random noise. Wunch et al. (2016) reported that the comparison of XCO_2 derived from the OCO-2 version 7Br data against co-located ground-based TCCON data that indicates the median differences between the OCO-2 and TCCON data were less than 0.50 ppm, and corresponding RMS differences of less than 1.50 ppm. The overall results of our comparisons were comparable with the report of Wunch et al. (2016). The OCO-2 product of XCO_2 was biased (satellite minus g-b FTS) with respect to the g-b FTS, which was slightly higher by 0.18 ppm with a standard deviation of 1.19 ppm, a corresponding RMS difference of 1.16 ppm. This bias could be attributed to the instrument uncertainty. In addition to that, we also obtained a strong correlation between the two datasets, which was quantified as a correlation coefficient of 0.94 (see Table 5 and Figure 13).

Table 5. Summary of the statistics of XCO_2 comparisons between OCO-2 and the g-b FTS from 2014 to 2017 are presented. N - coincident number of data, R - Pearson correlation coefficient, RMS - Root Mean Squares differences.

N	Mean Absolute.diff. (ppm)	Mean Relative diff (%)	R	RMS (ppm)
13	**0.18±1.19**	**0.04±0.29**	**0.94**	**1.16**

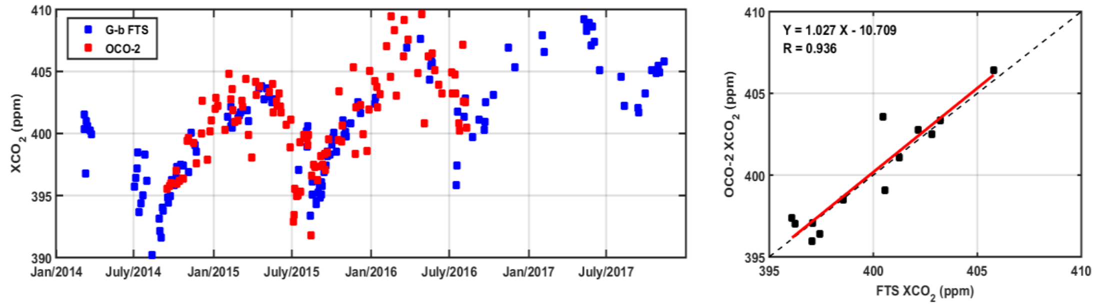

Figure 13. Left panel: The time series of XCO_2 from the g-b FTS (blue squares) and OCO-2 (red squares) over the Anmyeondo station from February 2014 to November 2017 are shown. Right panel: The linear regression curve between FTS and OCO-2 is shown. All results are given on a daily medians basis.

Table 6. Seasonal mean and standard deviations of XCO_2 from the g-b FTS and OCO-2 in the period between 2014 and 2016 are given below.

Season	g-b FTS XCO_2 mean ± std (ppm)	OCO-2 XCO_2 mean ± std (ppm)
Winter	401.52 ± 0.85	402.67 ± 2.67
Spring	402.72 ± 2.79	403.96 ± 2.77
Summer	396.92 ± 3.28	399.68 ± 3.77
Autumn	398.01 ± 2.83	398.48 ± 2.41

Both measurements capture the seasonal variability of XCO_2. As can be seen clearly from the temporal distribution of FTS XCO_2, the maximum and minimum values are discernible in spring and late summer seasons, respectively. The mean values in spring and summer were 402.72 and 396.92 ppm, respectively (see Table 6). This is because the seasonal variation of XCO_2 is most likely to be controlled by the imbalance of the terrestrial ecosystem exchange, and this could explain the larger XCO_2 values in the northern hemisphere in late April (Schneising et al. 2008, and references therein). The minimum value of XCO_2 occurs in August, which is most likely due to uptake of carbon into the biosphere associated with the period of plant growth. Furthermore, both instruments showed high standard deviations during summer, about 3.28 ppm in FTS and 3.77 ppm in OCO-2, and this suggests that the variability reflects strong sources and sink signals.

4 Conclusions

Monitoring of greenhouse gases is an essential issue in the context of global climate change. Accurate and precise continuous long-term measurements of greenhouse gases (GHGs) are substantial for investigating their sources and sinks. Today, several remote sensing instruments operated on different platforms are dedicated for measuring GHGs. Total column measurements of greenhouse gases such as XCO_2, XCH_4, XH_2O, XN_2O have been made using the g-b FTS at the Anmyeondo station since 2013. In this work, we focused on the measurements taken during the period of February 2014 to November 2017. The instrument has been operated in a semi-automated mode since then. The FTS instrument has been stable during the whole measurement period. Regular instrument alignment checks using the HCl cell measurements are performed. The TCCON standard GGG2014 retrieval software was used to retrieve XCO_2, XCO, and others GHG gases from the g-b FTS spectra.

In this work, the g-b FTS retrieval of XCO_2 and XCH_4 were compared with aircraft measurements that were conducted over Anmyeondo station on 22 May 2016, 29 October and 12 November, 2017. The mean absolute difference between FTS and aircraft XCO_2 were found to be -1.109 ± 0.802 ppm, corresponding to a mean relative difference of -0.273 ± 0.198 % for XCO_2, while the mean absolute difference for XCH_4 is 0.007 ± 0.0096 ppm, corresponding to a mean relative difference of 0.377 ± 0.518 %. These differences appeared in both species and were consistent with the combined instrument errors. The preliminary comparison results of XCO_2 between FTS and OCO-2 were also presented over the Anmyeondo station. The mean absolute difference of XCO_2 between FTS and OCO-2 was calculated on daily median basis, and it was estimated to be 0.18 ppm with a standard deviation of 0.19 with respect to the g-b FTS. This bias could be attributed to instrument uncertainty. Based on the seasonal cycle comparison, both the g-b FTS and OCO-2 showed a consistent pattern in capturing the seasonal variability of XCO_2, with maximum in spring and minimum in summer.

5 Acknowledgements

This research was supported by the Research and Development for KMA Weather, Climate, and Earth system Services (NIMS-2016-3100). D.W.T.G and V.A.V. would like to acknowledge financial support from the Australian Research Council (ARC) for TCCON activities (DP160101598, DP140101552, DP110103118). We are grateful for the Jeong-Hoo Park in Park National Institute of Environmental Research and Ryan Bennett in NASA Langley Research Center and NASA's KORUS campaign team. Many thanks goes to Dr. Haeyoung Lee for accessing in-situ surface data of the Anmyeondo station and Dr. Kei Shiomi and the team as well for the provision of Saga FTS data. We thank the OCO-2 and GOSAT science teams for the delivery of data. Finally, we strongly appreciate the two anonymous reviewers who helped us to improve this manuscript well.

References

Boland, S., Brown L. R., Burrows J. P., Ciais P., Connor B. J., Crisp D., Denning S., Doney S. C., Engelen R., Fung I. Y., Griffith P., Jacob D. J., Johnson B., Martin-Torres J., Michalak A. M., Miller C. E., Polonsky I., Potter C., Randerson J. T., Rayner P. J., Salawitch R. J., Santee M., Tans P. P., Wennberg P. O., Wunch D., Wofsy S. C., and Yung Y. L.: The Need for Atmospheric Carbon Dioxide Measurements from Space: Contributions from a Rapid Reflight of the Orbiting Carbon Observatory, 2009, http://www.nasa.gov/pdf/363474main_OCO_Reflight.pdf.

Brault, J. W.: New approach to high-precision Fourier transform spectrometer design. Appl. Opt. 35, 2891–2896, 1996.

Butz, A., Guerlet, S., Hasekamp, O., Schepers, D., Galli, A., Aben, I., Frankenberg, C., Hartmann, J.-M., Tran, H., Kuze, A., Keppel-Aleks, G., Toon, G., Wunch, D., Wennberg, P., Deutscher, N., Griffith, D., Macatangay, R., Messerschmidt, J., Notholt, J., and Warneke, T.: Toward accurate CO_2 and CH_4 observations from GOSAT, Geophys. Res. Lett., 38, L14812, https://doi.org/10.1029/2011GL047888, 2011.

Chen, H., Winderlich, J., Gerbig, C., Hoefer, A., Rella, C. W., Crosson, E. R., Van Pelt, A. D., Steinbach, J., Kolle, O., Beck, V., Daube, B. C., Gottlieb, E. W., Chow, V. Y., Santoni, G. W., and Wofsy, S. C: High-accuracy continuous airborne measurement of greenhouse gases (CO_2 and CH_4) using the cavity ring-down spectroscopy (CRDS) technique Atmos. Meas. Tech., 3, 375-386, 2010.

Connor B. J., Bösch H., Toon G., Sen B., Miller C. E., and Crisp D.: Orbiting carbon observatory: Inverse method and prospective error analysis, J. Geophys. Res., 113 doi: 10.1029/2006JD008336, 2008.

Crisp D., Miller C. E., DeCola P. L.: NASA Orbiting Carbon Observatory: measuring the column averaged carbon dioxide mole fraction from space. J. Appl. Remote Sens., 2, 023508, doi:10.1117/1.2898457, 2008.

Crisp D. for the OCO-2 Team: Measuring Atmospheric Carbon Dioxide from Space with the Orbiting Carbon Observatory-2 (OCO-2), Proc. SPIE 9607, Earth Observing Systems XX, 960702, doi: 10.1117/12.2187291, 2015.

Deutscher, N. M., Griffith, D. W. T., Bryant, G. W., Wennberg, P. O., Toon, G. C., Washenfelder, R. A., Keppel-Aleks, G., Wunch, D., Yavin, Y., Allen N. T., Blavier, J.-F., Jiménez R., Daube, B. C., Bright, A. V., Matross, D. M., Wofsy, S. C., and Park, S.: Total column CO_2 measurements at

Darwin, Australia-site description and calibration against in situ aircraft profiles, Atmos. Meas. Tech., 3, 947-958, doi:10.5194/amt-3-947-2010, 2010.

Frankenberg, C., Pollock, R., Lee, R. A. M., Rosenberg, R., Blavier, J.-F., Crisp, D., O'Dell C. W., Osterman, G. B., Roehl, C., Wennberg, P. O., and Wunch, D.: The Orbiting Carbon Observatory (OCO-2): spectrometer performance evaluation using pre-launch direct sun measurements. Atmospheric Measurement Techniques, 8(1), 301–313. doi:10.5194/amt-8-301-2015, 2015.

Hase, F., Blumenstock, T., and Paton-Walsh, C.: Analysis of the instrumental line shape of high resolution Fourier transform IR spectrometers with gas cell measurements and new retrieval software, Appl. Optics, 38, 3417–3422, doi:10.1364/AO.38.003417,1999.

Hase, F., Drouin, B. J., Roehl, C. M., Toon, G. C., Wennberg, P. O., Wunch, D., Blumenstock, T., Desmet F., Feist, D. G., Heikkinen, P., De Mazière, M., Rettinger, M., Robinson, J., Schneider, M., Sherlock, V., Sussmann, R., Té Y., Warneke, T., and Weinzierl, C.: Calibration of sealed HCl cells used for TCCON instrumental line shape monitoring, Atmospheric Measurement Techniques, 6(12), 3527–3537, doi:10.5194/amt-6-3527-2013, 2013.

Kiel, M., Wunch, D., Wennberg, P. O., Toon, G. C., Hase, F., and Blumenstock, T.: Improved retrieval of gas abundances from near-infrared solar FTIR spectra measured at the Karlsruhe TCCON station, Atmos. Meas. Tech., 9(2), 669–682, doi:10.5194/amt-9-669-2016, 2016.

Kivi, R. and Heikkinen, P.: Fourier transform spectrometer measurements of column CO_2 at Sodankylä, Finland, Geosci. Instrum. Method. Data Syst., 5, 271–279, 2016.

Messerschmidt, J., Macatangay, R., Notholt, J., Petri C., Warneke, T., and Weinzierl, C.: Side by side measurements of CO_2 by ground-based Fourier transform spectrometry (FTS), Tellus B, 62(5), 749-758, doi:10.1111/j.1600-0889.2010.00491.x., 2010.

Messerschmidt, J., H. Chen, N. M. Deutscher, C. Gerbig, P. Grupe, K. Katrynski, F.-T. Koch, J. V. Lavrič, J. Notholt, C. Rödenbeck, W. Ruhe, T. Warneke, and Weinzierl, C.: Automated ground-based remote sensing measurements of greenhouse gases at the Białystok site in comparison with collocated in situ measurements and model data, Atmospheric Chemistry and Physics, 12(15), 6741–6755, doi:10.5194/acp-12-6741-2012, 2012.

Miao, R., Lu N., Yao L., Zhu, Y., Wang, J., and Sun, J.: Multi-Year Comparison of Carbon Dioxide from Satellite Data with Ground-Based FTS Measurements (2003–2011), Remote Sensing, 5(7), 3431–3456, doi:10.3390/rs5073431, 2013.

Miller, C. E., Crisp, D. DeCola, P. L., Olsen, S. C., Randerson, J. T., Michalak, A. M., Alkhaled, A., Rayner, P., Jacob, D. J., Suntharalingam, P., Jones, D. B. A., Denning, A. S., Nicholls, M. E., Doney, S. C., Pawson, S., Boesch, H., Connor B. J., Fung I. Y., O'Brien, D., Salawitch, R. J., Sander, S. P., Sen, B., Tans, P., Toon, G. C., Wennberg, P. O., Wofsy, S. C., Yung, Y. L., and Law, R. M.: Precision requirements for space-based XCO_2 data, J. Geophys. Res-Atmos., 109, D02301, doi: 10.1029/2006JD007659, 2007.

Morino, I., Uchino, O., Inoue, M., Yoshida, Y., Yokota T., Wennberg, P. O., Toon, G. C., Wunch, D., Roehl, C. M., Notholt, J., Warneke, T., Messerschmidt, J., Griffith, D. W. T., Deutscher, N. M., Sherlock, V., Connor, B. J., Robinson, J., Sussmann, R., and Rettinger, M.: Preliminary validation of column-averaged volume mixing ratios of carbon dioxide and methane retrieved from GOSAT short-wavelength infrared spectra, Atmospheric Measurement Techniques, 4(6), 1061-1076, doi:10.5194/amt-4-1061-2011, 2011.

Miyamoto, Y., Inoue, M., Morino, I., Uchino, O., Yokota, T., Machida, T., Sawa, Y., Matsueda, H., Sweeney, C., Tans, P. P., Andrews, A. E., and Patra, P. K.: Atmospheric column-averaged mole fractions of carbon dioxide at 53 aircraft measurement sites, Atmos. Chem. Phys., 13, 52655275, 2013.

O'Dell, C. W., Connor, B., Bösch, H., O'Brien, D., Frankenberg C., Castano, R., Christi, M., Eldering, D., Fisher, B., Gunson, M., McDuffie, J., Miller, C. E., Natraj, V., Oyafuso, F., Polonsky, I., Smyth, M., Taylor, T., Toon, G. C., Wennberg, P. O., and Wunch, D.: The ACOS CO2 retrieval algorithm – Part 1: Description and validation against synthetic observations, Atmospheric Measurement Techniques, 5, 99–121, doi: 10.5194/amt-5-99-2012, http://www.atmos-meas-tech.net/5/99/2012/, 2012.

Ohyama, H., Morino, I., Nagahama, T., Machida, T., Suto H., Oguma, H., Sawa, Y., Matsueda, H., Sugimoto, N., Nakane, H., and Nakagawa, K.: Column-averaged volume mixing ratio of CO_2 measured with ground-based Fourier transform spectrometer at Tsukuba, J. Geophys. Res., 114, D18303 doi:10.1029/2008JD011465, 2009.

Ohyama, H., Kawakami, S., Tanaka, T., Morino, Uchino, I., O., Inoue, M., Sakai, T., Nagai, T., Yamazaki, A., Uchiyama, A., Fukamachi, T., Sakashita, M., Kawasaki, T., Akaho, T., Arai, K., and Okumura, H.: Observations of XCO_2 and XCH_4 with ground-based high-resolution FTS at Saga, Japan, and comparisons with GOSAT products, Atmos. Meas. Tech., 8(12), 5263–5276, doi:10.5194/amt-8-5263-2015.

Rayner P. J., and O'Brien D. M.: The utility of remotely sensed CO_2 concentration data in surface source inversions, Geophys. Res. Lett., 28, 175–178, doi: 10.1029/2000GL011912, 2001.

Schneising O., Buchwitz M., Burrows J. P., Bovensmann, H., Reuter, M., Notholt, J., Macatangay, R., and Warneke, T.: Three years of greenhouse gas column-averaged dry air mole fractions retrieved from satellite-Part 1: Carbon dioxide, Atmos. Chem. Phys., 8, 3827-3853, 2008.

Sun, Y., Palm, M., Weinzierl, C., Peteri, C., Notholt, J., Wang, Y., and Liu, C.: Technical note: Sensitivity of instrumental line shape monitoring for the ground-based high-resolution FTIR spectrometer with respect to different optical attenuators, Atmos. Meas. Tech. Discuss., doi:10.5194/amt-10-989- 2017.

S. A. Vay, S. C. Tyler, Y. Choi, D. R. Blake, N. J. Blake, G. W. Sachse, G. S. Diskin, and H. B. Singh.: Sources and transport of $\triangle^{14}C$ in CO_2 within the Mexico City Basin and vicinity, Atmos. Chem. Phys., 9, 4973-4985, 2009.

Sachse, G. W., G. F. Hill, L. O. Wade, and M. G. Perry, 1987: Fast-Response, High-Precision Carbon Monoxide Sensor Using a Tunable Diode Laser Technique. J. Geophys. Res., 92, 2071-2081.

Thoning, K. W., Tans, P. P. and Komhyr, W. D.: Atmospheric carbon dioxide at Mauna Loa Observatory. Analysis of the NOAA GMCC Data, 1974-1985, J. Geophys. Res., 94, 8549-8565, 1989.

Velazco, V., Morino, I., Uchino, O., Hori, A., Kiel, M., Bukosa, B., Deutscher, N., Sakai, T., Nagai, T., Bagtasa, G., Izumi, T., Youshida, Y. and Griffith, D.: TCCON Philippines: First Measurement Results, Satellite Data and Model Comparisons in Southeast Asia Remote Sensing, 9(12), 1228, doi: 10.3390/rs9121228, 2017

WMO (2016). The state of greenhouse gases in the atmosphere based on global observations through 2015, greenhouse gas. Greenhouse Gas Bulletin 2016. https://library.wmo.int/opac/doc_num.php.

Wang, W., Tian, Y., Liu, C., Sun, Y., Liu, W., Xie, P., Liu, J., Xu, J., Morino, I., Velazco, V., Griffith, D., Notholt, J., and Warneke, T.: Investigating the performance of a greenhouse gas observatory in Hefei, China, Atmos. Meas. Tech., 10, 2627–2643, 2017.

Wang, Y., Munger, J. W., Xu, S., McElroy, M. B., Hao, J., Nielsen, C. P., and Ma, H.: CO2 and its correlation with CO at a rural site near Beijing: implications for combustion efficiency in China, Atmos. Chem. Phys., 10, 8881–8897, https://doi.org/10.5194/acp-10-8881-2010, 2010.

Washenfelder R. A., Toon G. C., Blavier J-F., Yang Z., Allen N. T., Wennberg P. O., Vay S. A., Matross, D. M., and Daube B. C.: Carbon dioxide column abundances at the Wisconsin Tall Tower site, Journal of Geophysical Research, 2006, 111, doi:10.1029/2006JD00715, 2006. Warneke, T., Yang, Z., Olsen, S., Korner, S., Notholt J., Toon, G. C., Velazco, V., Schultz, A., and Schrems, O.: Seasonal and latitudinal variations of column averaged volume-mixing ratios of atmospheric CO_2, Geophysical Research Letters, 32(3), 2-5, doi:10.1029/2004GL021597, 2005.

Wunch, D., Toon G. C., Wennberg, P. O., Wofsy, S. C., Stephens, B., Fisher, M. L., Uchino O., Abshire, J. B., Bernath, P. F., Biraud, S. C., Blavier, J.-F. L., Boone, C. D., Bowman, K. P., Browell, E. V., Campos, T., Connor, B. J., Daube, B. C., Deutscher, N. M., Diao M., Elkins, J. W., Gerbig, C., Gottlieb, E., Griffith, D. W. T., Hurst, D. F., Jiménez, R., Keppel-Aleks, G., Kort, E. A., Macatangay, R., Machida, T., Matsueda, H., Moore, F. L., Morino, I., Park, S., Robinson, J., Roehl, C. M., Sawa, Y., Sherlock, V., Sweeney, C., Tanaka, T., and Zondlo, M. A.: Calibration of the Total Carbon Column Observing Network using aircraft profile data, Atmospheric Measurement Techniques, 3(5), 1351-1362, doi:10.5194/amt-3-1351-2010.

Wunch, D., Toon, G. C., Sherlock, V., Deutscher, N. M., Liu X., Feist, D. G., and Wennberg, P. O.: The Total Carbon Column Observing Network's GGG2014 Data Version. doi:10.14291/tccon.ggg2014.documentation.R0/1221662, 2015.

Wunch, D., Wennberg, P.O.,, Osterman, G., Fisher, B., Naylor, B., Roehl, C. M., O'Dell, C., Mandrake, L.,Viatte, C., Griffith, D. W. T., Deutscher, N. M., Velazco, V. A., Notholt, J.,Warneke, T.,Petri, C., Maziere, M. De, Sha, M. K., Sussmann,R., Rettinger, M., Pollard, D., Robinson, J.,Morino, I., Uchino O., Hase, F., Blumenstock, T., Kiel, M., Feist, D. G., Arnold S.G., Strong, K., Mendonca, J., Kivi, R.,Heikkinen, P., Iraci, L., Podolske, J., Hillyard, P. W., Kawakami, S., Dubey, M. K., Parker, H. A., Sepulveda, E., Rodriguez, O. E. G., Te, Y., Jeseck, P., Gunson, M. R., Crisp, D., and Eldering A., Comparisons of the Orbiting Carbon Observatory-2 (OCO-2) XCO_2 measurements with TCCON, Atmos. Meas. Tech. Discuss., doi:10.5194/amt-2016-227, 2016.